Electronic Supplementary Information (ESI)

Functionalization Methodology for Synthesis of Silane-End-Functionalized Linear and Star Poly(aryl isocyanide)s by Combination of Cationic Polymerization and Hydrosilylation Reaction

*Tuemay Abadi Belay, Jupeng Chen, HuanXu, ShaowenZhang,ShiluChen,*Xiaofang Li**

Key Laboratory of Cluster Science of Ministry of Education, School of Chemistry and Chemical Engineering, Beijing Institute of Technology, 5 South Zhongguancun Street, Haidian District, Beijing 10081, China

Table of contents

Experimental Section

Materials

General Methods

Scheme S1. Synthesis of 1,3,5-Tris(dimethylsilyl) Benzene

Scheme S2. Synthesis of 4-Ethoxycarbonyl Phenyl Isocyanides (**EPI**)

Synthesis of 4-Aminobenzoate

Synthesis of 4-Formamidobenziate

Synthesis of 4-Ethoxycarbonyl Phenyl Isocyanide

Scheme S3. Synthesis of 4-Isocyano-4-(1,1,2-Triphenylvinyl)-1-Phenyl (**ITPP**)

Synthesis of (2-(4-Aminophenyl)-Ethene-1,1,2-Triyl)-Tribenzene

Synthesis of (2-(4-Formamidophenyl)-Ethene-1,1,2-Triyl-Tribenzene

Synthesis of (2-(4-Isocyanophenyl)-Ethene-1,1,2-Triyl)-Tribenzene

Scheme S4. Synthesis of 4-Isocyano-4-(1,1,2-Triphenylvinyl)-1-Phenyl-1-Anisol (**ITPPA**)

Synthesis of 4-Methoxytetraphenylethene

Synthesis of N-(4-Iodophenyl)-Formamide

Synthesis of N-(4'-(1,2,2-Triphenylvinyl)-[1-Phenoxy-1-Phenyl]-4-yl)-Formamide

Synthesis of 4-Isocyano-4'-(1,2,2-Triphenylvinyl)-1-Phenyl-1-Anisol

Scheme S5. Synthesis of (*1S,2R,5S*)-2-Isopropyl-5-Metheylcyclohexyl-4-Isocyanobezoate (**D-IMCI**) and (*1R,2S,5R*)-2-Isopropyl-5-Metheylcyclohexyl-4-Isocyanobezoate (**L-IMCI**)

Synthesis of (*1S,2R,5S*)-2-Isopropyl-5-Metheylcyclohexyl-4-Nitrobezoate

Synthesis of (*1S,2R,5S*)-2-Isopropyl-5-Metheylcyclohexyl-4-Aminobezoate

Synthesis of (*1S,2R,5S*)-2-Isopropyl-5-Metheylcyclohexyl-4-Formamidobezoate

Synthesis of (*1S,2R,5S*)-2-Isopropyl-5-Metheylcyclohexyl-4-Isocyanobezoate

Synthesis of (*1R,2S,5R*)-2-Isopropyl-5-Metheylcyclohexyl-4-Nitrobezoate

Synthesis of (*1R,2S,5R*)-2-Isopropyl-5-Metheylcyclohexyl-4-Aminobezoate

Synthesis of (*1R,2S,5R*)-2-Isopropyl-5-Metheylcyclohexyl-4-Formamidobezoate

Synthesis of (*1R,2S,5R*)-2-Isopropyl-5-Metheylcyclohexyl-4-Isocyanobezoate

A typical procedure for the linear polymerization of 4-ethoxycarbonyl phenyl isocyanide (EPI) with Et_3Si-H as end-functionalized agent (Table 1, entry 4).

A typical procedure for the three star random and homo-copolymerization of (*1S*,*2R*,*5S*)-2-isopropyl-5-methylcyclohexyl-4-isocyanobenzoate (D-IMCI) with 4-isocyano-4'-(1,2,2-triphenylvinyl)-1-phenyl-1-anisol (ITPPA) with 1,3,5-tris(dimethylsilyl)benzene as core-first functional agent (Table 3, entry 5).

Figure S1. ^{1}H NMR spectrum of4-ethoxycarbonyl phenyl isocyanide (**a**).

Figure S2. ^{13}C NMR spectrum of4-ethoxycarbonyl phenyl isocyanide (**a**).

Figure S3. ^{1}H NMR spectrum of 4-isocysno-4-(1,1,2-triphenylvinyl)-1-phenyl (ITPP) (**b**).

Figure S4. ^{13}C NMR spectrum of 4-isocysno-4-(1,1,2-triphenylvinyl)-1-phenyl (ITPP) (**b**).

Figure S5. ^{1}H NMR spectrum of 4-isocysno-4-(1,1,2-triphenylvinyl)-1-phenoxy-1-anisol (ITPPA) (**c**).

Figure S6. ^{13}C NMR spectrum of 4-isocysno-4-(1,1,2-triphenylvinyl)-1-phenoxy-1-anisol (ITPPA) (**c**).

Figure S7. ^{1}H NMR spectrum of (*1S,2R,5S*)-2-isopropyl-5-metheylcyclohexyl-4-isocyanobezoate (**d**).

Figure S8.^{13}C NMR spectrum of (*1S,2R,5S*)-2-isopropyl-5-metheylcyclohexyl-4-isocyanobezoate (**d**).

Figure S9.^{1}H NMR spectrum of (*1R,2S,5R*)-2-isopropyl-5-metheylcyclohexyl-4-isocyanobezoate (**e**).

Figure S10.^{13}C NMR spectrum of (*1R,2S,5R*)-2-isopropyl-5-metheylcyclohexyl-4-isocyanobezoate (**e**).

Figure S11. ^{1}H NMR spectra of Et_3SiH.

Figure S12. (a) ^{1}H NMR spectra of Et_3SiH and (b) corresponding cationic species in situ generated by reaction of Et_3SiH with catalyst $[Ph_3C][B(C_6F_5)_4]$.

Figure S13. ^{1}H NMR of poly(EPI) with Et_3SiH as end group (Table 2, entry 4).

Figure S14. (a) ^{1}H NMR of poly(EPI) (Table 2, entry 4), (b) Poly(ITPPA) (Table 2, entry 8), (c) Poly(D-IMCI) (Table 3, entry 9) and (d) Poly(L-IMCI) (Table 2, entry 10).

Figure S15. ^{1}H NMR of poly(EPI) with different silane source as end group (Table 2, entries 1–2).

Figure S16. ^{1}H NMR of poly(EPI) with different silane source as end group (Table 2, entries 3, 5–6).

Figure S17. ^{29}SiNMR spectrum of Et_3SiH and Et_3Si-end-functionalized poly(EPI) (Table 2, entry 4).

Figure S18. (^{1}H + ^{29}Si) gHMBC NMR spectrum of Et_3Si-end-functionalized poly(EPI) (Table 2, entry 4).

Figure S19. ^{29}Si-NMR spectrum of Et_3SiH and Et_3Si-end-functionalized poly(ITPPA) (Table 2, entry 8).

Figure S20. ^{29}Si-NMR spectrum of $PhSiH_3$ and PhSi-end-functionalized star poly(EPI) (Table 3, entry1).

Figure S21. ^{29}Si-NMR spectrum of $PhMe_2Si$-end-functionalized poly(EPI)(Table 2, entry 1).

Figure S22. ^{29}Si-NMR spectrum of (4-^{i}PrC_6H_4)Me_2Si-end-functionalized poly(EPI)(Table 2, entry 2).

Figure S23. ^{29}Si-NMR spectrum of Ph_3Si-end-functionalized poly(EPI) (Table 2, entry 3).

Figure S24. ^{29}Si-NMR spectrum of $^{i}Pr_3Si$-end-functionalized poly(EPI) (Table 2, entry 5).

Figure S25. ^{29}Si-NMR spectrum of $(OEt)_3Si$-end-functionalized poly(EPI) (Table 2, entry 6).

Figure S26. FT-IR spectra of monomers (a) Et_3SiH, (b) EPI, (c) ITPPA, (d) D-IMCIand (e) L-IMCI.

Figure S27. FT-IR spectra of (a) Poly(EPI) (Table 2, entry 4), (b) Poly(ITPPA) (Table 2, entry 8), (c) Poly(D-IMCI) (Table 2, entry 9), (d) Poly(L-IMCI) (Table 2, entry 10).

Figure S28. FT-IR spectra of $PhSiH_3$ and PhSi-end-functionalized star poly(EPI) (Table 3, entry1).

Figure S29. FT-IR spectra of $PhMe_2SiH$ and $PhMe_2Si$-end-functionalized poly(EPI) (Table 2, entry 1).

Figure S30. FT-IR spectra of (4-$^iPrC_6H_4$)Me_2SiH and (4-$^iPrC_6H_4$)Me_2Si-end-functionalized poly(EPI) (Table 2, entry 2).

Figure S31. FT-IR spectra of Ph_3SiH and Ph_3Si-end-functionalized poly(EPI) (Table 2, entry 3).

Figure S32. FT-IR spectra of $^iPr_3SiH$ and $^iPr_3Si$-end-functionalized poly(EPI) (Table 2, entry 5).

Figure S33. FT-IR spectra of $(OEt)_3SiH$ and $(OEt)_3Si$-end-functionalized poly(EPI) (Table 2, entry 6).

Figure S34. Plots of fluorescence intensity vs water fraction in THF/water mixture (0.01 mg/mL) (A) ITPP, (B) Poly(ITPP) (Table 2, entry 7), (C) ITPPA, (D) Poly(ITPPA) (Table 3, entry 8) (conditions: EX wavelength: 290 nm, EX slit: 5 nm, EM slit: 5 nm, 700 V).

Figure S35. UV absorption and transmittance spectra of (A) ITPP, (B) Poly(ITPP) (Table 2, entry 7), (C) ITPPA and (D) Poly(ITPPA) (Table 2, entry 8) with the water fraction in THF/water mixture ranging from 0 to 95%.

Figure S36. CD Spectra of Et_3Si-end-functionalized poly(D-IMCI) and Et_3Si-end-functionalized poly(L-IMCI) (Table 2, entries 9–10).

Figure S37. (a) ^1H NMR spectra of 1,3,5-$(SiMe_2H)_3$-C_6H_3 and (b) corresponding cationic species *in situ* generated by reaction of Poly-Si-H with catalyst $[Ph_3C][B(C_6F_5)_4]$.

Figure S38. ^1H NMR spectra of Poly(ITPPA) (Table 2, entry 8), Poly(D-IMCI-*co*-ITPPA)s (Table 3, entries 4–8) and Poly(D-IMCI) (Table 3, entry 9).

Figure S39. ^1H NMR spectra of Poly(ITPPA) (Table 2, entry 8), Poly(L-IMCI-*co*-ITPPA)s (Table 4, entries 9–13) and Poly(L-IMCI) (Table 3, entry 10).

Figure S40. ^{29}Si-NMR spectrum of poly(D-IMCI) (Table 3, entry 2).

Figure S41. ^{29}Si-NMR spectrum of poly(D-IMCI-*co*-ITPPA) (Table 3, entry 6).

Figure S42. Plots of fluorescence intensity vs water fraction in THF/water mixture (0.01 mg/mL) (A) Poly(D-IMCI-*co*-ITPPA) (Table 3, entry 4), (B) Poly(D-IMCI-*co*-ITPPA) (Table 3, entry 5), (C) Poly(D-IMCI-*co*-ITPPA) (Table 3, entry 6), (D) Poly(D-IMCI-*co*-ITPPA) (Table 3, entry 8), (F) Poly(L-IMCI-*co*-ITPPA) (Table 3, entry 9), (G) Poly(L-IMCI-*co*-ITPPA) (Table 3, entry 10), (H) Poly(L-IMCI-*co*-ITPPA)

(Table 3, entry 11) and (I) Poly(L-IMCI-*co*-ITPPA) (Table 3, entry 13) (conditions: EX wavelength: 290 nm, EX slit: 5 nm, EM slit: 5 nm, 700 V).

Figure S43. UV absorption and transmittance spectra of (a) baseline, (b) ITPPA, (c) Poly(ITPPA) (Table 2, entry 8), (d-g) (Poly(D-IMCI-*co*-ITPPA)s (Table 3, entries 4–8) and (h-l) Poly(L-IMCI-*co*-ITPPA)s (Table 3, entries 9–13) in THF.

Figure S44. CD spectra of poly(D-IMCI) (Table 3, entry 2) and poly(L-IMCI) (Table 3, entry 3).

Figure S45. MALDI-TOF mass spectrum of EPI oligomer obtained by the binary $[Ph_3C][B(C_6F_5)_4]/Et_3SiH$ system.

Figure S46. GPC curve of Poly(EPI) by cationic catalyst $[Ph_3C][B(C_6F_5)_4$ in Table 1, entry 1.

Figure S47. GPC curve of Poly(EPI) by cationic catalyst $[(Et_3Si)_2H][B(C_6F_5)_4]$ in Table 1, entry 2.

Figure S49. GPC curve of Et_3Si-end-functionalized poly(EPI) in Table 1, entry 3.

Figure S49. GPC curve of Et_3Si-end-functionalized poly(EPI) in Table 1, entry 4.

Figure S49. GPC curve of Et_3Si-end-functionalized poly(EPI) in Table 1, entry 5.

Figure S50. GPC curve of Et_3Si-end-functionalized poly(EPI) in Table 1, entry 6.

Figure S51. GPC curve of Et_3Si-end-functionalized poly(EPI) in Table 1, entry 7.

Figure S52. GPC curve of Et_3Si-end-functionalized poly(EPI) in Table 1, entry 8.

Figure S53. GPC curve of Et_3Si-End-Functionalized Poly(EPI) in Table 1, entry 9.

Figure S54. GPC curve of Et_3Si-end-functionalized poly(EPI) in Table 1, entry 10.

Figure S55. GPC curve of Et_3Si-end-functionalized poly(EPI) in Table 1, entry 11.

Figure S56. GPC curve of Et_3Si-end-functionalized poly(EPI) in Table 1, entry 12.

Figure S57. GPC curve of Et_3Si-end-functionalized poly(EPI) in Table 1, entry 13.

Figure S58. GPC curve of Et_3Si-end-functionalized poly(EPI) in Table 1, entry 14.

Figure S59. GPC curve of Et_3Si-end-functionalized poly(EPI) in Table 1, entry 15.

Figure S60. GPC curve of Et_3Si-end-functionalized poly(EPI) in Table 1, entry 16.

Figure S61. GPC curve of Et_3Si-end-functionalized poly(EPI) in Table 1, entry 17.

Figure S62. GPC curve of Et_3Si-end-functionalized poly(EPI) in Table 1, entry 18.

Figure S63. GPC curve of $PhMe_2Si$-end-functionalized poly(EPI) in Table 2, entry 1.

Figure S64. GPC curve of (4-$^{i}PrC_6H_4$)Me_2Si-end-functionalized poly(EPI) in Table 2, entry 2.

Figure S65. GPC curve of Ph_3Si-end-functionalized poly(EPI) in Table 2, entry 3.

Figure S66. GPC curve of $^{i}Pr_3Si$ -end-functionalized poly(EPI) in Table 2, entry 5.

Figure S67. GPC curve of $(OEt)_3Si$-end-functionalized poly(EPI) in Table 2, entry 6.

Figure S68. GPC curve of $(OEt)_3Si$-end-functionalized poly(EPI) in Table 2, entry 7.

Figure S69. GPC curve of Et_3Si-end-functionalized poly(ITPP) in Table 2, entry 8.

Figure S70. GPC curve of Et_3Si-end-functionalized poly(ITPPA) in Table 2, entry 9.

Figure S71. GPC curve of Et_3Si-end-functionalized poly(D-IMCI) in Table 2, entry 10

Figure S72. GPC curve of PhSi-end-functionalized star poly(EPI) in Table 3, entry 1.

Figure S73. GPC curve of C_6H_3-1,3,5-$(Me_2Si)_3$-end-functionalized poly(D-IMCI) in Table 3, entry 2.

Figure S74. GPC curve of C_6H_3-1,3,5-$(Me_2Si)_3$-end-functionalized poly(L-IMCI) in Table 3, entry 3.

Figure S75. GPC curve of C_6H_3-1,3,5-$(Me_2Si)_3$-end-functionalized poly(D-IMCI-*co*-ITPPA) in Table 3, entry 4.

Figure S76. GPC curve of C_6H_3-1,3,5-$(Me_2Si)_3$-end-functionalized poly(D-IMCI-*co*-ITPPA) in Table 3, entry 5.

Figure S77. GPC curve of C_6H_3-1,3,5-$(Me_2Si)_3$-end-functionalized poly(D-IMCI-*co*-ITPPA) in Table 3, entry 6.

Figure S78. GPC curve of C_6H_3-1,3,5-$(Me_2Si)_3$-end-functionalized poly(D-IMCI-*co*-ITPPA) in Table 3, entry 7.

Figure S79. GPC curve of C_6H_3-1,3,5-$(Me_2Si)_3$-end-functionalized poly(D-IMCI-*co*-ITPPA) in Table 3, entry 8.

Figure S80. GPC curve of C_6H_3-1,3,5-$(Me_2Si)_3$-end-functionalized poly(L-IMCI-*co*-ITPPA) in Table 3, entry 9.

Figure S81. GPC curve of C_6H_3-1,3,5-($Me_2Si)_3$-end-functionalized poly(L-IMCI-*co*-ITPPA) in Table 3, entry 10.

Figure S82. GPC curve of C_6H_3-1,3,5-($Me_2Si)_3$-end-functionalized poly(L-IMCI-*co*-ITPPA) in Table 3, entry 11.

Figure S83. GPC curve of C_6H_3-1,3,5-($Me_2Si)_3$-end-functionalized poly(L-IMCI-*co*-ITPPA) in Table 3, entry 12.

Figure S84. GPC curve of C_6H_3-1,3,5-($Me_2Si)_3$-end-functionalized poly(L-IMCI-*co*-ITPPA) in Table 3, entry 13.

COMPUTATIONALMETHODS

Density functional calculations

Figure S85. Optimized structures of the adduct between Ph_3C^+ and a substrate **a** (Ph_3C-$(a)_1^+$) and the transition state (**TS$_A$**) for the A^+ formation activated by Ph_3C^+.

Figure S86. Free energy profile for the polymerization initiated by Ph_3C^+.

Figure S87. Free energy profile for the polymerization initiated by A^+.

Figure S88. Optimized structures of stationary points in the polymerization initiated by A^+.

Figure S89. Optimized structures of stationary points in the polymerization initiated by Ph_3C^+.

Figure S90. DSC curve of PhSi-end-functionalized star poly(EPI) in Table 3, entry 1.

Figure S91. DSC curve of Ph_3Si-end-functionalized poly(EPI) in Table 2, entry 3.

Figure S92. DSC curve of $^iPr_3Si$-end-functionalized poly(EPI) in Table 2, entry 5.

Figure S93. DSC curve of $(OEt)_3Si$-end-functionalized poly(EPI) in Table 2, entry 6.

Figure S94. DSC curve of triethylsilane-end-capped Poly(D-IMCI) Table 2, entry 9.

Figure S95. DSC curve of triethylsilane-end-capped Poly(L-IMCI) in Table 2, entry 10.

Figure S96. DSC curve of silane-end-capped star Poly(D-IMCI) in Table 3, entry 2.

Figure S97. DSC curve of silane-end-capped star Poly(L-IMCI) in Table 3, entry 3.

Figure S98. AFM image of silane-end-capped star Poly(L-IMCI) in Table 3, entry 3.

Figure S99. SEM image of silane-end-capped star Poly(L-IMCI) in Table 3, entry 3.

Figure S100. The *in situ* ^{1}H NMR spectra of the polymerization of EPI by the $[Ph_3C][B(C_6F_5)_4]/PhSiH_3$ binary system under the molar ratio of $[EPI]/\{[Ph_3C][B(C_6F_5)_4]\}/[PhSiH_3]$ as 10:1:10 at room temperature in d^8-THF.

Figure S101. The *in situ* ^{29}Si NMR spectra of the polymerization of EPI by the $[Ph_3C][B(C_6F_5)_4]/PhSiH_3$ binary system under the molar ratio of $[EPI]/\{[Ph_3C][B(C_6F_5)_4]\}/[PhSiH_3]$ as 10:1:10 at room temperature in d^8-THF.

Figure S102. The reaction of $[Ph_3C][B(C_6F_5)_4]$ and $PhSiH_3$ under the molar ratio of $[EPI]/\{[Ph_3C][B(C_6F_5)_4]\}/[PhSiH_3]$ as 10:1:10 at room temperature in 1h.

References

EXPERIMENTAL SECTION

Materials

All manipulations of air and moisture-sensitive compounds were performed under a dry and oxygen free nitrogen atmosphere by using schlenk techniques or under nitrogen atmosphere in an Mbraunglovebox. Nitrogen (Beijing AP beifen gases Industrial Co.Ltd.) was purified through a dry clean column (4A molecular sieves, Dalian Replete Science and Technology Co.Ltd.) and a gas clean column (Dalian Replete Science and Technology Co.Ltd.). The nitrogen in glovebox was constantly circulated through copper/molecular sieves catalyst unit. The oxygen and moisture concentrations in the glovebox atmosphere were monitored by an O_2/H_2O Combi-Analyzer (Mbraun) to ensure both were always below 0.1ppm. THF, Hexane, Toluene, Chlorobenzene, Dichlorobenzene and 1,1,2,2-tetrachloroethane were purified by a solvent purification system (SPS-800, Mbraun), and dried over fresh Na Chips in the glovebox. $[Ph_3C][B(C_6F_5)_4]$, $[PhMe_2NH][B(C_6F_5)_4]$, and $B(C_6F_5)_3$ were purchased from Tosoh finechem corporation and used without purification. All Silane monomers were also purchased from Tosoh Finechem Corporation and dried with CaH_2 and Distilled.

Isocyanide monomers were synthesized according to literatures.[1] The 1,3,5-tris(dimethylsilyl)benzene also synthesized according to literature.[2] The deuterated solvents benzene-d6 (99.6 atom% D) and Chloroforum-d1 (99.8 atom% D) were obtained from Cambridge Isotope.

General Methods

^1H and ^{13}C NMR spectra were recorded on a BrukerAvance (III-HD 400 MHz) Spectrometer. The molecular Weights and molecular weight distributions of EPI Polymers were determined against polystyrene standard at 25°C by GPC on waters HPLC-515 apparatus, $CHCl_3$ was employed as the eluent at a flow rate of 1 ml/min. The molecular Weights and molecular weight distributions of the D-(or L-) IMCI and ITPA Polymers were determined against polystyrene standard at 25 °C by GPC on waters HPLC-8320GPC apparatus, THF was employed as the eluent at a flow rate of 1 mL/min.

FT-IR spectra were recorded on a thermo IS5 FT-IR system using KBr Pellets at room temperature. The UV-Vis spectra were recorded on a HITACHI F-7000 Fluorescence spectrometer. Quartz cells with 10.0 mm length were used in UV-Vis and fluorescence measurement, and the slit widths were set at 5.0 nm for both excitation and emission during the fluorescence measurement. Circular dichroism spectra were collected on a Jasco J-810 and quartz cell length was 1.0 nm. Optical rotations were measured on a Kruss P8000-T polarimeter using a 0.5 cm cell with a Na 589 nm filter. High resolution mass spectra were collected on an Agilent 6520 Accurate-mass Q-TOF LC/MS.

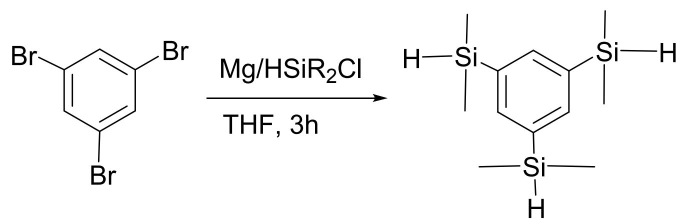

Scheme S1. Synthesis of 1,3,5-Tris(dimethylsilyl) Benzene

Synthesis of 1,3,5-tris(dimethylsilyl) benzene: The 1,3,5-tris(dimethylsilyl) benzene was synthesized according to the literature procedures.[3]To a mixture of dimethylchlorosilane (4.73 g, 50.0 mmol) and magnesium (1.22 g, 50.0 mmol) in dry THF (15 mL) was added a solution of 1,3,5-tribromobenzene (3.15 g, 100 mmol) in THF (10 mL). The rate of the addition was adjusted to maintain a reflux. When the addition was finished the reaction was heated under reflux for 3 h. The volatiles were removed in vacuo and the product extracted from the solid residue of hexane (3 × 20 mL). The solvent was removed in vacuo. The product was purified by distillation under reduced pressure, Yield 75%. ^1H-NMR ($CDCl_3$): 0.21 (18H, d, –CH_3, J ¼ 3 Hz), 4.29 (3H, septet, Si–H, J ¼ 3 Hz), 7.58 (3H, s, H–Ar).

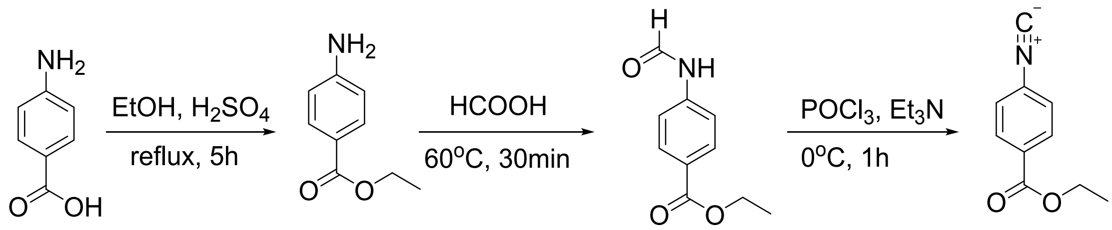

Scheme S2. Synthesis of 4-Ethoxycarbonyl Phenyl Isocyanides (**EPI**)

Synthesis of ethyl-4-aminobenzoate: To a solution of 4-aminobenzoic acid (5.26 g, 30.0 mmol) in 120 mL of EtOH was slowly added 16.3 mL of aqueous con.H_2SO_4 (300 mmol) at room temperature. The mixture was refluxed for 7 h, cooled to room temperature, neutralized with a saturated K_2CO_3 aqueous solution and extracted with ethyl acetate (3 × 60 mL), the combined organic phases were washed with brine (2 × 40 mL), dried over anhydrous Na_2SO_4 and concentrated in vacuum, the residue was purified by column chromatography (silica gel, 4:1-2:1 hexane to ethyl acetate, v/v) to afford compoundas a white solid (4.35 g, 93% yield). ^{1}H NMR (400 MHz, $CDCl_3$): 1.36 (t, *J*= 7.0 Hz, 3H), 4.06 (br, 2H), 4.31 (q, *J*= 7.2 Hz, 2H), 6.63 (d, *J*= 8.8 Hz, 2H), 7.85 (d, *J*= 8.4 Hz, 2H).

Synthesis of ethyl-4-formamidobenzoate: Compoundethyl 4-aminobenzoate (4.35 g, 26.3 mmol) was dissolved in a formic acid (1.5 mL, 39.5 mmol) the resulting mixture was heated at 60^{o}C for 30min. After the reaction mixture was cooled to room temperature, the excess formic acid was removed under reduced pressure, the residue was washed with saturated aqueous Na_2CO_3 (25 mL) and filtered, the filter cake was washed twice with water and dried in vacuum to afford crude compoundas a white solid (4.71 g, crude), this compound was used directly for the next step without purification.

Synthesis of 4-ethoxycarbonyl phenyl isocyanide: Compound ethyl-4-formamidobenzoate (4.71 g, 28.5 mmol) and triethylamine (27.60 mL, 191.0 mmol) were dissolved in dry THF (45 mL) under an atmosphere of nitrogen, after the mixture was cooled to 0^{o}C, $POCl_3$ (4.50 mL, 48.4 mmol) was added drop wise to the mixture, the resulting mixture was slowly warmed to room temperature and stirred for 1h, then the reaction mixture was slowly poured into 40 mL saturated aqueous Na_2CO_3 and stirred at room temperature for 1h, the mixture was extracted with CH_2Cl_2 (3 ×60 mL), the combined organic layers were washed with brine, dried over anhydrous Na_2SO_4 and concentrated under reduced pressure, the residue was purified by column chromatography (neutral Al_2O_3, 10:1 hexane to ethyl acetate, v/v) to afford the desired compound as brown solid (3.71 g, 87% yield). ^{1}H NMR (400

MHz,$CDCl_3$): 1.40 (t, *J*= 7.2 Hz, 3H), 4.39 (q, *J*= 7.2 Hz, 2H), 7.43 (d, *J*= 8.4 Hz, 2H), 7.43 (d, *J*= 8.4 Hz, 2H), 8.08 (dt, *J*= 2.0, 8.8 Hz, 2H); ^{13}C NMR (100 MHz,$CDCl_3$):14.33, 61.66, 126.48, 129.94 , 130.88, 131.38, 165.06, 167.10.

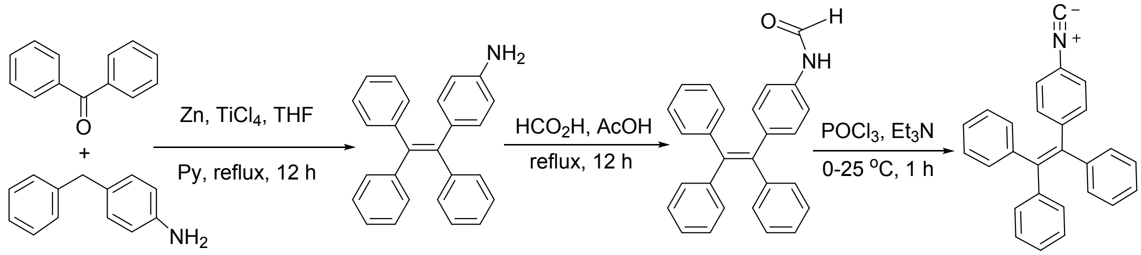

Scheme S3. Synthesis of 4-Isocyano-4-(1,1,2-Triphenylvinyl)-1-Phenyl (**ITPP**)

Synthesis of (2-(4-aminophenyl)ethene-1,1,2-triyl)tribenzene: The (2-(4-aminophenyl)ethene-1,1,2-triyl)tribenzene was synthesized by the typical McMurry reaction according to the literature procedures.[4] Into a two-necked round-bottom flask (100 mL) with reflux condenser were added of Zinc powder (Zn, 1.49 g, 22.8 mmol) and THF (60 mL). The flask was evacuated and flushed with dry nitrogen three times. After cooling to -15^{o}C, $TiCl_4$ (4.33 g, 22.8 mmol) was slowly added. The mixture was stirred for 2.5 h at room temperature. After cooling to -5^{o}C, again, Pyridine (1.53 mL, 19.0 mmol) was added and the mixture was stirred for 10 min. Then the solution of benzophenone (1.50 g, 7.6 mmol) and 4-benzylaniline (1.66 g, 9.1 mmol) in THF (40 mL) was added, the mixture was refluxed overnight. Afterwards, K_2CO_3 solution was added to quench the reaction. After cooling to room temperature, THF was removed by a rotary evaporator. The solution was poured in to water and extracted with DCM. The collected organic layer was dried over anhydrous Na_2SO_4. After extraction and evaporation of solvent, the crude product was recrystallized from Methanol. A yellow solid was obtained in 56%. ^{1}H NMR (400 MHz, $CDCl_3$): 7.13–6.99 (m, 17H); 6.85–6.82 (d, 2H); 6.52–6.49 (d, 2H).^{13}C NMR (100MHz, $CDCl_3$): 114.69, 144.57, 144.52, 144.44, 141.25, 139.87, 135.04, 132.94, 131.89.

Synthesis of (2-(4-formamidophenyl) ethene-1,1,2-triyl) tribenzene: Into a 100 mL two-necked flask was added compound (2-(4-aminophenyl)ethene-1,1,2-triyl)tribenzene(1.50 g, 4.3 mmol) and THF (40 mL). After cooling to 0^{o}C, acetic formal anhydride was tardily added by a syringe. The mixture was stirred at room temperature for 2 h. Then the reaction was quenched by the saturated solution of $NaHCO_3$. The mixture was extracted with ethyl acetate (EA), and then the collected organic layer was dried over anhydrous Na_2SO_4

and concentrated in Vacuum. The crude product was recrystallized from Methanol. A crude yellow solid was obtained in 82% and used directly for next step.

Synthesis of 4-Isocyano-4-(1,1,2-Triphenylvinyl)-1-Phenyl(ITPP): Compound (2-(4-formamidophenyl) ethene-1,1,2-triyl) tribenzene(1.39 g, 3.7 mmol) and triethylamine (3.50 mL, 24.8 mmol) were dissolved in dry THF (20 mL) under an atmosphere of nitrogen, after the mixture was cooled to 0°C, $POCl_3$ (0.60 mL, 6.3 mmol) was added drop wise to the mixture, the resulting mixture was slowly warmed to room temperature and stirred for 1h, then the reaction mixture was slowly poured into 15 mL saturated aqueous Na_2CO_3 and stirred at room temperature for 1 h, the mixture was extracted with CH_2Cl_2 (3 × 20 mL), the combined organic layers were washed with brine, dried over anhydrous Na_2SO_4 and concentrated under reduced pressure, the residue was purified by column chromatography (neutral Al_2O_3, 30:1 hexane to ethyl acetate, v/v) to afford the desired compound as light yellow solid (0.84g, 63% yield). ^1H NMR (400 MHz, $CDCl_3$): 7.17–7.10 (m, 11H), 7.21–6.93 (m, 8H); ^{13}C NMR (101 MHz, $CDCl_3$): 167.01, 148.40, 145.13, 145.08, 144.94, 144.78, 141.27, 133.38, 133.15, 132.35, 132.29, 129.09, 129.05, 128.86, 128.12, 126.99, 127.96, 126.88, 125.55.

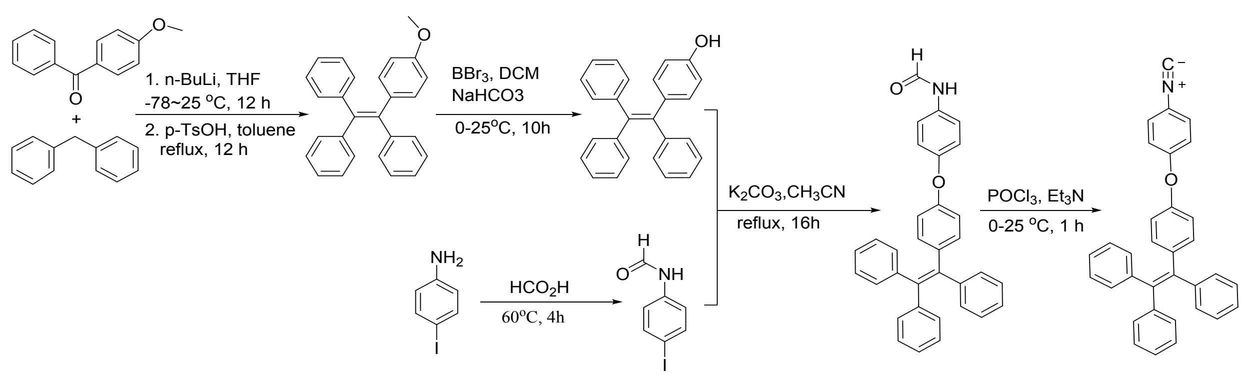

Scheme S4. Synthesis of 4-Isocyano-4-(1,1,2-Triphenylvinyl)-1-Phenyl-1-Anisol(**ITPPA**)

Synthesis of 4-methoxytetraphenylethene: Under nitrogen atmosphere, compounddiphenylmethane(8.60 g, 51.0 mmol) was dissolved in 50 mL of dry THF, after the solution was cooled to -78°C, n-BuLi (22.30 mL, 2.5 M in hexane) was added drop wise and the resulting mixture was stirred at -10°C for 2 h, then compound (4-methoxyphenyl)(phenyl)methanone (9.0 g, 42.4 mmol) in 15 mL THF was added drop wise and the mixture was allowed to warmed to room temperature and stirred for 10 h. Then the reaction mixture was quenched with an aqueous solution of ammonium chloride, extracted with CH_2Cl_2 (3 × 100 mL), the combined organic layers were dried over anhydrous Na_2SO_4 and evaporated to remove the solvent. The residue was dissolved in toluene (100 mL), p-toluene sulfonic acid (1.06 g, 6.2 mmol) as catalyst was added, the resulting mixture was refluxed for 10 h. after the reaction mixture was cooled to room temperature, the solvent was removed under reduced pressure, the residue was recrystallized from methanol to afford the desired compound 4-methoxytetraphenyletheneas a white solid (14.8 g, 86% yield). ^{1}H NMR (400 MHz, $CDCl_3$): 7.21–7.01 (m, 15H, Ar–*H*), 6.97 (d, *J* = 8.4 Hz, 2H, Ar–*H*), 6.67 (d, *J* = 8.6 Hz, 2H, Ar–*H*), 3.77 (s, 3H, CH_3).

Synthesis of 4-hydroxytetraphenylethene: Two-necked flask containing compound 4-methoxytetraphenylethene (8.25 g, 22.7 mmol) and dried DCM (120 mL) was cooled to -20^{o}C, and BBr_3 (17.10 g, 68.2 mmol) was slowly added. The mixture was warmed to room temperature and allows standing for 8 h, and then poured into saturated aqueous solution of $NaHCO_3$. The organic phase was dried over Na_2SO_4, and the crude product was recrystallized from petroleum ether to obtained white solid (7.65 g, 97% yield).^{1}H NMR (400 MHz, $CDCl_3$): 7.01−7.13 (m, 15H, Ar–*H*). 6.90 (d, *J* = 8.0 Hz, 2H, Ar–*H*). 6.56 (d, *J* = 8.0 Hz, 2H, Ar–*H*),4.60 (s, 1H, O–*H*). ^{13}C NMR (100 MHz, $CDCl_3$): 154.08, 144.12, 144.01, 140.54, 140.34, 136.54, 132.87, 131.49, 131.46, 127.84,127.74, 126.52, 126.4, 114.72.

Synthesis of N-(4-iodophenyl) formamide: The synthetic procedure was the same with that of compound (2-(4-formamidophenyl) ethene-1, 1, 2-triyl) tribenzene, and the crude product was directly used for the next step without further purification (11.5g, 92% yield).

Synthesis of N-(4'-(1,2,2-triphenylvinyl)-[1-phenyl-1-anisol]-4-yl) formamide: Compound N-(4-iodophenyl) formamide (4.40 g, 17.8 mmol), 4-hydroxytetraphenylethene (5.64 g, 16.2 mmol) and K_2CO_3 (3.26 g, 24.3 mmol) in 100 mL CH_3CN were reflux overnight (16 h). After the reaction completed, water was added and the resulting mixture was extracted with ethyl acetate. The organic layer was collected, washed with water and brine, dried over anhydrous $MgSO_4$ and evaporated. The crude product was washed with Petroleum ether to obtain a yellow solid (8.5 g, 84.7% yield) and directly used for next the step without further purification.

Synthesis of 4-isocyano-4'-(1,2,2-triphenylvinyl)-1-phenyl-1-anisol (ITPPA): The synthetic procedure was the same with that of compound 4-Isocyano-4-(1, 1, 2-Triphenylvinyl)-1-Phenyl (ITPP). (Weight solid, 83% yield). ^{1}H NMR (400 MHz, $CDCl_3$): 7.03−7.15 (m, 17H), 7.32 (d, *J*= 8.0 Hz, 2H), 7.40 (d, *J*= 8.4 Hz, 2H), 7.56 (dt, *J*= 1.6, 8.4 Hz, 2H); ^{13}C NMR (100 MHz, $CDCl_3$): 125.50, 126.36, 126.69, 126.73, 126.76, 126.83, 127.81, 127.84, 127.90, 127.95, 131.43, 131.46, 131.50, 132.15, 137.06, 140.28, 141.75, 141.99, 143.64, 143.69, 144.02, 164.69.

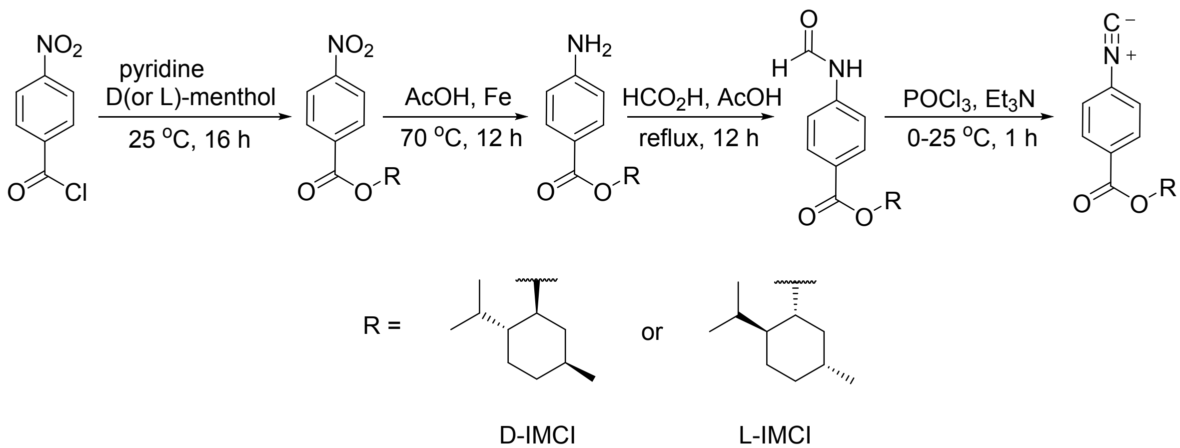

Scheme S5. Synthesis of (*1S,2R,5S*)-2-Isopropyl-5-Metheylcyclohexyl-4-Isocyanobezoate (**D-IMCI**) and (*1R,2S,5R*)-2-Isopropyl-5-Metheylcyclohexyl-4-Isocyanobezoate (**L-IMCI**)

Synthesis of (*1S,2R,5S*)-2-isopropyl-5-metheylcyclohexyl-4-nitrobezoate: Under nitrogen atmosphere, compound 4-nitrobenzoyl chloride (1.80 g, 9.7 mmol) was dissolved in dry pyridine (20 mL), then D-menthol (1.50 g, 9.7 mmol) was added in one portion and the resulting mixture was stirred at room temperature for 16 h, after removal of pyridine under reduced pressure, the residue was dissolved indichloromethane(30 mL) and washed with 1N HCl, saturated $NaHCO_3$ aqueous solution and brine, the separated organic layer was dried over anhydrous Na_2SO_4 and concentrated under reduced pressure, the residue was purified by column chromatography (silica gel, 10:1 hexane to ethyl acetate, v/v) to afford the desired compound (*1S*,*2R*,*5S*)-2-isopropyl-5-metheylcyclohexyl-4-nitrobezoate as a yellow solid (2.40 g, 81% yield) ^{1}H NMR (400 MHz, $CDCl_3$): 0.79 (d, *J* = 7.2 Hz, 3H), 0.93 (t, *J* = 6.4 Hz, 6H), 0.88-0.98 (m, 1H), 1.08−1.17 (m, 2H), 1.54−1.62 (m, 2H), 1.74 (d, *J* = 12.4 Hz, 2H), 1.88−1.95 (m, 1H), 2.12 (d, *J* = 11.6 Hz, 1H), 4.97 (dt, *J* = 4.4, 11.2 Hz, 1H), 8.20 (d, *J* = 8.8 Hz, 2H), 8.28 (d, *J* = 8.4 Hz, 2H).

Synthesis of (*1S,2R,5S*)-2-isopropyl-5-metheylcyclohexyl-4-aminobezoate: Under nitrogen atmosphere, compound (*1S*,*2R*,*5S*)-2-isopropyl-5-metheylcyclohexyl-4-nitrobezoate (2.40 g, 7.9 mmol) was dissolved in 30 mL of acetic acid, then iron powder (4.4 g, 78.6 mmol) was added in one portion, the resulting mixture was stirred at 70°C overnight. Then the mixture was filtered and the filter cake was washed with ethyl acetate (20 mL), the filtrate was concentrated under reduced pressure, the residue was purified by column chromatography (silica gel, 4:1 hexane to ethyl acetate, v/v) to afford the desired compound (*1S*,*2R*,*5S*)-2-isopropyl-5-metheylcyclohexyl-4-aminobezoate as yellow solid (1.55 g, 72% yield) ^{1}H NMR (400 MHz, $CDCl_3$): 0.78 (d, *J* = 7.2 Hz, 3H), 0.90 (d, *J* = 6.8 Hz, 3H), 0.91 (d, *J* = 6.4 Hz, 3H), 0.85−0.96 (m, 1H), 1.02−1.14 (m, 2H), 1.48−1.54 (m, 2H), 1.69−1.72 (m, 2H), 1.94−1.98 (m, 1H), 2.09−2.12 (m, 1H), 4.04 (s, 2H), 4.87 (dt, *J* = 4.4, 10.8 Hz, 1H), 6.63 (d, *J* = 8.4 Hz, 2H), 7.85 (d, *J* = 8.8 Hz, 2H).

Synthesis of (*1S,2R,5S*)-2-isopropyl-5-metheylcyclohexyl 4-formamidobezoate: Compound (*1S*,*2R*,*5S*)-2-isopropyl-5-metheylcyclohexyl-4-aminobezoate (1.55 g, 5.6 mmol) was dissolved in a mixture of formic acid (16 mL) and acetic acid (3 mL), the resulting mixture was refluxed overnight. After the reaction mixture was cooled to room temperature, the solvents were removed under reduced pressure, the residue was washed with saturated aqueous Na_2CO_3 (10 mL) and filtered, the filter cake was washed twice with water and dried in vacuum to afford crude compound (*1S,2R,5S*)-2-isopropyl-5-metheylcyclohexyl 4-formamidobezoateas a white solid (1.70 g, crude), this compound was used directly for the next step without purification.

Synthesis of (*1S,2R,5S*)-2-isopropyl-5-metheylcyclohexyl 4-isocyanobezoate: Compound (*1S,2R,5S*)-2-isopropyl-5-metheylcyclohexyl 4-formamidobezoate (1.70g, crude) and triethylamine (5.2 mL, 37.5 mmol) were dissolved in dry THF (15 mL) under an atmosphere of nitrogen, after the mixture was cooled to 0^oC, $POCl_3$ (0.90 mL, 9.5 mmol) was added drop wise to the mixture, the resulting mixture was slowly warmed to room temperature and stirred for 1.5 h, then the reaction mixture was slowly poured into 20 mL saturated aqueous Na_2CO_3 and stirred at room temperature for 1 h, the mixture was extracted with DCM (3 × 20 mL), the combined organic layers were washed with brine, dried over anhydrous Na_2SO_4 and concentrated under reduced pressure, the residue was purified by column chromatography (neutral Al_2O_3,10:1 hexane to ethyl acetate, v/v) to afford the desired compound (*1S,2R,5S*)-2-isopropyl-5-metheylcyclohexyl 4-isocyanobezoateas a black syrup (1.35g, 81% yield for two steps) ^{1}H NMR (400 MHz, $CDCl_3$): 0.77 (d, *J*= 6.8 Hz, 3H), 0.91 (dd, *J*= 5.6, 6.8 Hz, 6H), 0.86−0.96 (m, 1H), 1.05−1.17 (m, 2H), 1.50−1.59 (m,2H), 1.70−1.74 (m, 2H), 1.86−1.94 (m, 1H), 2.07−2.12 (m, 1H), 4.93 (dt, *J*= 4.4, 10.8 Hz, 1H), 7.43 (d, *J*= 8.4 Hz, 2H), 8.07 (dt, *J*= 2.0, 8.8 Hz, 2H); ^{13}C NMR (100 MHz, $CDCl_3$): 16.60, 20.82, 22.10, 23.71, 26.66, 31.53, 34.32, 40.98, 47.30, 75.75, 126.48, 129.88, 130.90, 131.74, 164.58, 167.05.

Synthesis of (*1R,2S,5R*)-2-isopropyl-5-metheylcyclohexyl 4-nitrobezoate: was the same with that of (*1S,2R,5S*)-2-isopropyl-5-methylcyclohexyl 4-isocyanobenzoate.

Synthesis of (*1R,2S,5R*)-2-isopropyl-5-metheylcyclohexyl 4-aminobezoate: (yellow solid, 83% yield). ^{1}H NMR (400 MHz, $CDCl_3$): 0.79 (d, *J*= 6.8 Hz, 3H), 0.93 (t, *J*= 6.2 Hz, 6H), 0.88−0.98 (m, 1H), 1.08−1.19 (m, 2H), 1.54−1.61 (m, 2H), 1.71−1.78 (m, 2H), 1.85−1.97 (m, 1H), 2.13 (d, *J*= 12.0 Hz, 1H), 4.97 (dt, *J*= 4.4, 10.8 Hz, 1H), 8.20 (d, *J*= 9.2 Hz, 2H), 8.28 (d, *J*= 8.8 Hz, 2H).

Synthesis of (*1R,2S,5R*)-2-isopropyl-5-metheylcyclohexyl 4-formamidobezoate: (yellow oil, 72% yield). ^{1}H NMR (400 MHz, *d6*-DMSO): 0.73 (d, *J* = 6.8 Hz, 3H), 0.87 (t, *J* = 7.4 Hz, 6H), 0.82−0.92 (m, 1H), 0.97−1.09 (m, 2H), 1.43−1.49 (m, 2H), 1.62−1.66 (m, 2H), 1.82−1.89 (m, 1H), 1.92−1.95 (m, 1H), 4.72 (dt, *J* = 4.4, 10.8 Hz, 1H), 5.92 (s, 2H), 6.56 (d, *J* = 8.8 Hz, 2H), 7.62 (d, *J* = 8.8 Hz, 2H).

Synthesis of (*1R,2S,5R*)-2-isopropyl-5-metheylcyclohexyl 4-isocyanobezoate: (black syrup, 80% yield). ^{1}H NMR (400 MHz, $CDCl_3$): 0.78 (d, *J* = 6.8 Hz, 3H), 0.92 (t, *J* = 6.4 Hz, 6H), 0.87−0.90 (m, 1H), 1.04−1.18 (m, 2H), 1.51−1.60 (m, 2H), 1.70−1.76 (m, 2H), 1.86−1.94 (m, 1H), 2.08−2.13 (m, 1H), 4.93 (dt, *J* = 4.4, 11.2 Hz, 1H), 7.43 (d, *J* = 8.4 Hz, 2H), 8.07 (dt, *J* = 2.0, 8.8 Hz,2H); ^{13}C NMR (100 MHz, $CDCl_3$): 16.63, 20.86, 22.13, 23.74, 26.69, 31.57, 34.35, 41.01, 47.35, 75.81, 126.52, 129.92, 130.94, 131.78, 164.63, 167.03.

A typical procedure for the linear polymerization of 4-ethoxycarbonyl phenyl isocyanide (EPI) with Et_3SiHas end-functionalized agent (Table 1, entry 4). In the glove box, a 50 mL round bottom flask was charged with a solution of $[Ph_3C][B(C_6F_5)_4]$ (9.22 mg, 10.0 μmol) in chlorobenzene (2 mL), then 11.5 mg (10 equiv.) of triethylsilane was added. After stirring for 5 min, a solution of 4-ethoxycarbonyl phenyl isocyanide (875 mg, 5 mmol) in chlorobenzene (3 mL) was added in one portion. The reaction mixture was stirred at 25^{o}C for 1min, then the flask was taken out of the glove box and the reaction mixture was poured into methanol (100 mL) to precipitate the polymer product, the yellow polymer solid was collected by filtration, and dried in vacuum at 40^{o}C to a constant weight (868 mg, 99% yield), The product obtained is soluble thoroughly in $CHCl_3$ at 25^{o}C.

A typical procedure for the three star random and homocopolymerization of (*1S*,*2R*,*5S*)-2-isopropyl-5-methylcyclohexyl-4-isocyanobenzoate (D-IMCI) with 4-isocyano-4'-(1,2,2-triphenylvinyl)-1-phenyl-1-anisol (ITPPA) with 1,3,5-tris(dimethylsilyl)benzene as core-first functional agent (Table 2, entry 5). In the glove box, a 50 mL round bottom flask was charged with a solution of $[Ph_3C][B(C_6F_5)_4]$ (7.5 mg, 8.1 μmol) in chlorobenzene (2 mL). Then 1,3,5-tris(dimethylsilyl)benzene (0.68 mg, 2.7 μmol) was added tothe bottom, after stirring for 5 min, 10.8 μmol (4 equiv.) of 1,3,5-tris(dimethylsilyl)benzene was added and subsequently,a solution of (*1S,2R,5S*)-2-isopropyl-5-methylcyclohexyl 4-isocyanobenzoate (77 mg, 0.3 mmol) and 4-isocyano-4'-(1,2,2-triphenylvinyl)-1-biphenyl-1-anisol (121 mg, 0.3 mmol) in chlorobenzene (3 mL) was added, the reaction mixture was stirred at 25^{o}C for 2 min, then the flask was taken out of the glove box and the reaction mixture was poured into methanol (100 mL) to precipitate the copolymer product, the orange copolymer solid was collected by filtration, and dried in vacuum at 40^{o}C to a constant weight (149 mg, 91% yield). The product obtained is soluble thoroughly in $CHCl_3$ and THF at 25^{o}C.

Calculation for the activity of catalyst

$$A= m_{polymer} / (n_{cat.} \cdot t)$$

A: the activity of (co)polymerization (g of polymer/(mol$_{cat.}$·h)), $m_{polymer}$: the mass of (co)polymer (g), t: the reaction time of (co)polymerization (h), $n_{cat.}$: molar amount of catalyst (mol).

$$n_{cat.}=m_{catalyst}/M_{catalyst}$$

$m_{catalyst}$: the mass of catalysts (g), and $M_{catalysts}$: the relative molecular weight of catalyst.

Calculation of the IMCI contents of the copolymers

The IMCI contents of the copolymers were calculated from the ^{1}H NMR spectra according to the following formula

$$\omega(mol\%)_{IMCI} = \{[23(I_{H3}+I_{H4})]/[19(I_{H1}+I_{H2}+I_{H3}+I_{H4})]\}\times 100$$

In which I_{H1} is the integration of the peak at 7.05 ppm which assigned to the aryl protons of ITPPA units and the *β*-H of the aryl ring of IMCI units. I_{H2} is the integration of the peak at 5.76 ppm which assigned to the *α*-H of the aryl ring of IMCI units. I_{H3} is the integration of the peak at 4.86 ppm ascribed to the proton of the cyclohexyl carbon connected with the oxygen. I_{H4} is the integration of the peaks between 0.3 to 2.5 ppm which assigned to the rest protons of the cyclohexyl group as well as the substituted methyl and the isopropyl.

The IMCI contents of poly(D-IMCI-*co*-ITPA)s and poly(L-IMCI-*co*-ITPA)s were calculated from the ^{1}H NMR spectra according to the following formula:

$$\omega(mol\%)IMCI = \{[5\times I_{H4}-6(I_{H1}+I_{H2}+I_{H3})]/[12(I_{H1}+I_{H2}+I_{H3})]\}\times 100$$

In which I_{H1} is the integration of the peak at 7.05 ppm which assigned to the aryl protons of ITPPA units and the H of the aryl ring of IMCI units. I_{H2} is the integration of the peak at 5.76 ppm which assigned to the H of the aryl ring of IMCI and ITPA units. I_{H3} is the integration of the peak at 4.86 ppm ascribed to the proton of the cyclohexyl carbon connected with the oxygen and the proton of the isopropyl carbon connected with the oxygen. I_{H4} is the integration of the peaks between 0.3 to 2.5 ppm which assigned to the rest protons of the cyclohexyl group as well as the substituted methyl and the isopropyl and the rest protons of the isopropyl.

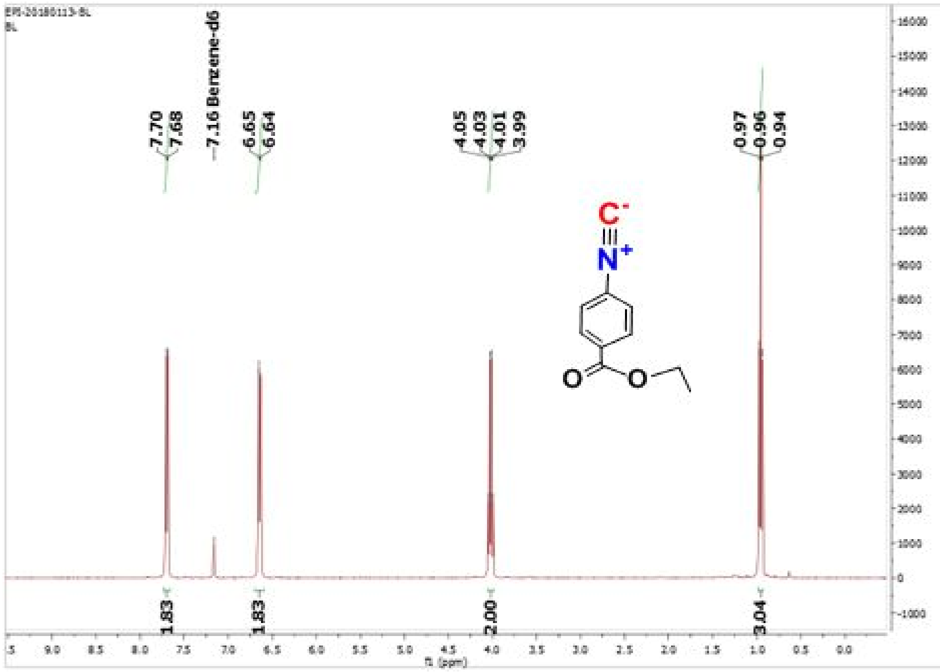

Figure S1. [1]H NMR spectrum of 4-ethoxycarbonyl phenyl isocyanide (**a**).

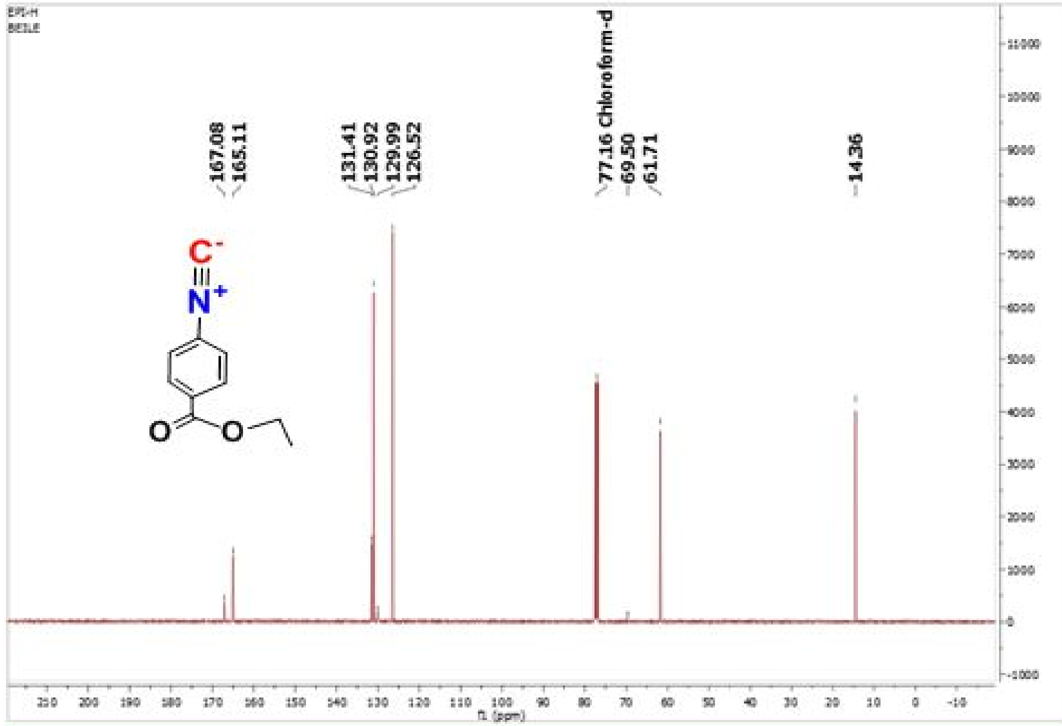

Figure S2. ^{13}C NMR spectrum of 4-ethoxycarbonyl phenyl isocyanide (**a**).

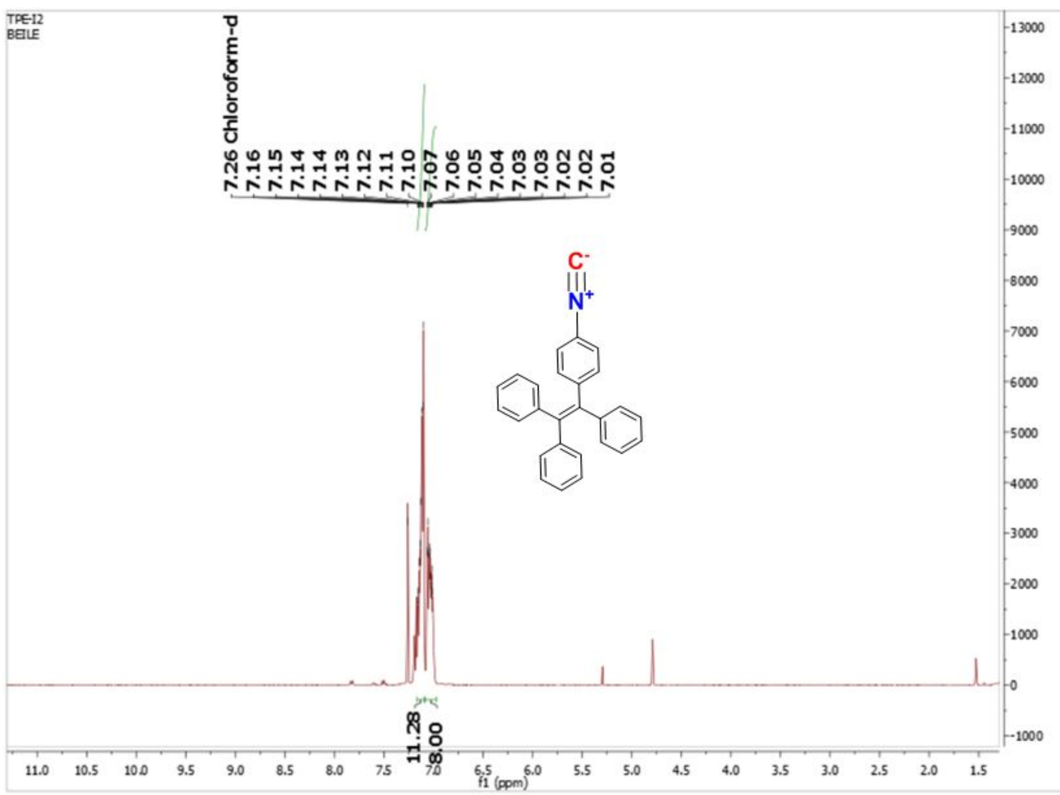

Figure S3. ^{1}H NMR spectrum of 4-isocysno-4-(1,1,2-triphenylvinyl)-1-phenyl (ITPP) (**b**).

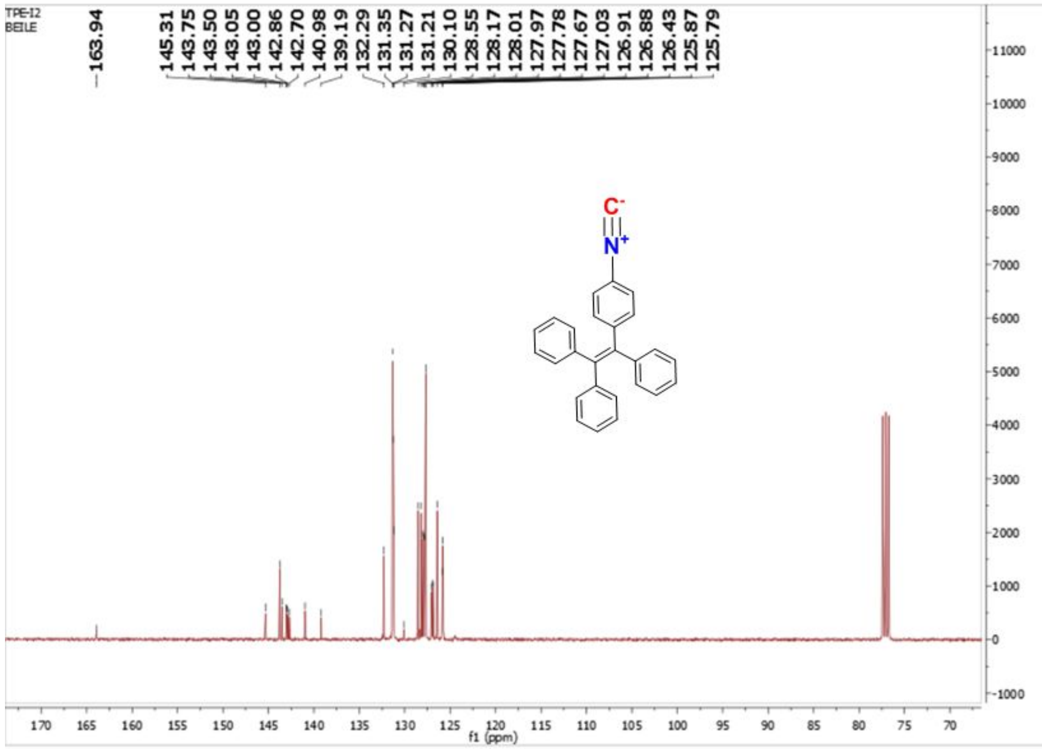

Figure S4. ^{13}C NMR spectrum of 4-isocysno-4-(1,1,2-triphenylvinyl)-1-phenyl (ITPP) (**b**).

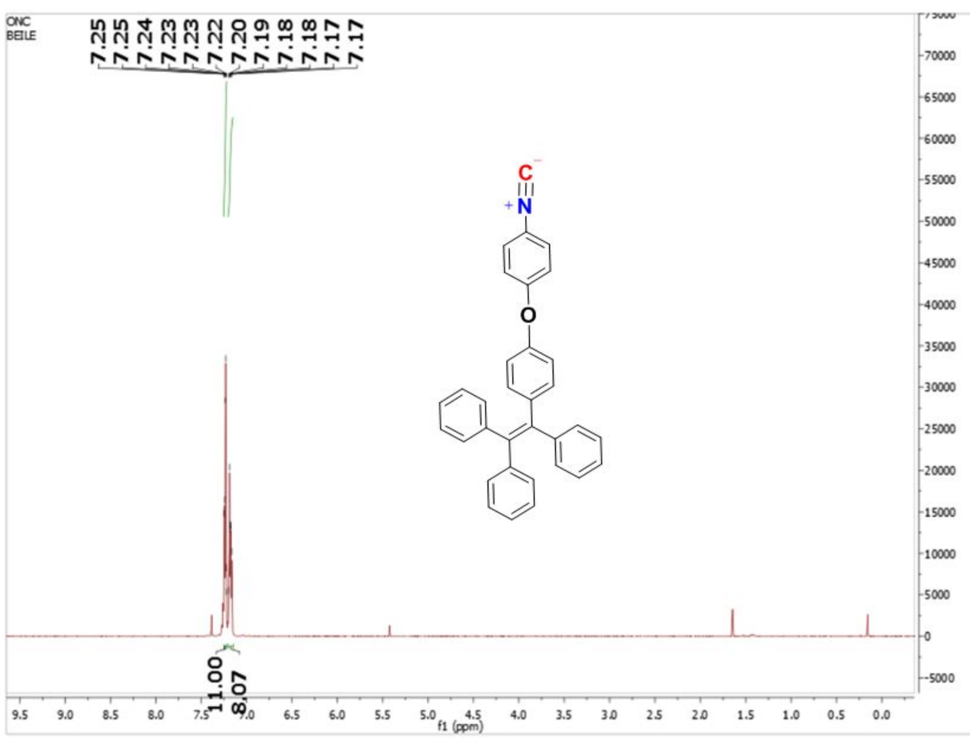

Figure S5. ^{1}H NMR spectrum of 4-isocysno-4-(1,1,2-triphenylvinyl)-1-phenoxy-1-anisol (ITPPA) (**c**).

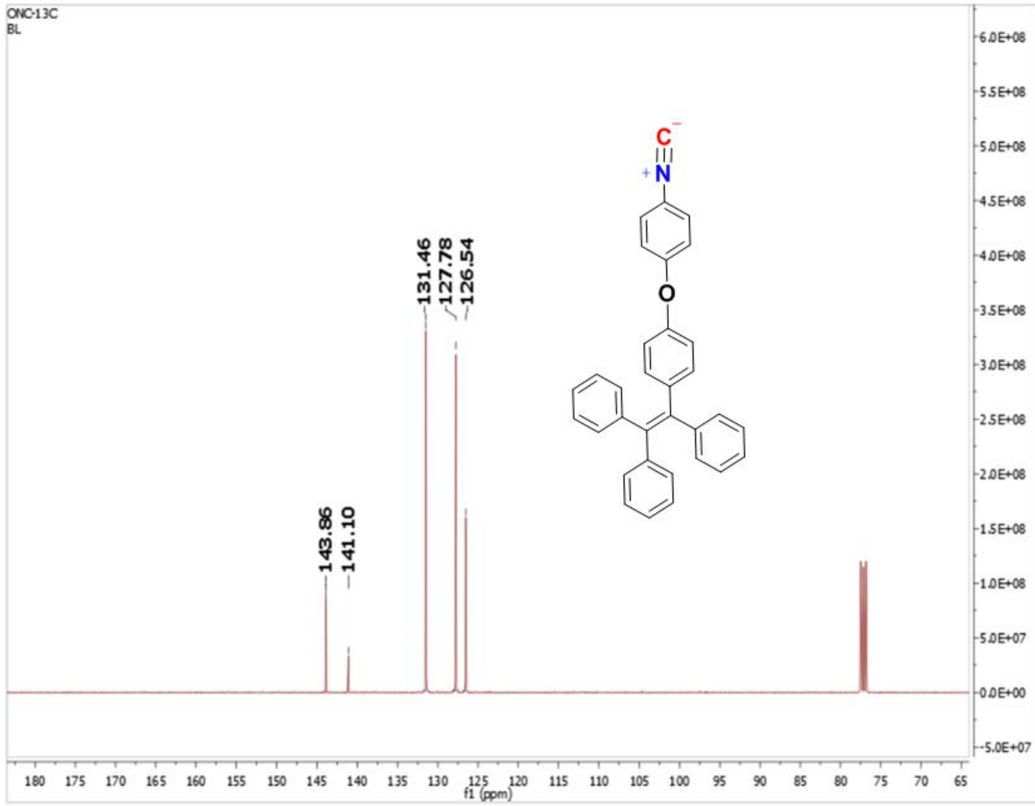

Figure S6. ^{13}C NMR spectrum of 4-isocysno-4-(1,1,2-triphenylvinyl)-1-phenoxy-1-anisol (ITPPA) (**c**).

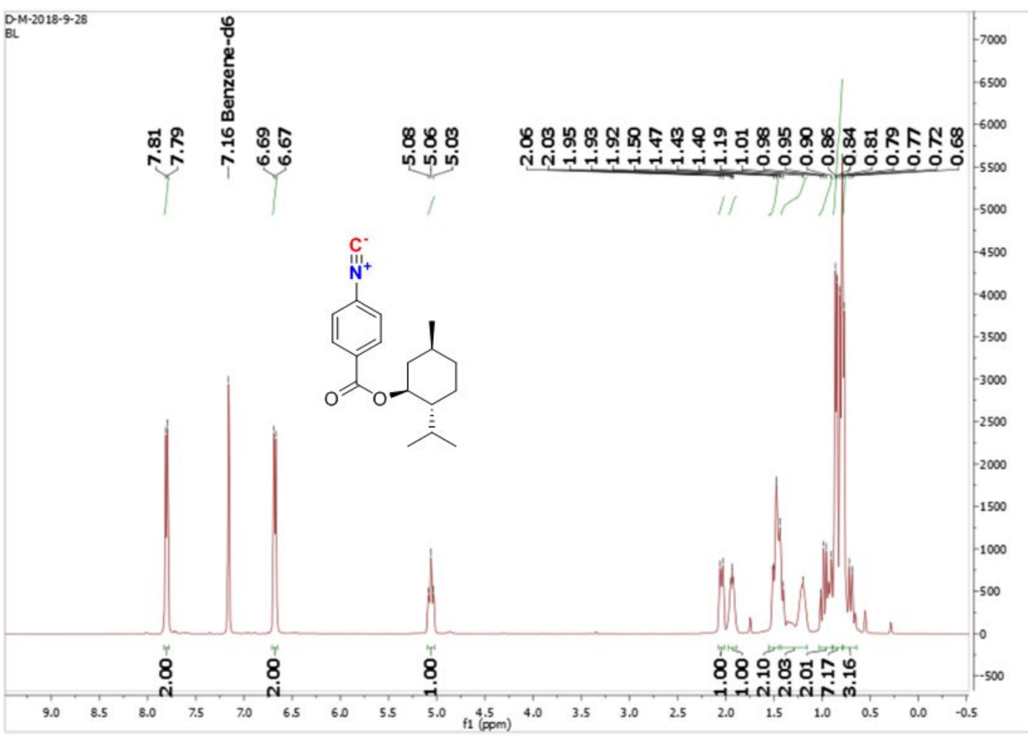

Figure S7. ^{1}H NMR spectrum of (*1S,2R,5S*)-2-isopropyl-5-metheylcyclohexyl-4-isocyanobezoate (**d**).

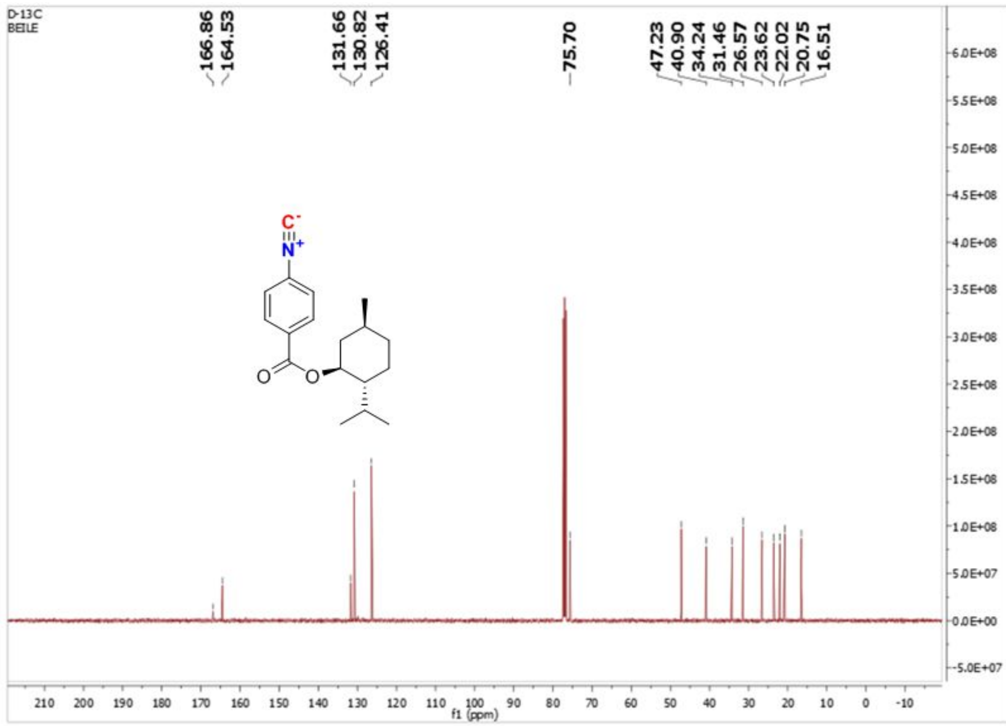

Figure S8. ^{13}C NMR spectrum of (*1S,2R,5S*)-2-isopropyl-5-metheylcyclohexyl-4-isocyanobezoate (**d**).

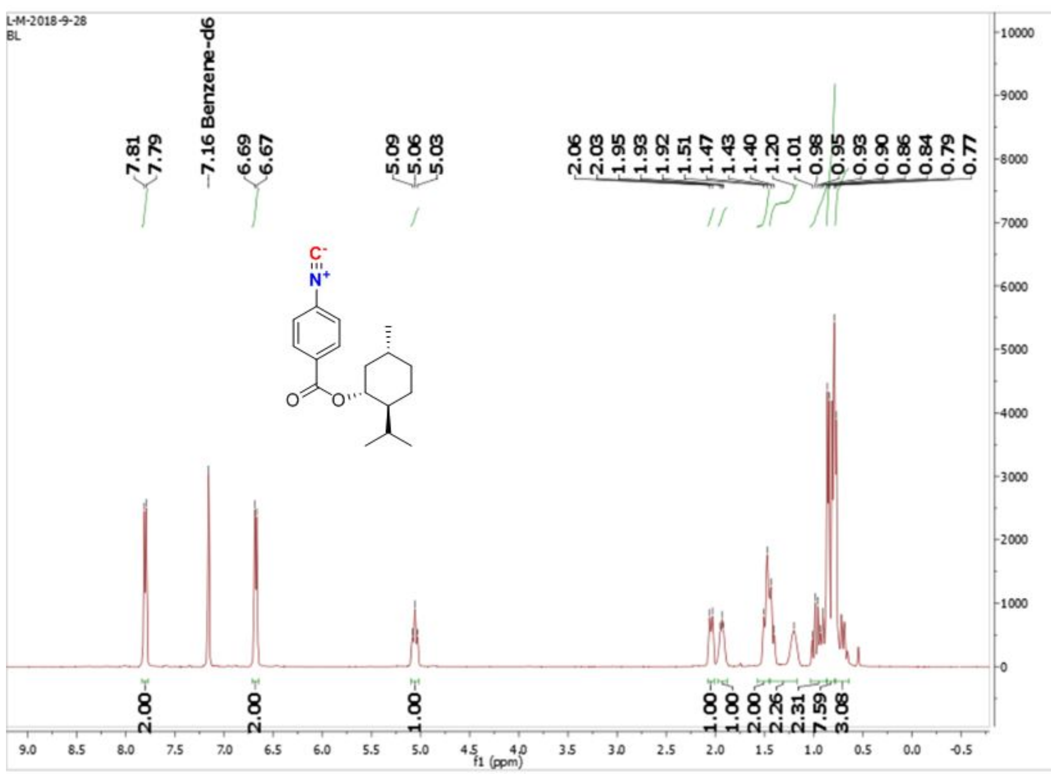

Figure S9. ^{1}H NMR spectrum of (*1R,2S,5R*)-2-isopropyl-5-metheylcyclohexyl-4-isocyanobezoate (**e**).

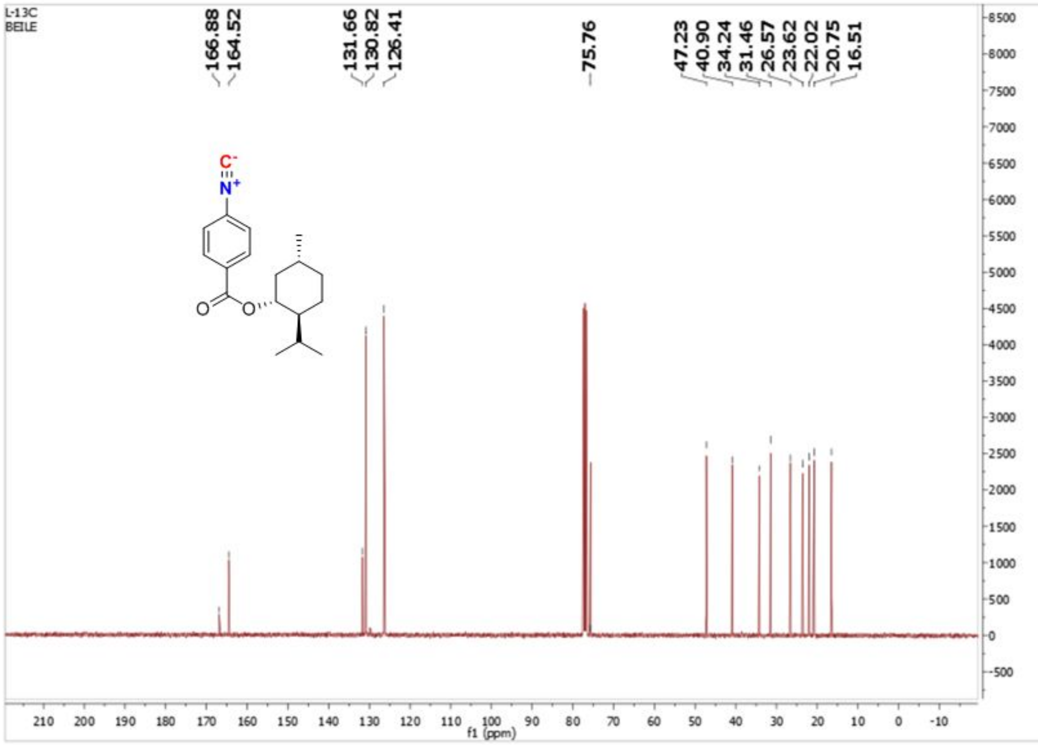

Figure S10. ^{13}C NMR spectrum of (*1R,2S,5R*)-2-isopropyl-5-metheylcyclohexyl-4-isocyanobezoate (**e**).

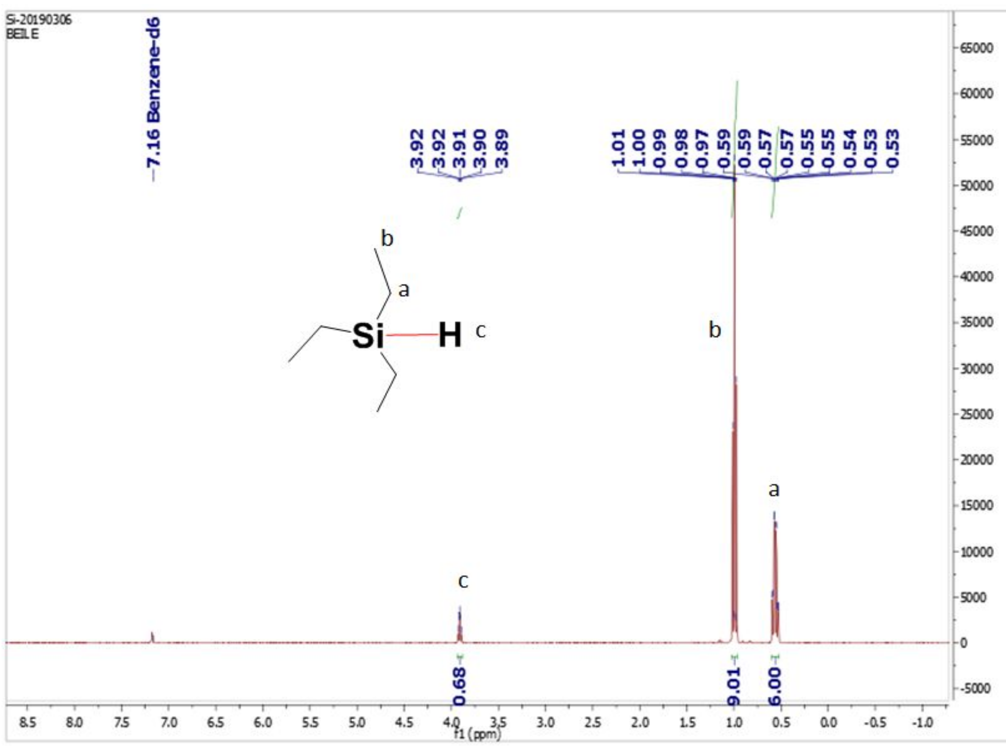

Figure S11. ^{1}H NMR spectra of Et_3SiH.

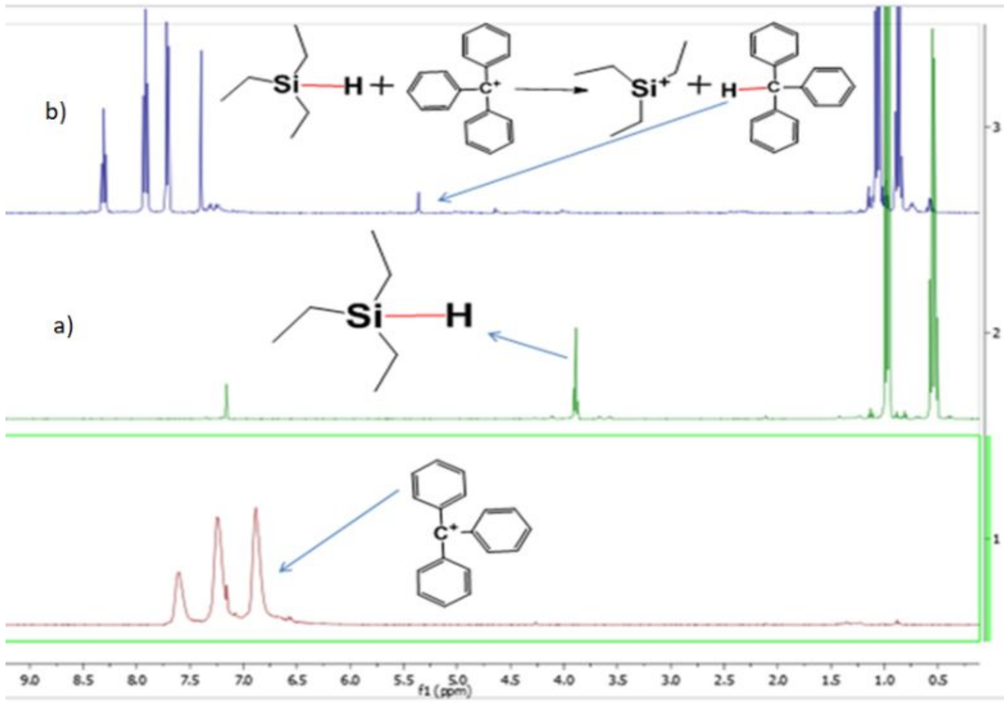

Figure S12. (a) [1]H NMR spectra of Et_3SiH and (b) corresponding cationic species *in situ* generated by reaction of Et_3SiH with catalyst $[Ph_3C][B(C_6F_5)_4]$.

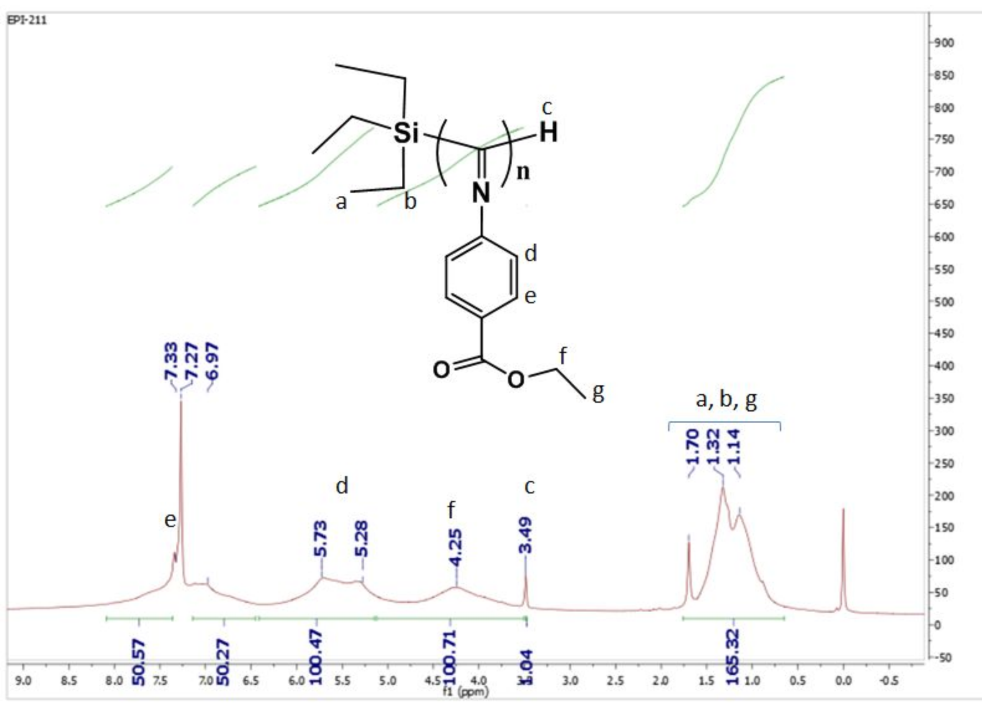

Figure S13. [1]H NMR of poly(EPI) with Et_3SiH as end group (Table 1, entry 4).

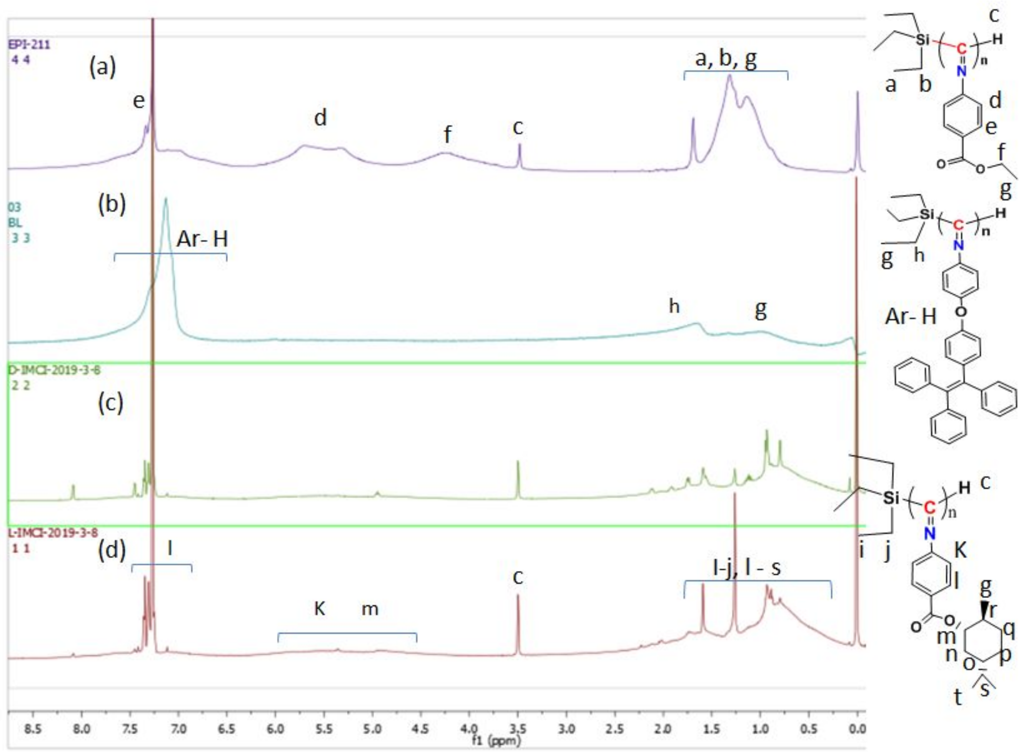

Figure S14. (a) [1]H NMR of poly(EPI) (Table 2, entry 4), (b) Poly(ITPPA) (Table 2, entry 8), (c) Poly(D-IMCI) (Table 2, entry 9) and (d) Poly(L-IMCI) (Table 2, entry 10).

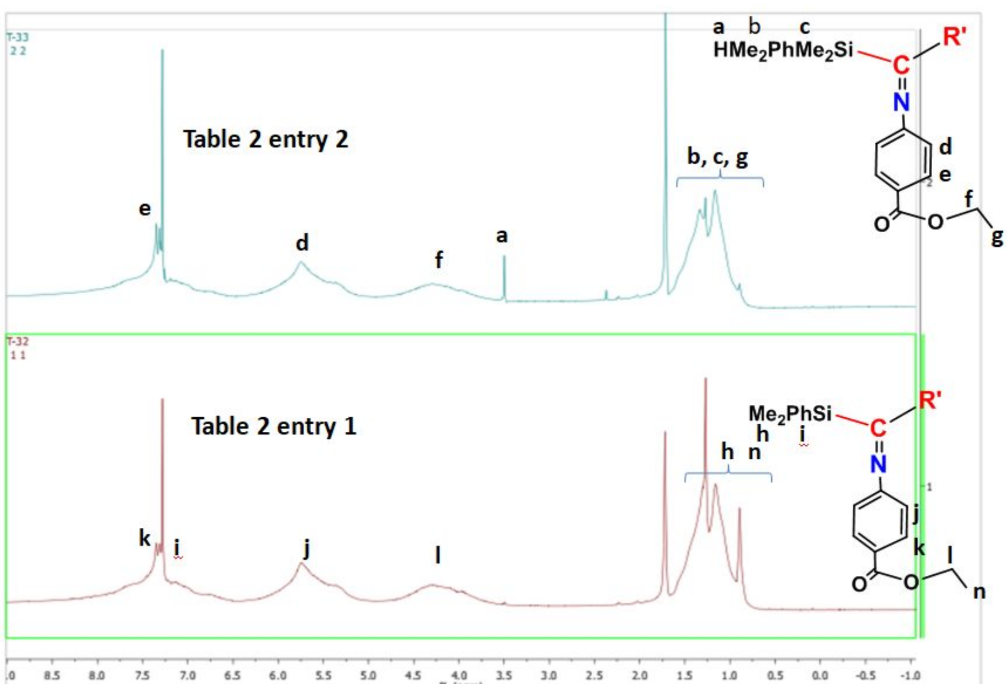

Figure S15. [1]H NMR of poly(EPI) with different silane source as end group (Table 2, entries 1–2).

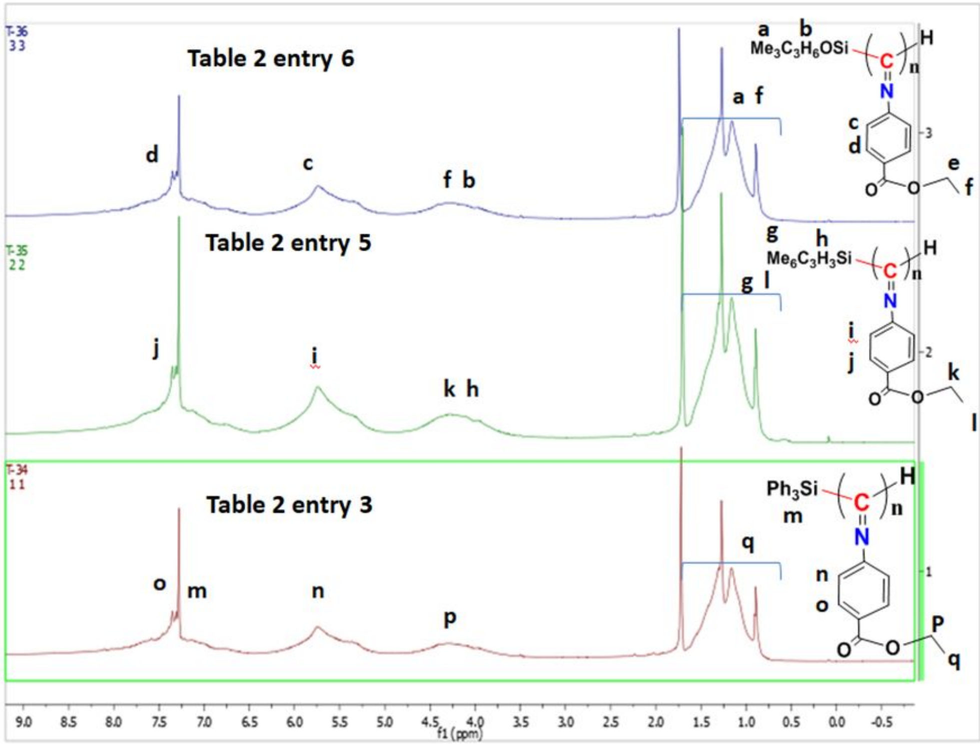

Figure S16. ^{1}H NMR of poly(EPI) with different silane source as end group (Table 2, entries 3,5–6).

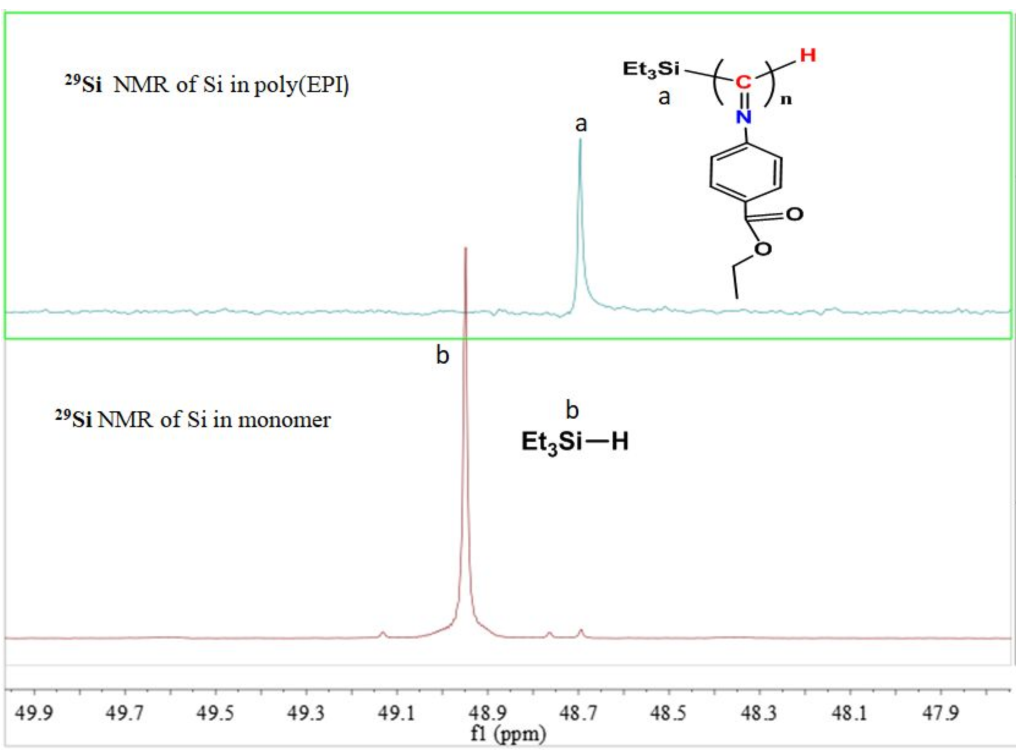

Figure S17. ^{29}SiNMR spectrum of Et_3SiH and Et_3Si-end-functionalized poly(EPI) (Table 2, entry 4).

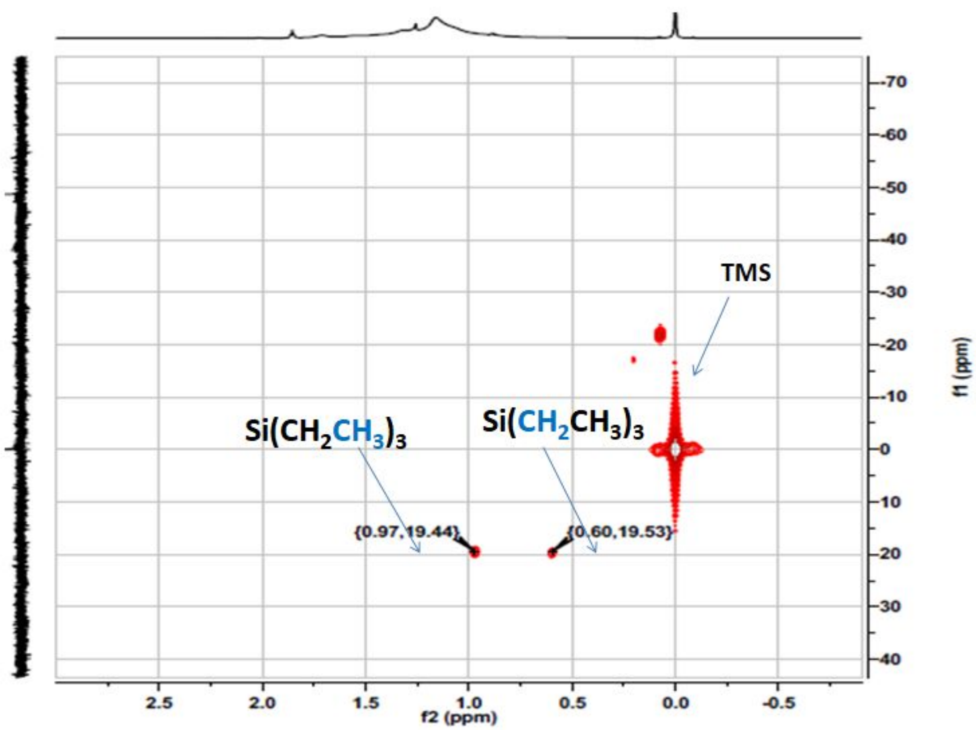

Figure S18. (^{1}H + ^{29}Si) gHMBC NMR spectrum of Et_3Si-end-functionalized poly(EPI) (Table 2, entry 4).

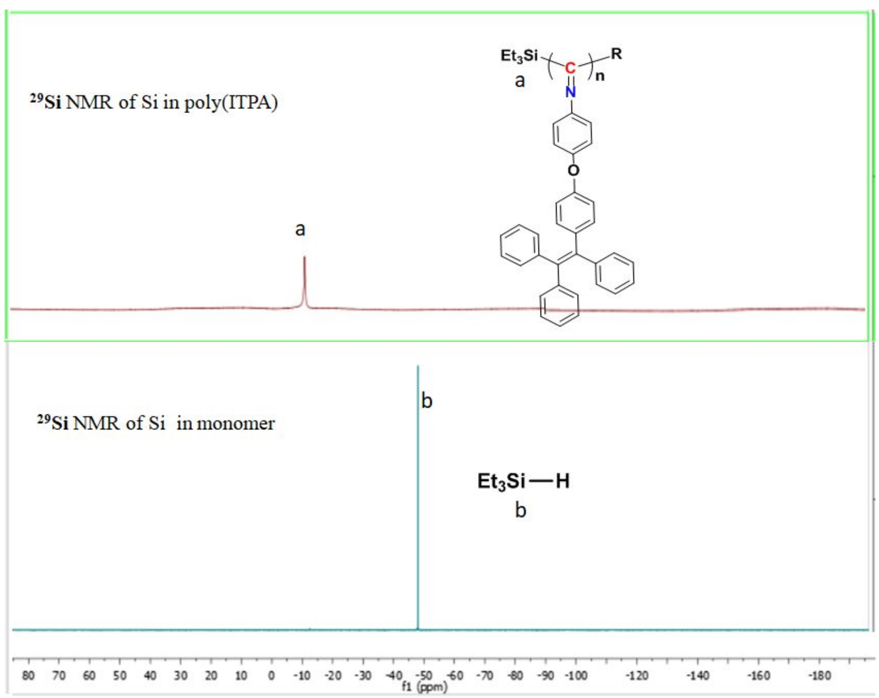

Figure S19. ^{29}Si-NMR spectrum of Et_3SiH and Et_3Si-end-functionalized poly(ITPPA) (Table 2, entry 8).

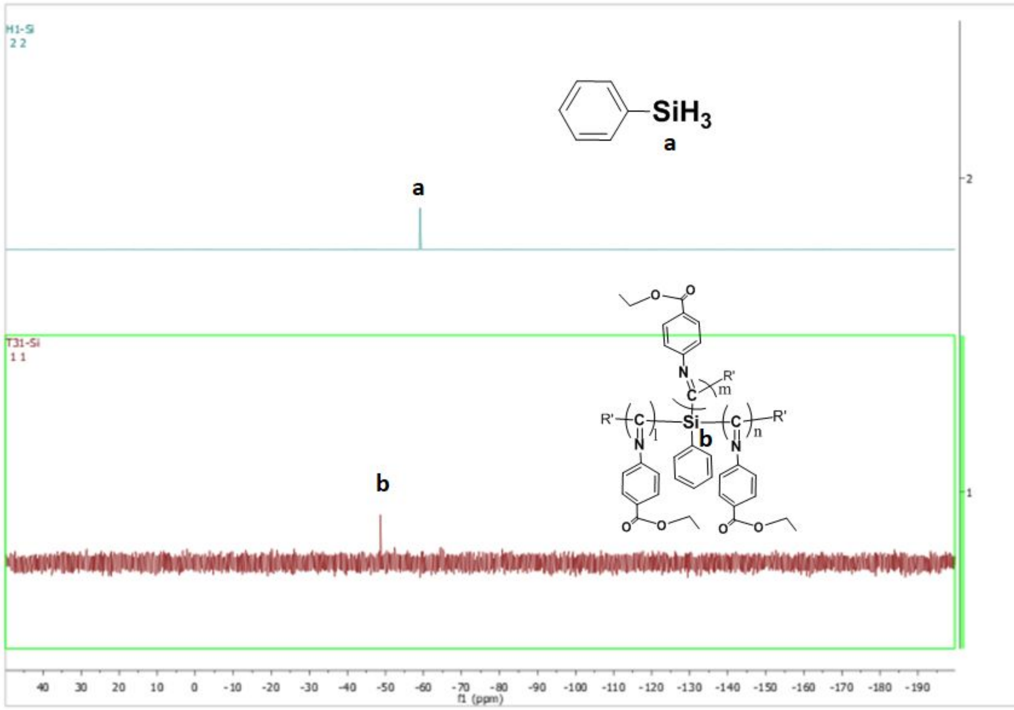

Figure S20. ^{29}Si-NMR spectrum of $PhSiH_3$ and PhSi-end-functionalized star poly(EPI) (Table 3, entry1).

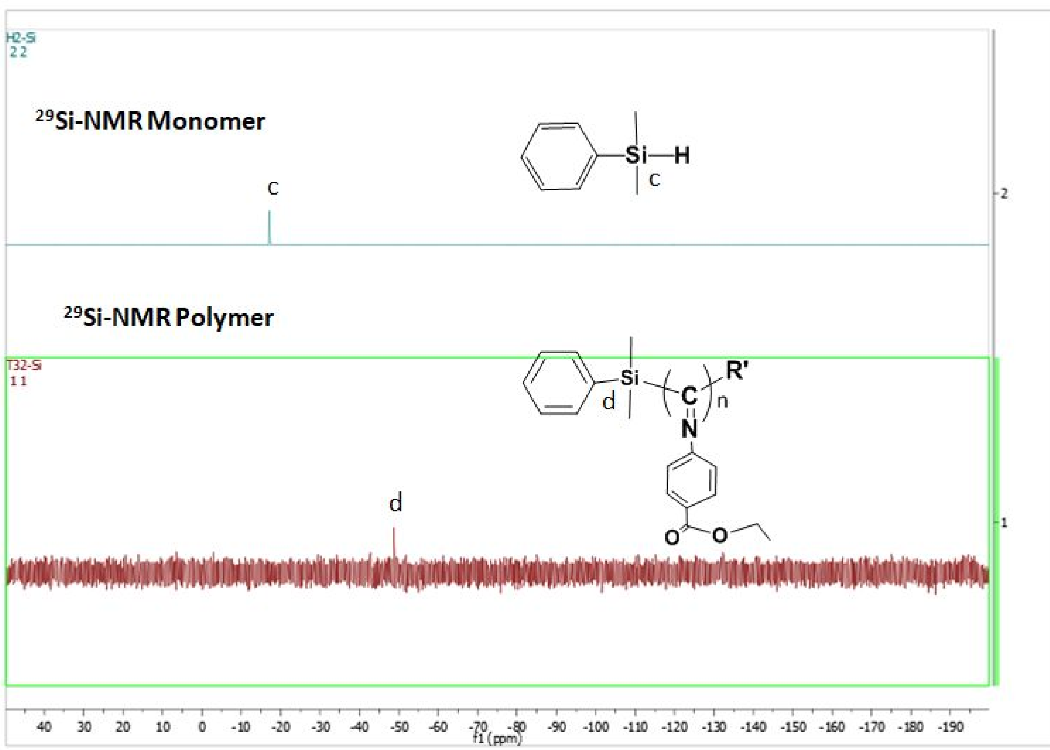

Figure S21. ^{29}Si-NMR spectrum of $PhMe_2Si$-end-functionalized poly(EPI) (Table 2, entry 1).

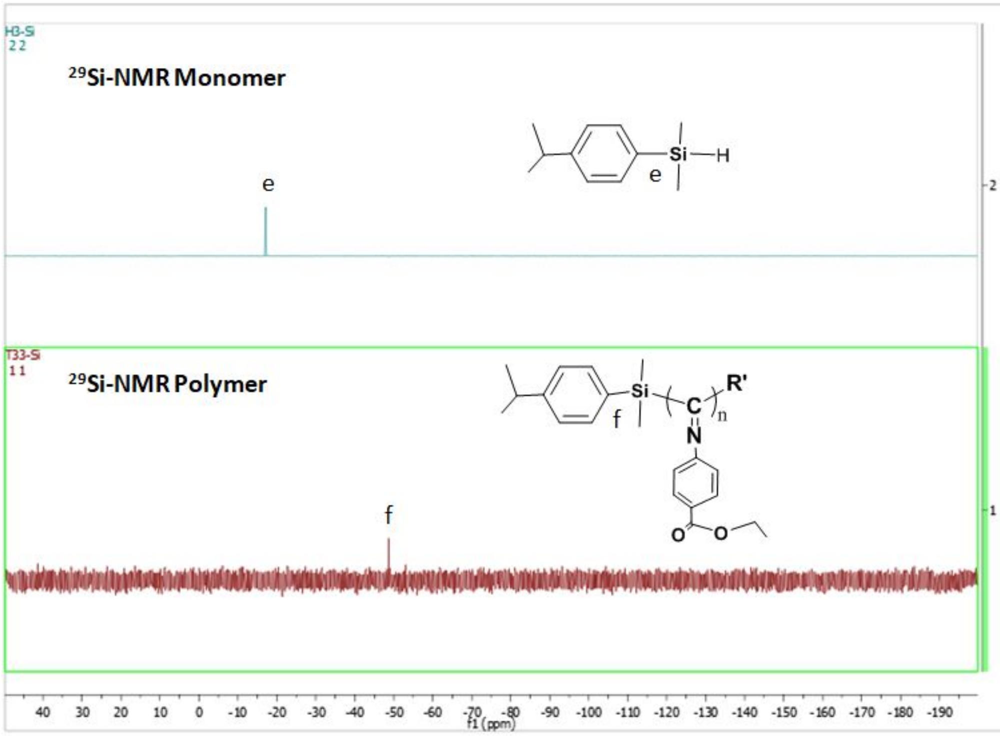

Figure S22. ^{29}Si-NMR spectrum of (4-^{i}PrC$_6$H$_4$)Me$_2$Si-end-functionalized poly(EPI) (Table 2, entry 2).

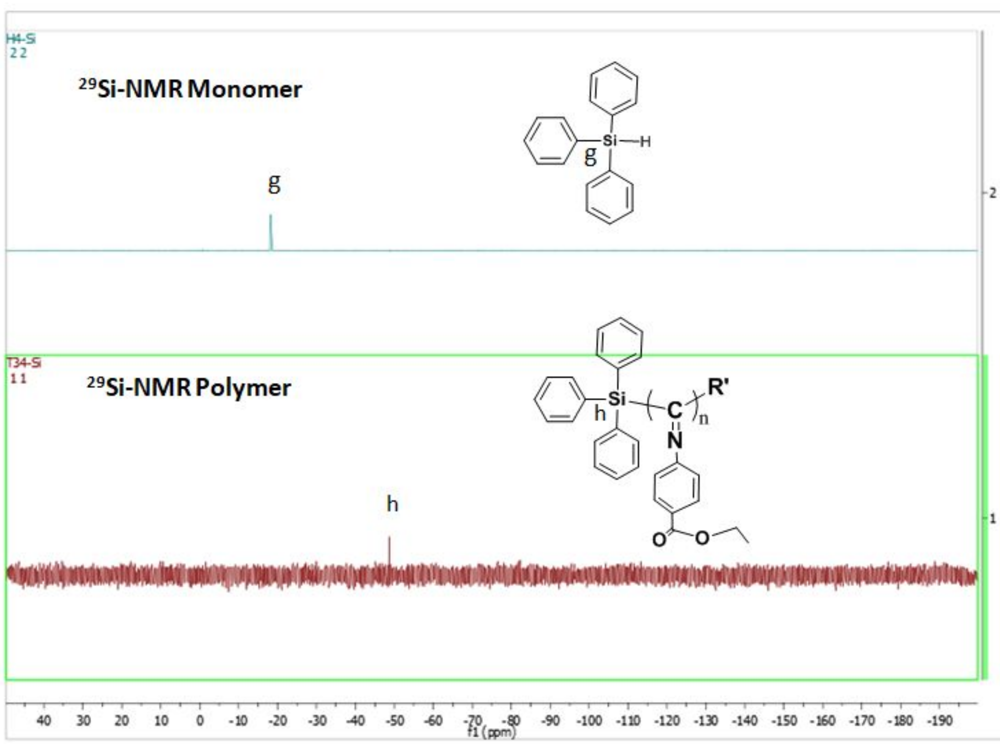

Figure S23. ^{29}Si-NMR spectrum of Ph$_3$Si-end-functionalized poly(EPI) (Table 2, entry 3).

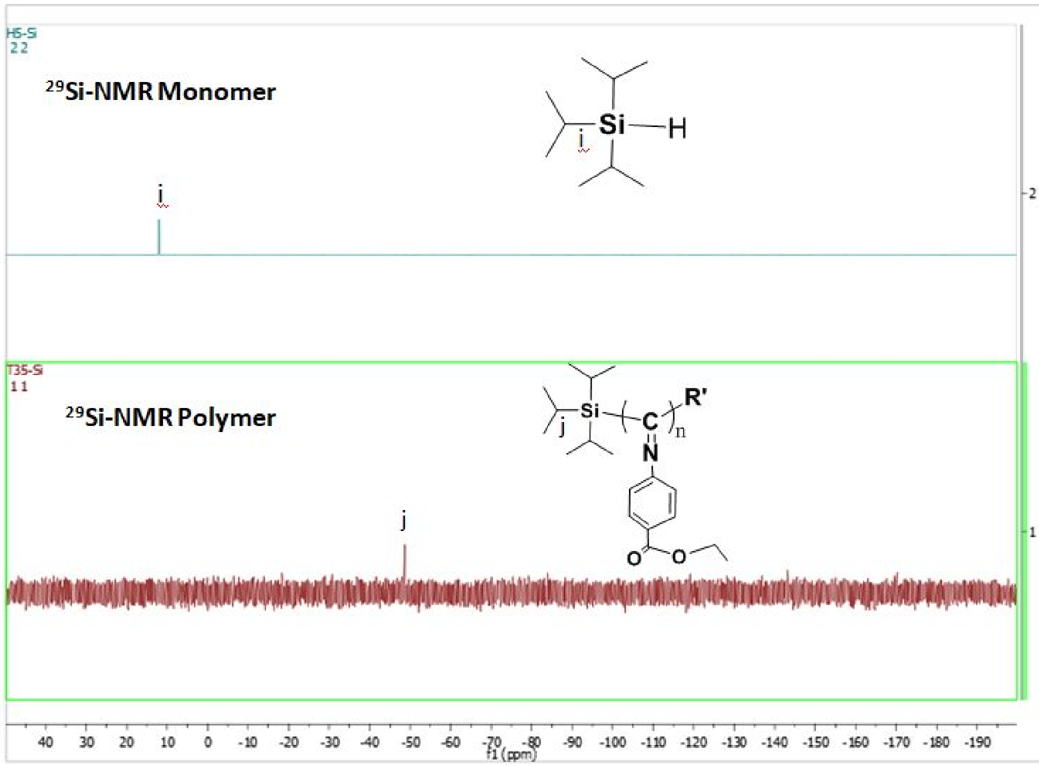

Figure S24. ^{29}Si-NMR spectrum of $^{i}Pr_3$Si-end-functionalized poly(EPI) (Table 2, entry 5).

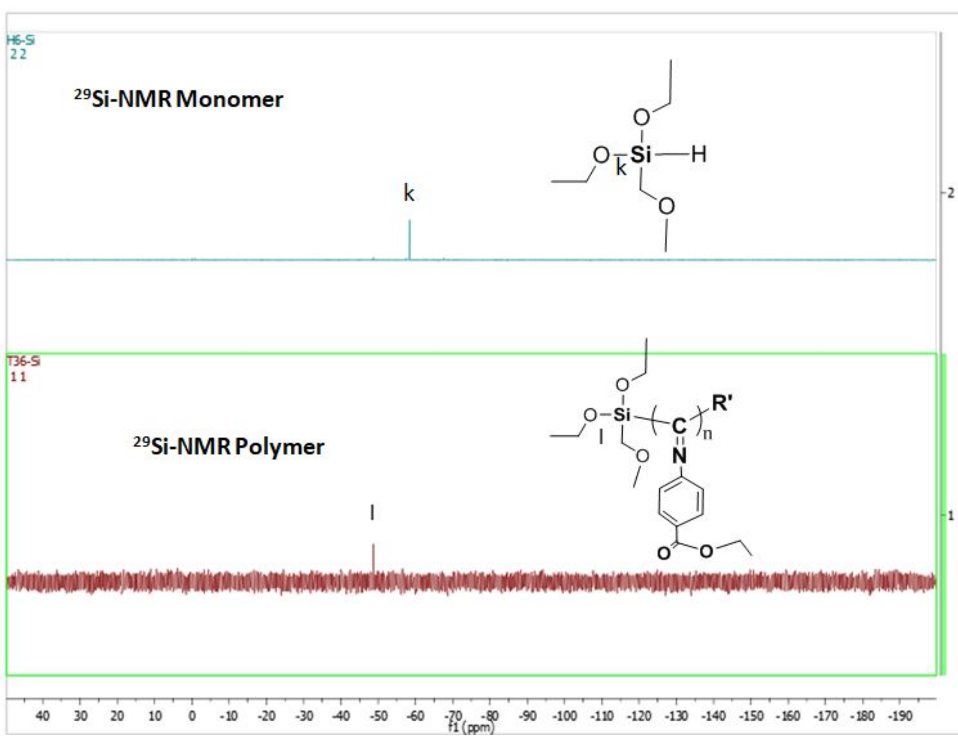

Figure S25. ^{29}Si-NMR spectrum of $(OEt)_3$Si-end-functionalized poly(EPI) (Table 2, entry 6).

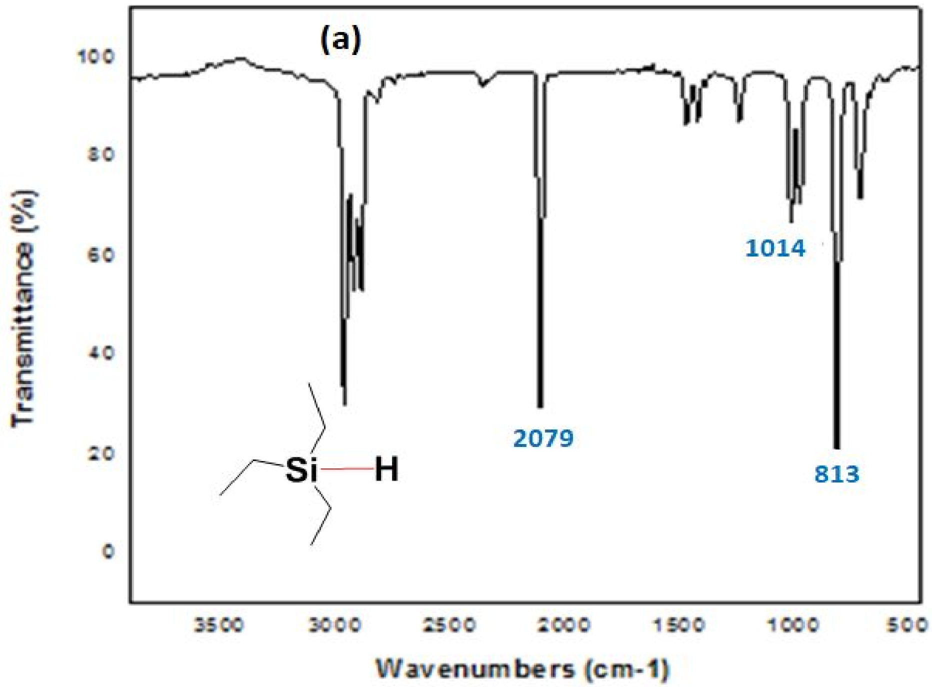

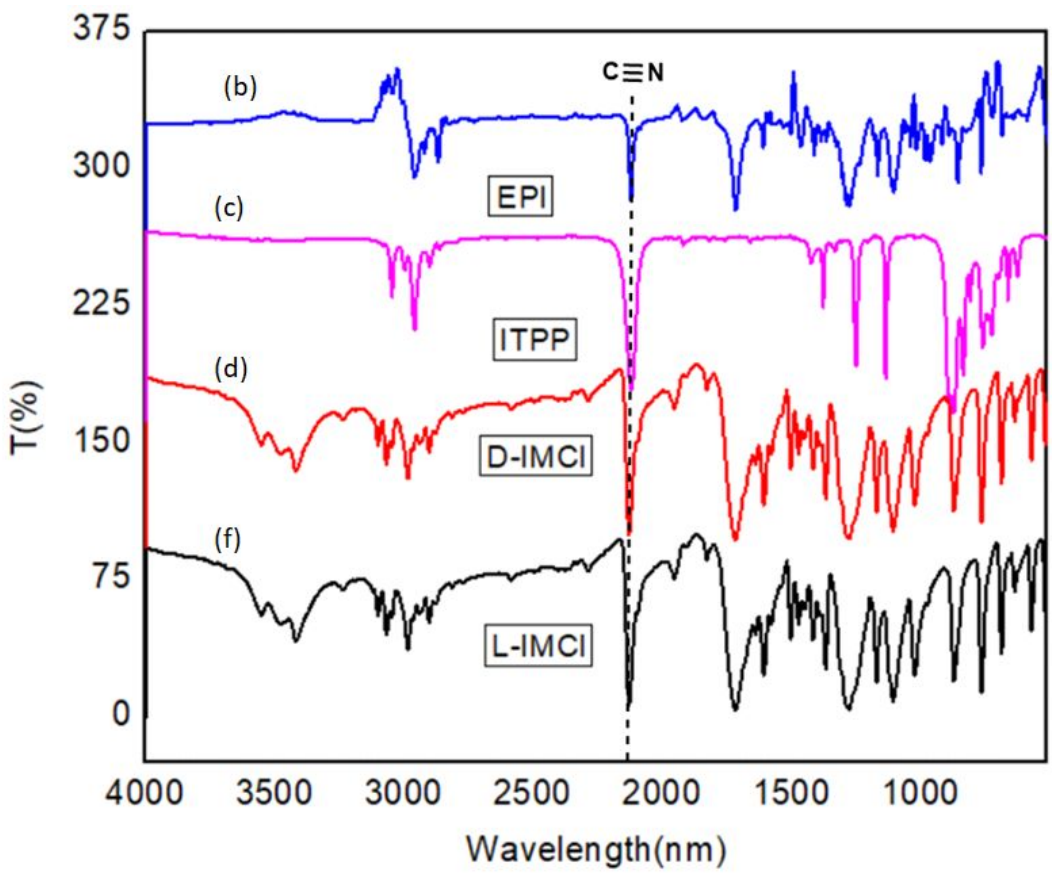

Figure S26. FT-IR spectra of monomers (a) Et_3SiH, (b) EPI, (c) ITPPA, (d) D-IMCI and (e) L-IMCI.

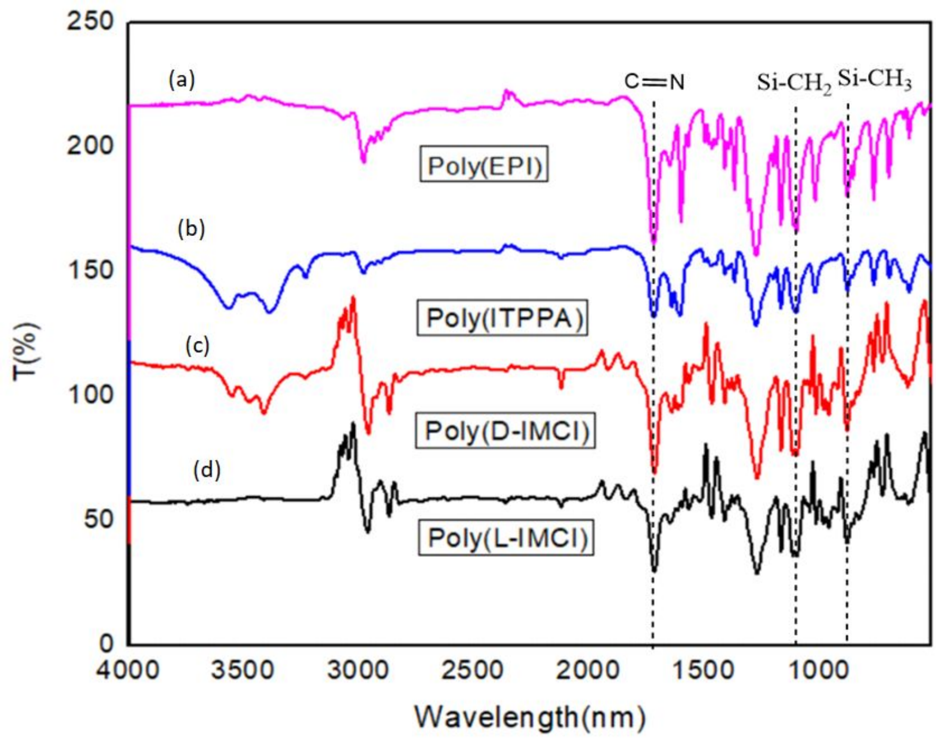

Figure S27. FT-IR spectra of (a) Poly(EPI) (Table 2, entry 4), (b) Poly(ITPPA) (Table 2, entry 8), (c) Poly(D-IMCI) (Table 2, entry 9), (d) Poly(L-IMCI) (Table 2, entry 10).

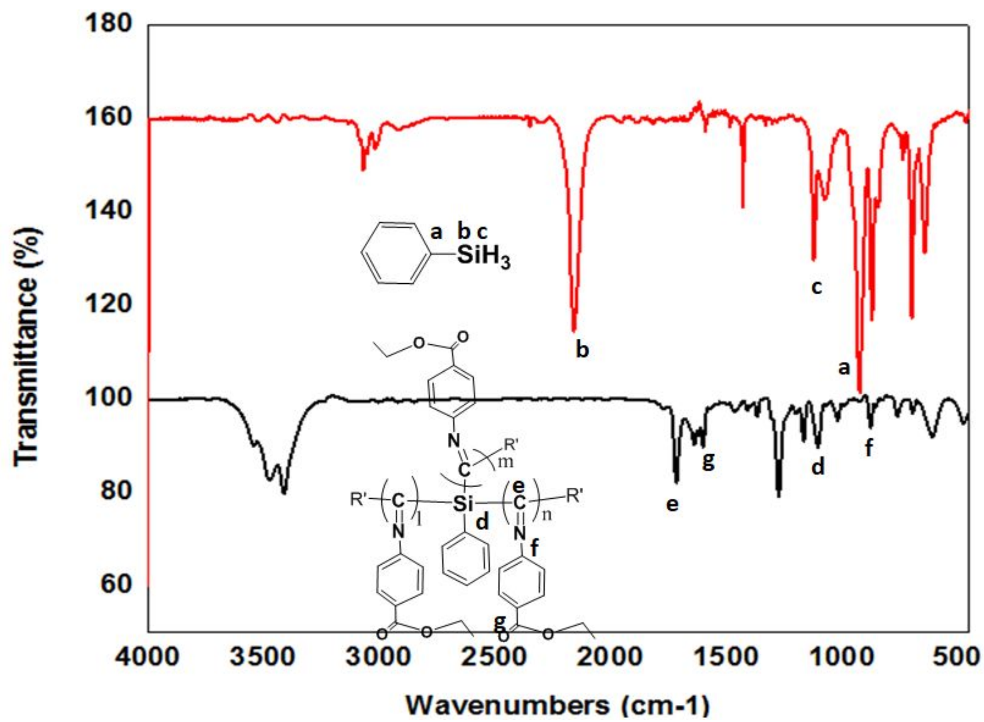

Figure S28. FT-IR spectra of $PhSiH_3$ and PhSi-end-functionalized star poly(EPI) (Table 3, entry1).

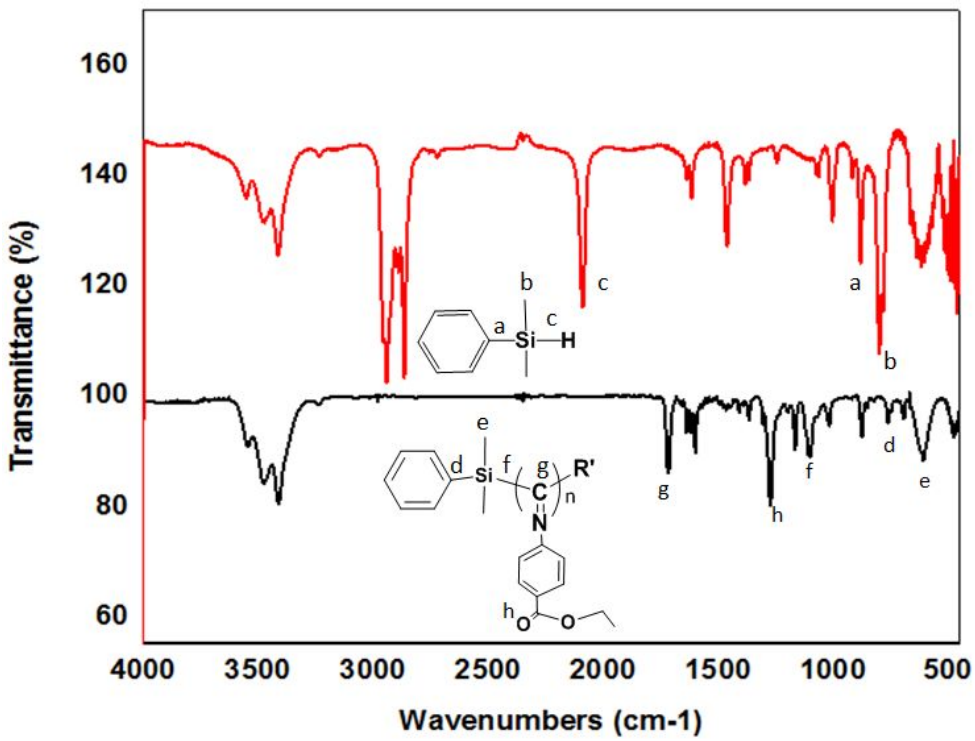

Figure S29. FT-IR spectra of $PhMe_2SiH$ and $PhMe_2Si$-end-functionalized poly(EPI) (Table 2, entry 1).

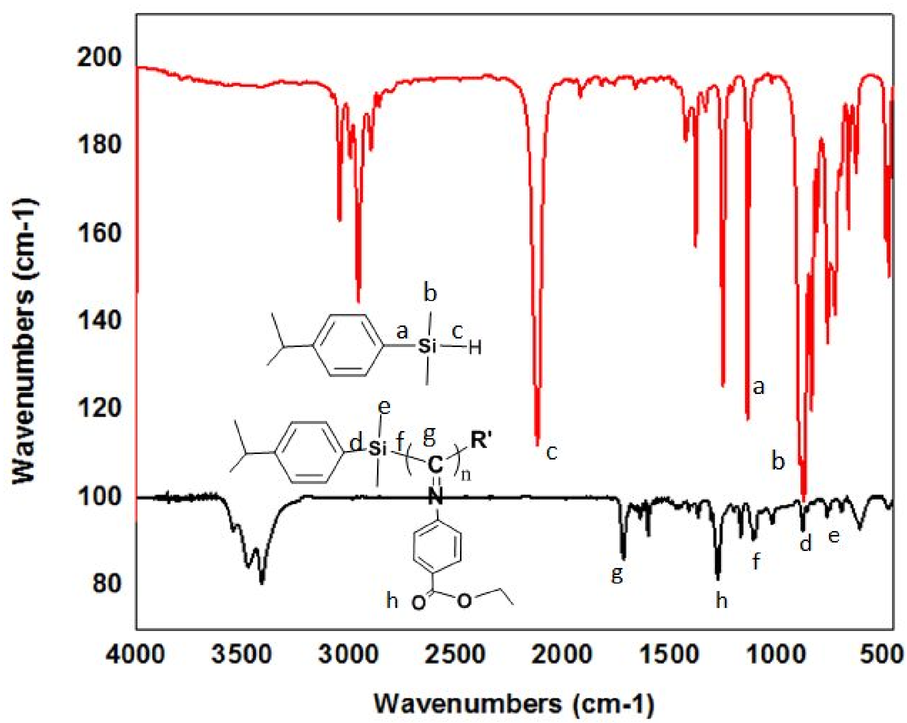

Figure S30. FT-IR spectra of (4-$^{i}PrC_6H_4$)Me_2SiH and (4-$^{i}PrC_6H_4$)Me_2Si-end-functionalized poly(EPI) (Table 2, entry 2).

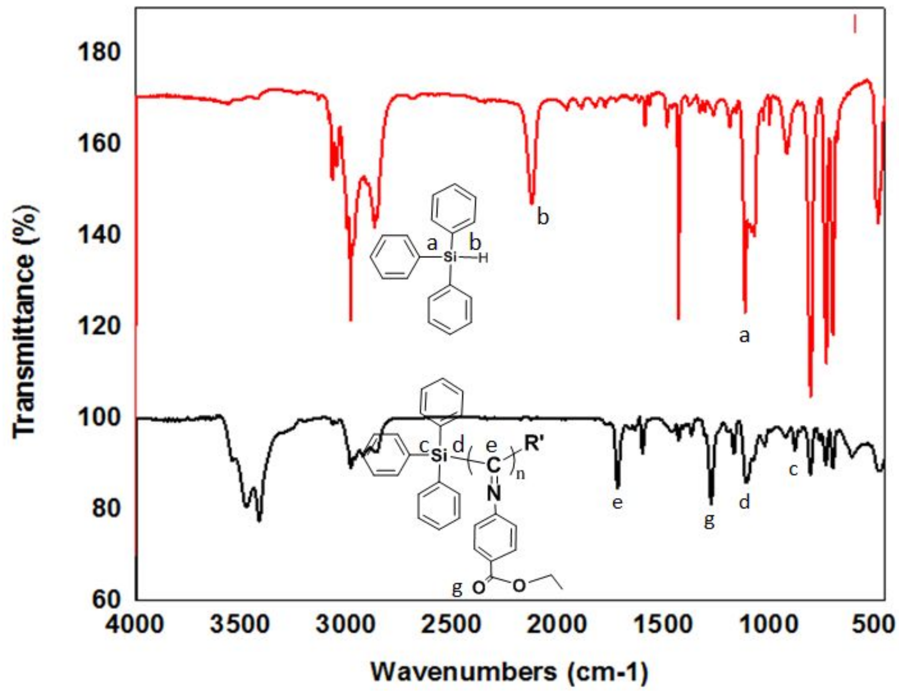

Figure S31. FT-IR spectra of Ph_3SiH and Ph_3Si-end-functionalized poly(EPI) (Table 2, entry 3).

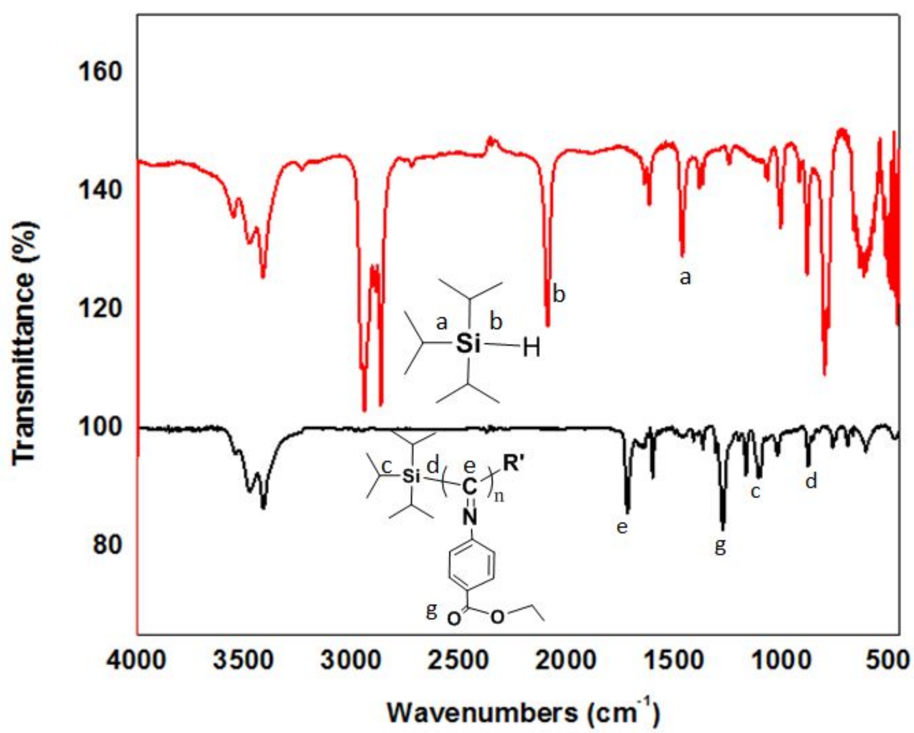

Figure S32. FT-IR spectra of $^{i}Pr_3SiH$ and $^{i}Pr_3Si$-end-functionalized poly(EPI) (Table 2, entry 5).

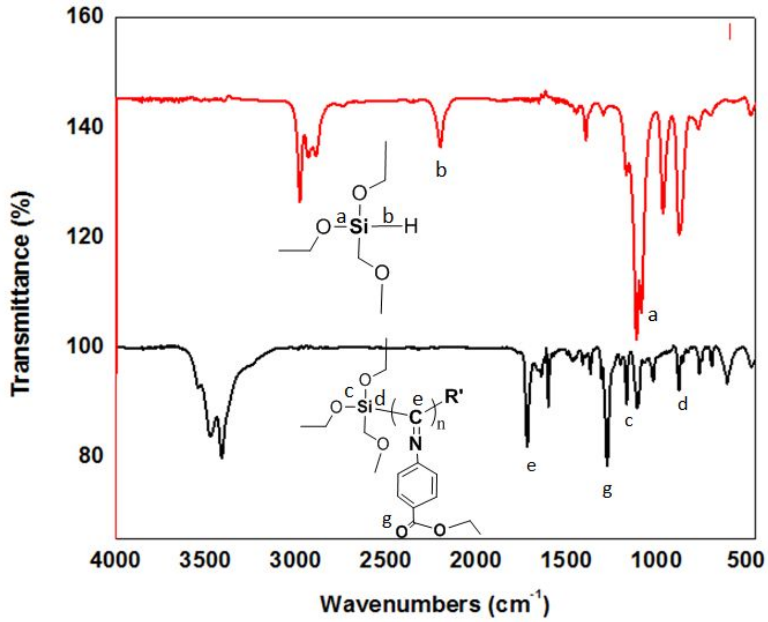

Figure S33. FT-IR spectra of $(OEt)_3SiH$ and $(OEt)_3Si$-end-functionalized poly(EPI) (Table 2, entry 6).

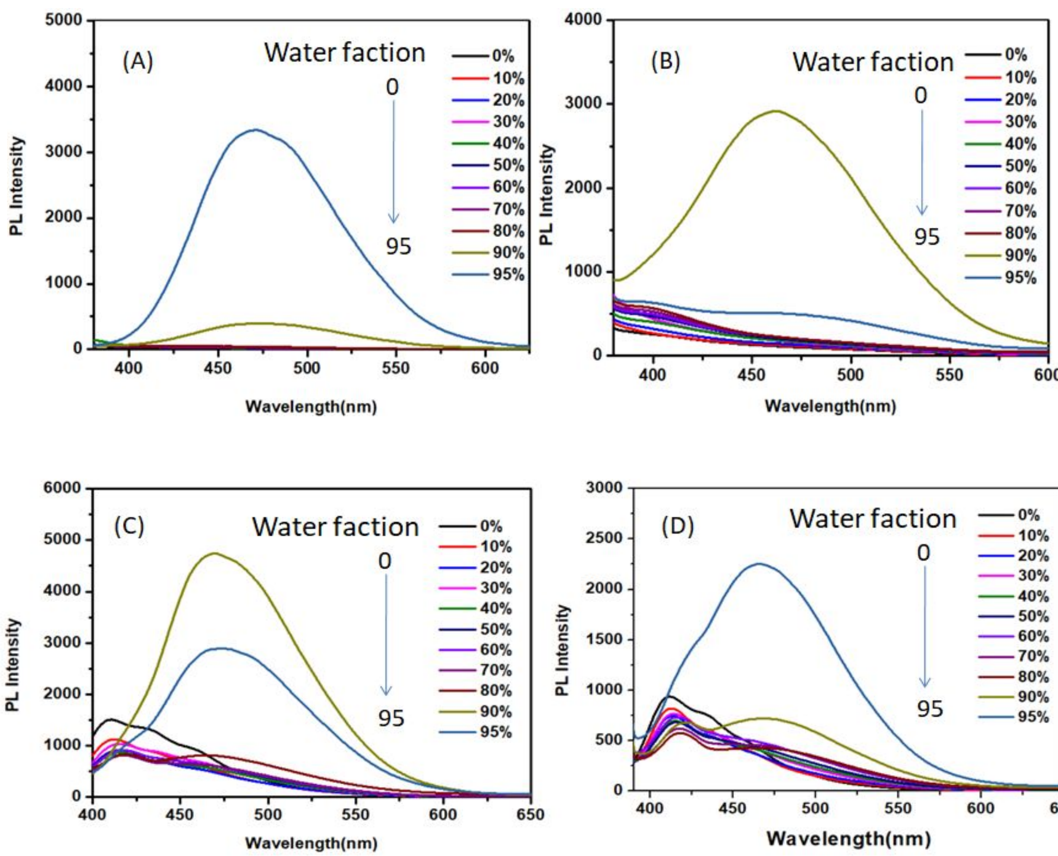

Figure S34. Plots of fluorescence intensity vs water fraction in THF/water mixture (0.01 mg/mL) (A) ITPP,

(B) Poly(ITPP) (Table 2, entry 7), (C) ITPPA, (D) Poly(ITPPA) (Table 3, entry 8) (conditions: EX wavelength: 290 nm, EX slit: 5 nm, EM slit: 5 nm, 700 V).

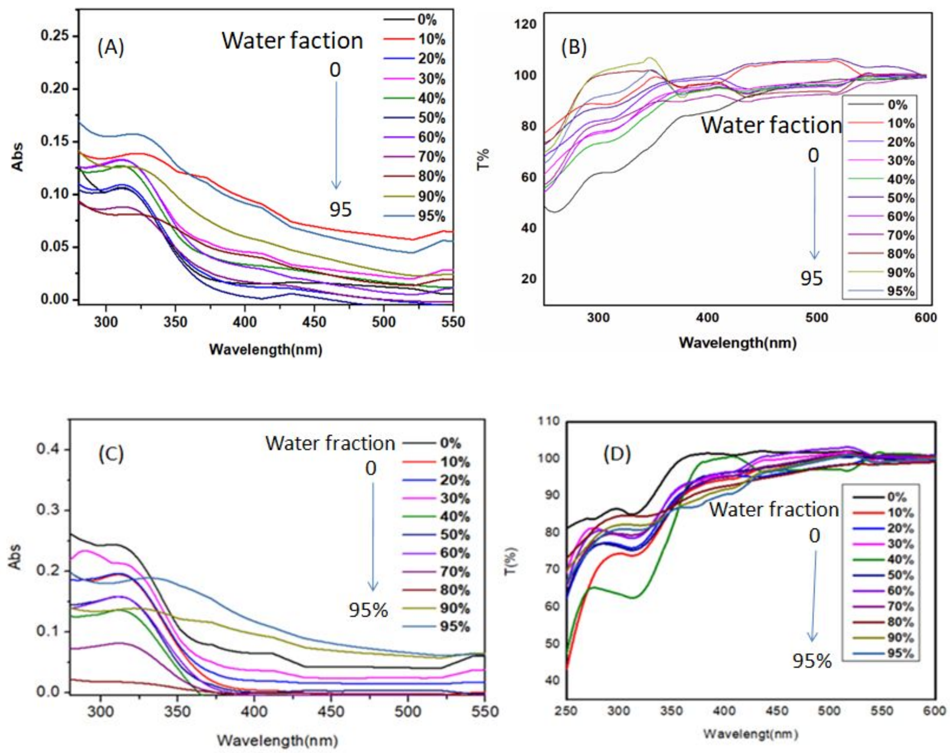

Figure S35. UV absorption and transmittance spectra of (A) ITPP, (B) Poly(ITPP) (Table 2, entry 7), (C) ITPPA and (D) Poly(ITPPA) (Table 2, entry 8) with the water fraction in THF/water mixture ranging from 0 to 95%.

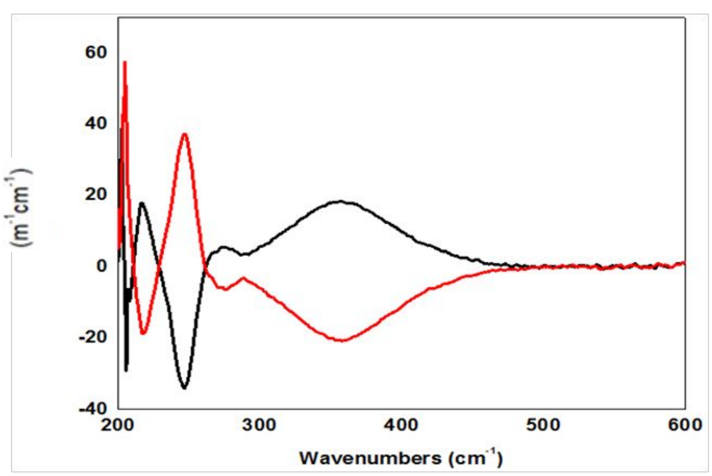

Figure S36. CD Spectra ofEt_3Si-end-functionalized poly(D-IMCI) and Et_3Si-end-functionalizedpoly(L-IMCI) (Table 2, entries 9–10).

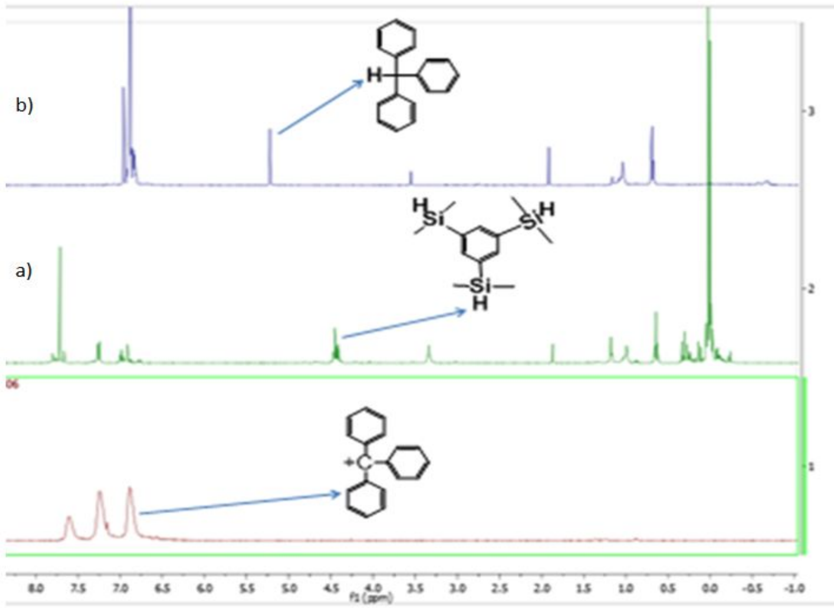

Figure S37. (a) ^{1}H NMR spectra of 1,3,5-$(SiMe_2H)_3$-C_6H_3 and (b) corresponding cationic species *in situ* generated by reaction of Poly-Si-H with catalyst $[Ph_3C][B(C_6F_5)_4]$.

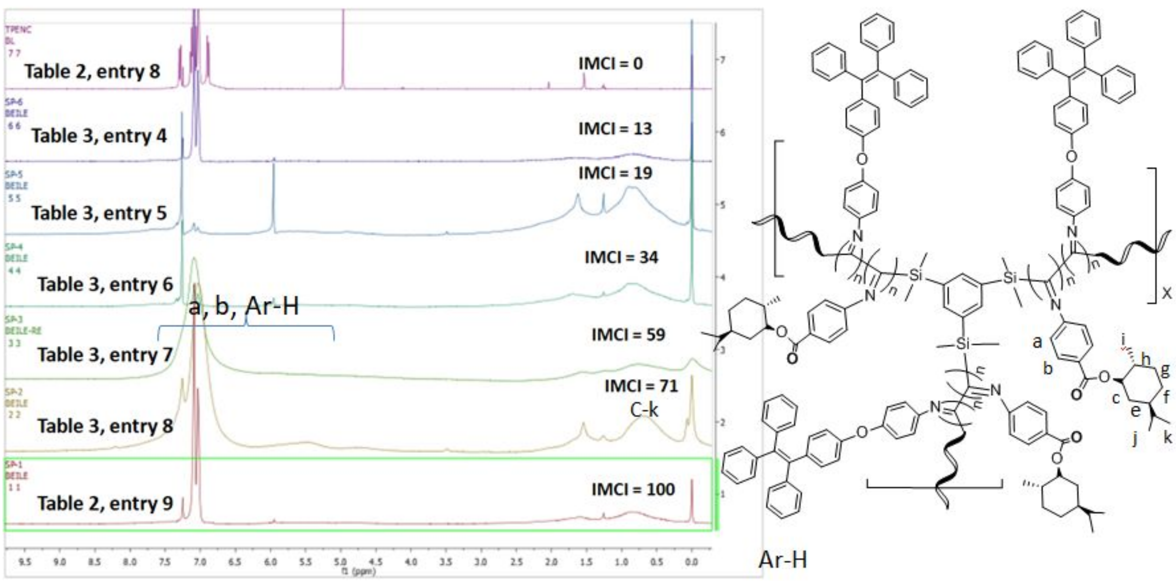

Figure S38. ^{1}H NMR spectra of Poly(ITPPA) (Table 2, entry 8), Poly(D-IMCI-*co*-ITPPA)s (Table 3, entries 4–8) and Poly(D-IMCI) (Table 3, entry 9).

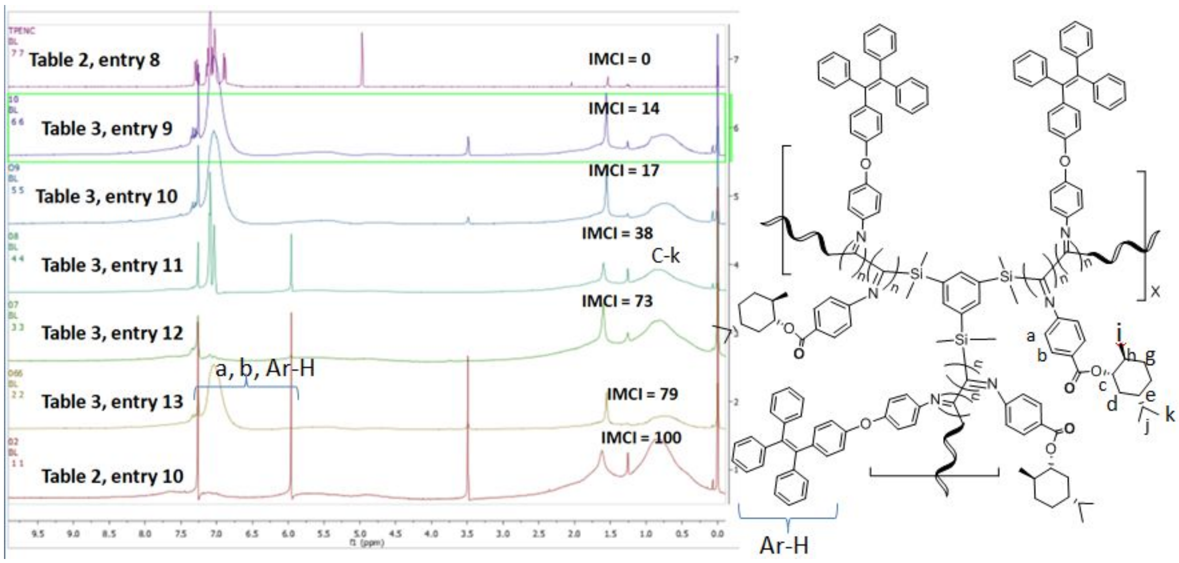

Figure S39. ^{1}H NMR spectra of Poly(ITPPA) (Table 2, entry 8), Poly(L-IMCI-*co*-ITPPA)s (Table 4, entries 9–13) and Poly(L-IMCI) (Table 3, entry 10).

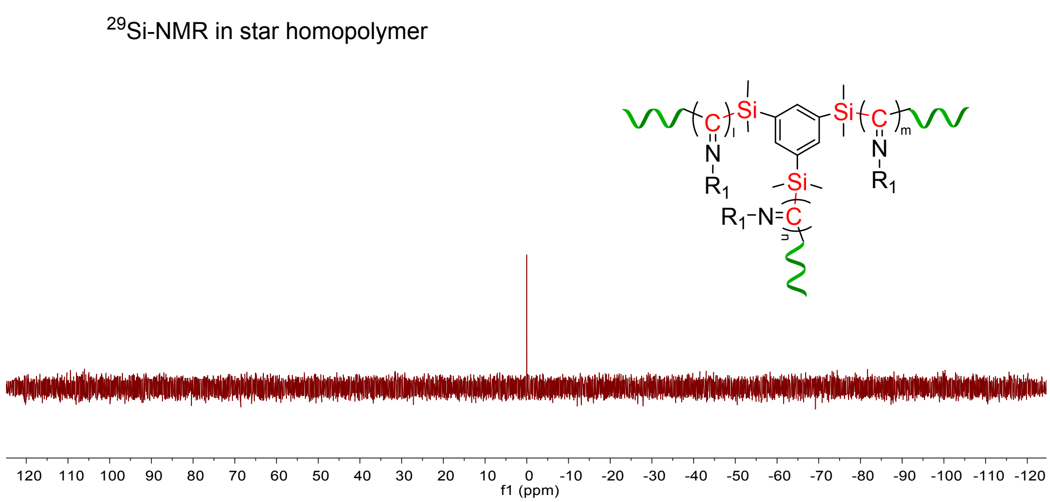

Figure S40. ^{29}Si-NMR spectrum of poly(D-IMCI) (Table 3, entry 2).

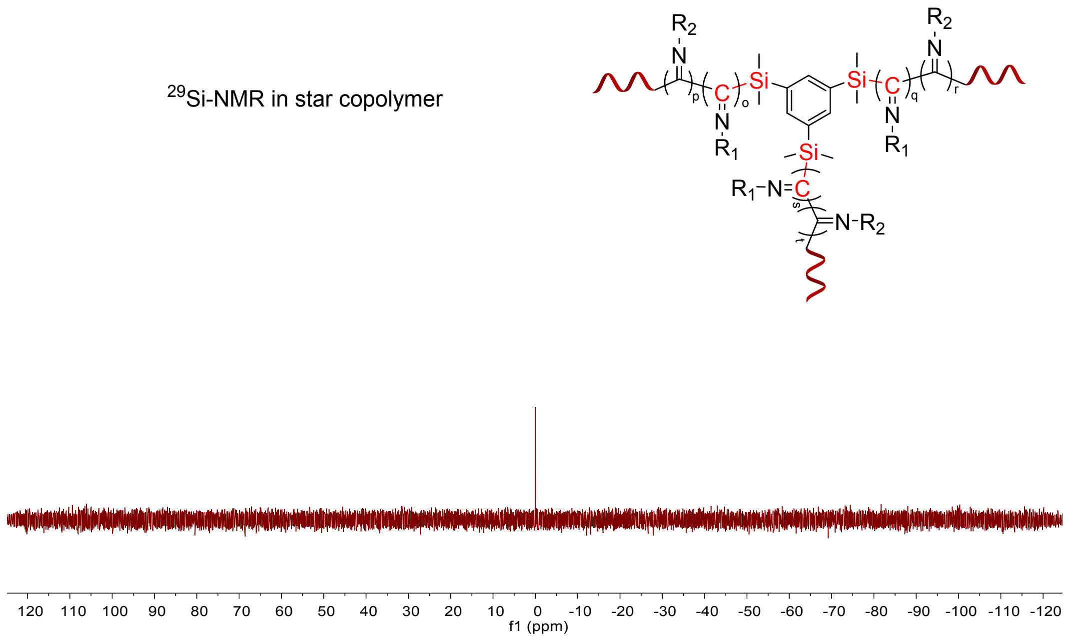

Figure S41. ^{29}Si-NMR spectrum of poly(D-IMCI-*co*-ITPPA) (Table 3, entry 6).

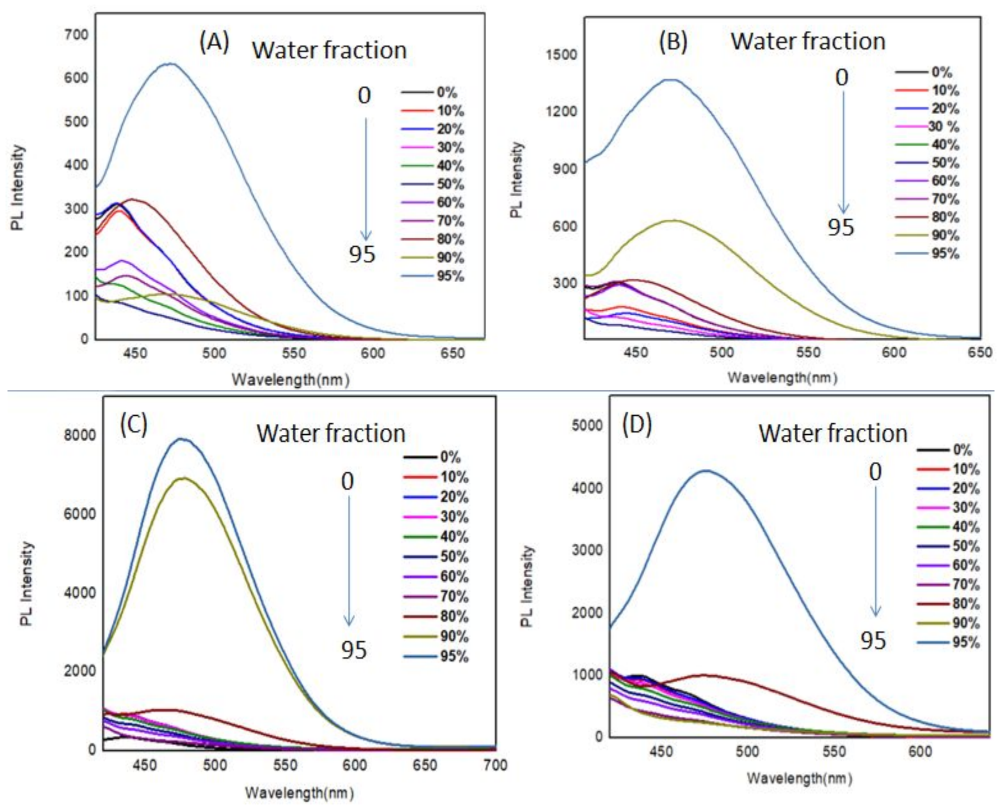

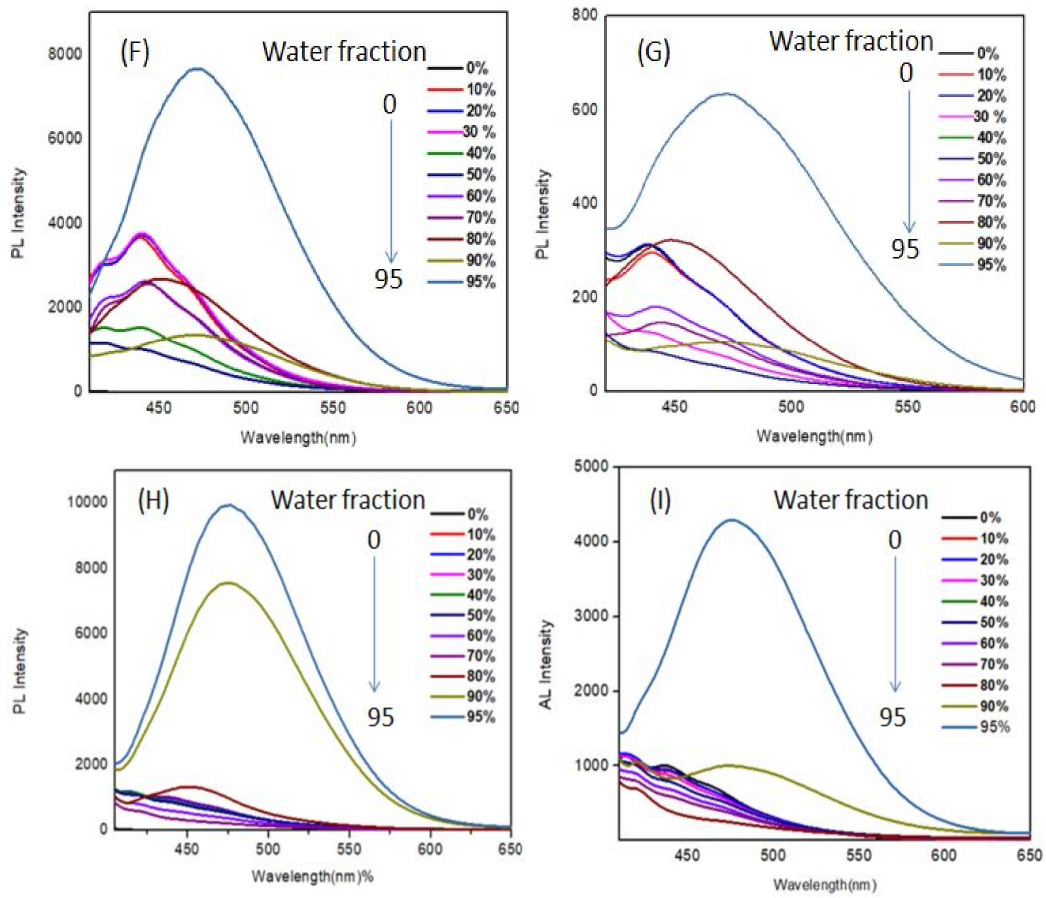

Figure S42. Plots of fluorescence intensity vs water fraction in THF/water mixture (0.01 mg/mL) (A) Poly(D-IMCI-*co*-ITPPA) (Table 3, entry 4), (B) Poly(D-IMCI-*co*-ITPPA) (Table 3, entry 5), (C) Poly(D-IMCI-*co*-ITPPA) (Table 3, entry 6), (D) Poly(D-IMCI-*co*-ITPPA) (Table 3, entry 8), (F) Poly(L-IMCI-*co*-ITPPA) (Table 3, entry 9), (G) Poly(L-IMCI-*co*-ITPPA) (Table 3, entry 10), (H) Poly(L-IMCI-*co*-ITPPA) (Table 3, entry 11) and (I) Poly(L-IMCI-*co*-ITPPA) (Table 3, entry 13) (conditions: EX wavelength: 290 nm, EX slit: 5 nm, EM slit: 5 nm, 700 V).

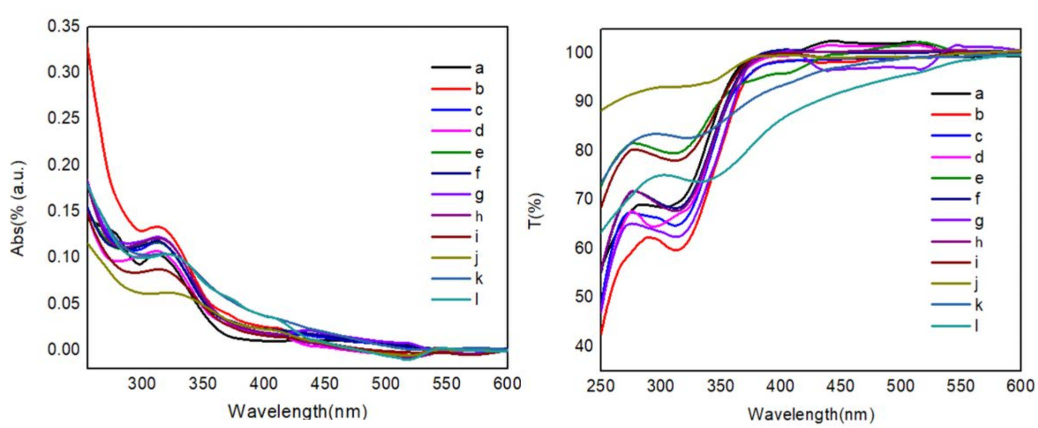

Figure S43. UV absorption and transmittance spectra of (a) baseline, (b) ITPPA, (c) Poly(ITPPA) (Table 2, entry 8), (d-g) (Poly(D-IMCI-*co*-ITPPA)s (Table 3, entries 4–8) and (h-l) Poly(L-IMCI-*co*-ITPPA)s (Table 3, entries 9–13) in THF.

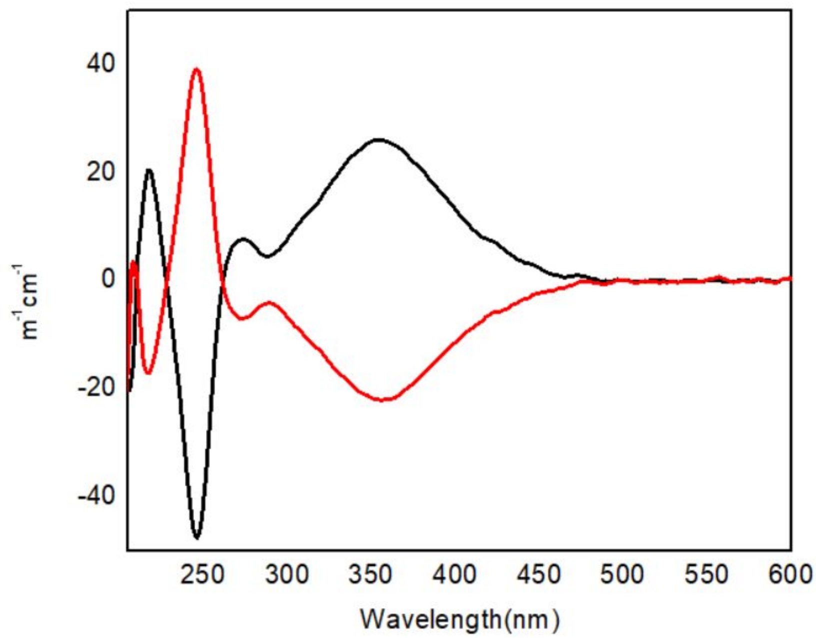

Figure S44. CD spectra of poly(D-IMCI) (Table 3, entry 2) and poly(L-IMCI) (Table 3, entry 3).

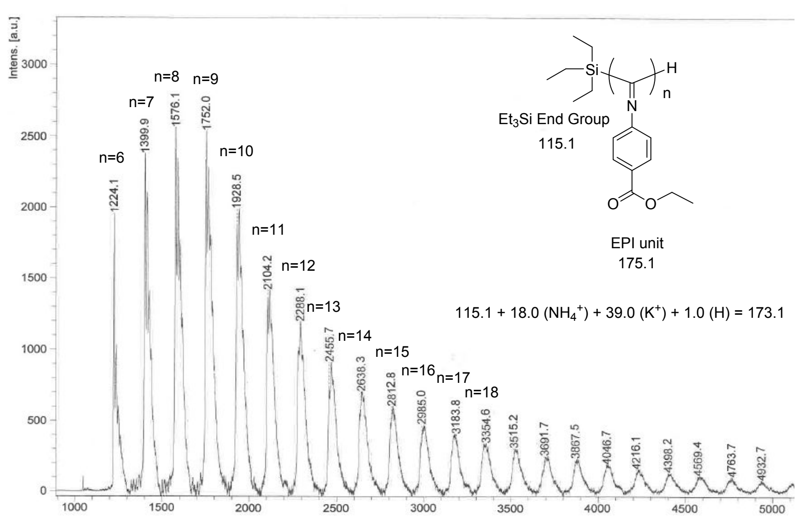

Figure S45. MALDI-TOF mass spectrum of EPI oligomer obtained by the binary $[Ph_3C][B(C_6F_5)_4]/Et_3SiH$ system.

GPC Curve Synthesis of Silane-End-Functionalized Linear Poly(aryl isocyanide)s through Cationic Polymerization of Aryl Isocyanides Promoted by Cationic Initiator Borates or Borane in the Presence of Hydrosilane.

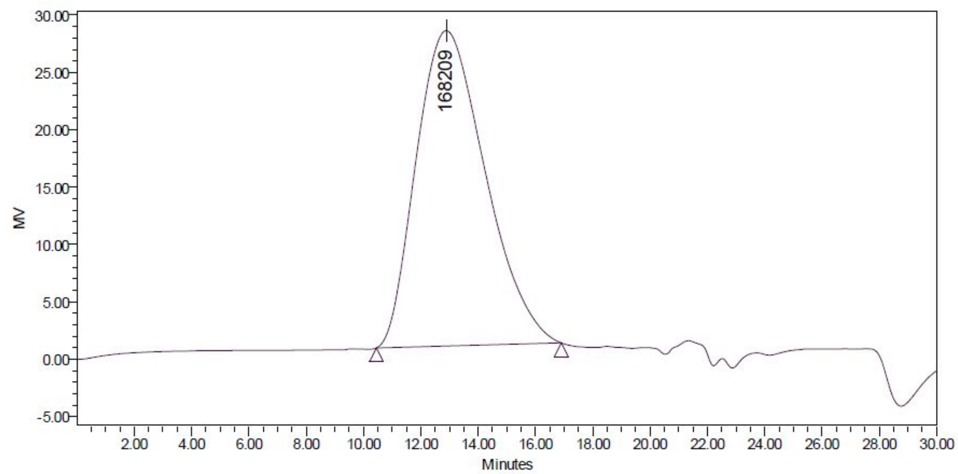

Broad Unknown Modified Universal Peak Table

	Distribution Name	Mv (Daltons)	K (dl/g)	alpha	Intrinsic Viscosity (dl/g)	Mn (Daltons)	Mw (Daltons)	MP (Daltons)	Mz (Daltons)	Mz+1 (Daltons)	Polydispersity	Mz/Mw
1						59102	229311	168209	549354	912038	3.879944	2.395673

Figure S46. GPC curve of Poly(EPI)by cationic catalyst[Ph_3C][$B(C_6F_5)_4$ in Table 1, entry 1.

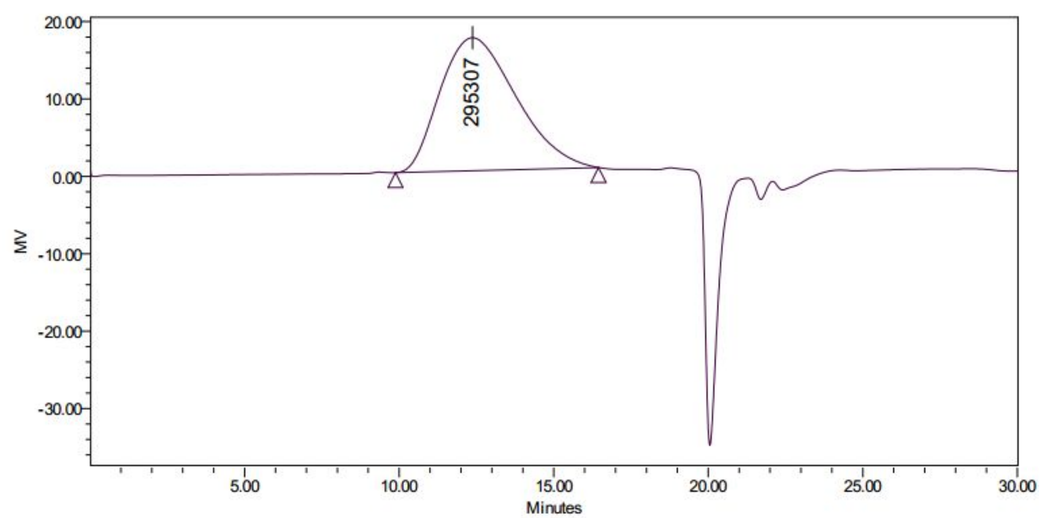

Broad Unknown Modified Universal Peak Table

	Distribution Name	Mv (Daltons)	K (dl/g)	alpha	Intrinsic Viscosity (dl/g)	Mn (Daltons)	Mw (Daltons)	MP (Daltons)	Mz (Daltons)	Mz+1 (Daltons)	Polydispersity	Mz/Mw
1						95602	405689	295307	1011338	1701846	4.243529	2.492891

Figure S47. GPC curve of Poly(EPI) by cationic catalyst [$(Et_3Si)_2H$][$B(C_6F_5)_4$] in Table 1, entry 2.

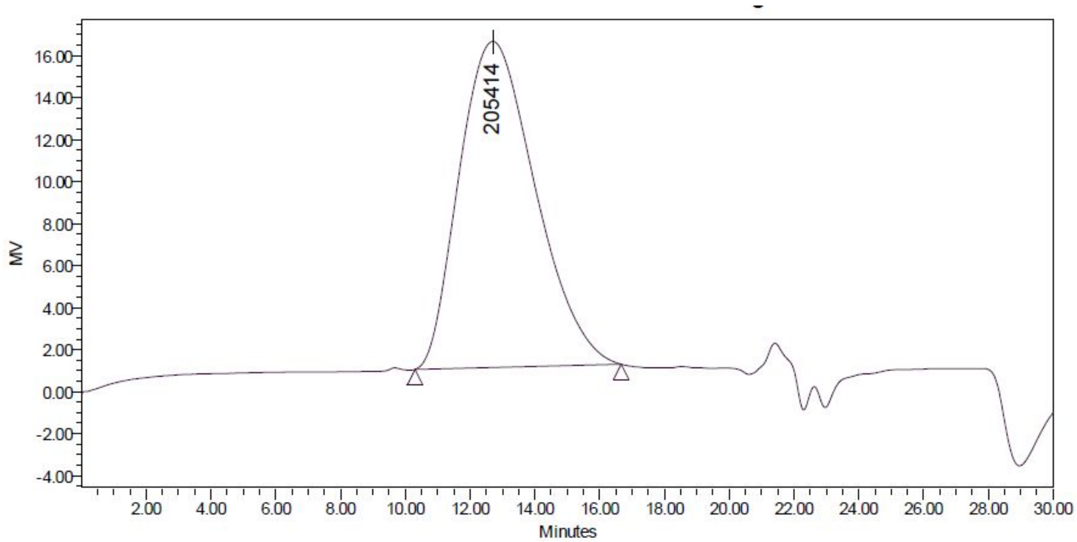

Broad Unknown Modified Universal Peak Table

	Distribution Name	Mv (Daltons)	K (dl/g)	alpha	Intrinsic Viscosity (dl/g)	Mn (Daltons)	Mw (Daltons)	MP (Daltons)	Mz (Daltons)	Mz+1 (Daltons)	Polydispersity	Mz/Mw
1						77439	281900	205414	657661	1081943	3.640275	2.332958

Figure S49. GPC curve of Et_3Si-end-functionalized poly(EPI) in Table 1, entry 3.

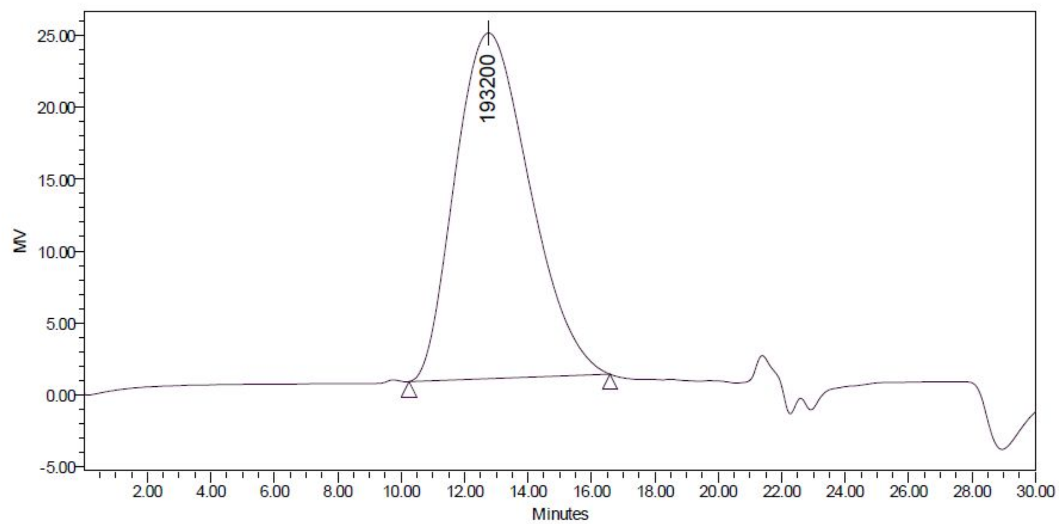

Broad Unknown Modified Universal Peak Table

	Distribution Name	Mv (Daltons)	K (dl/g)	alpha	Intrinsic Viscosity (dl/g)	Mn (Daltons)	Mw (Daltons)	MP (Daltons)	Mz (Daltons)	Mz+1 (Daltons)	Polydispersity	Mz/Mw
1						75636	272626	193200	648352	1087787	3.604437	2.378169

Figure S49. GPC curve of Et_3Si-end-functionalized poly(EPI) in Table 1, entry 4.

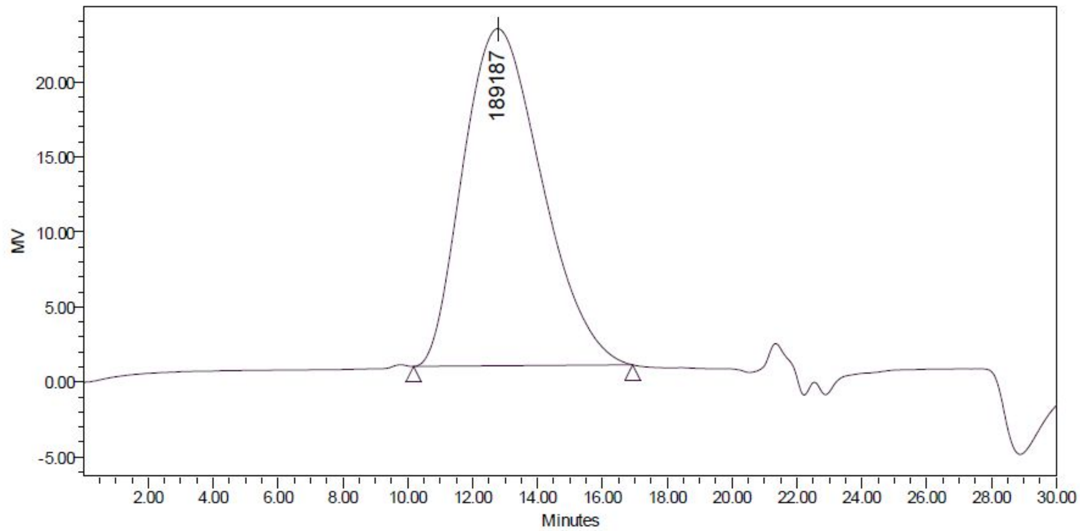

Broad Unknown Modified Universal Peak Table

	Distribution Name	Mv (Daltons)	K (dl/g)	alpha	Intrinsic Viscosity (dl/g)	Mn (Daltons)	Mw (Daltons)	MP (Daltons)	Mz (Daltons)	Mz+1 (Daltons)	Polydispersity	Mz/Mw
1						67507	268870	189187	665567	1132481	3.982856	2.475423

Figure S49. GPC curve of Et_3Si-end-functionalized poly(EPI) in Table 1, entry 5.

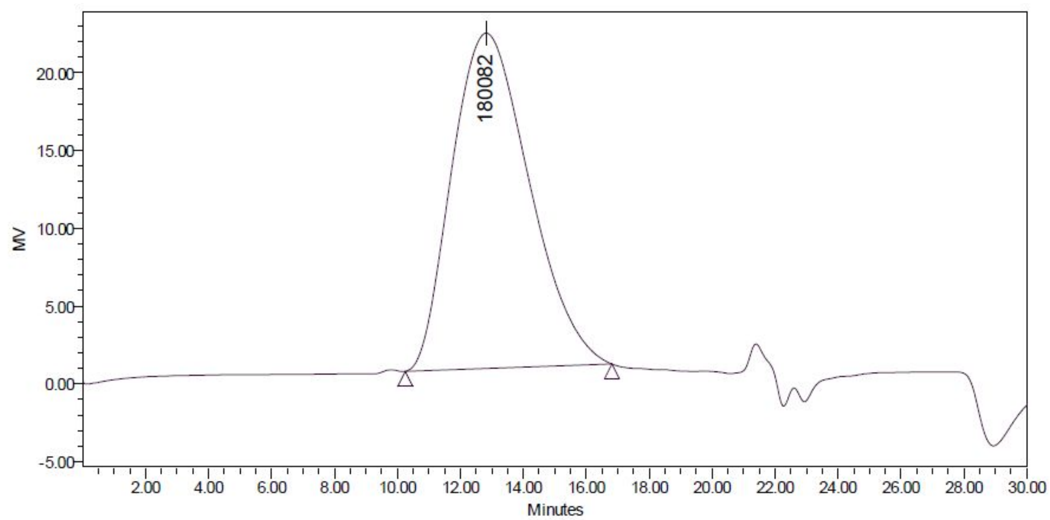

Broad Unknown Modified Universal Peak Table

	Distribution Name	Mv (Daltons)	K (dl/g)	alpha	Intrinsic Viscosity (dl/g)	Mn (Daltons)	Mw (Daltons)	MP (Daltons)	Mz (Daltons)	Mz+1 (Daltons)	Polydispersity	Mz/Mw
1						64750	259807	180082	645787	1093301	4.012448	2.485644

Figure S50. GPC curve of Et_3Si-end-functionalized poly(EPI) in Table 1, entry 6.

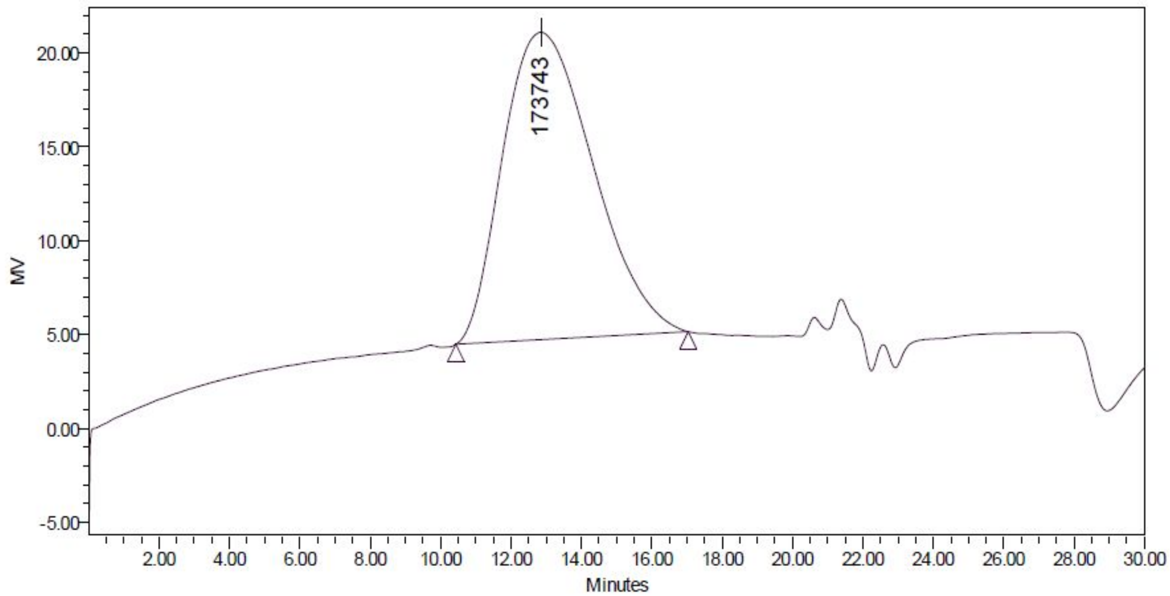

Broad Unknown Modified Universal Peak Table

	Distribution Name	Mv (Daltons)	K (dl/g)	alpha	Intrinsic Viscosity (dl/g)	Mn (Daltons)	Mw (Daltons)	MP (Daltons)	Mz (Daltons)	Mz+1 (Daltons)	Polydispersity	Mz/Mw
1						55478	237557	173743	589276	975952	4.282008	2.480563

Figure S51. GPC curve of Et_3Si-end-functionalized poly(EPI) in Table 1, entry 7.

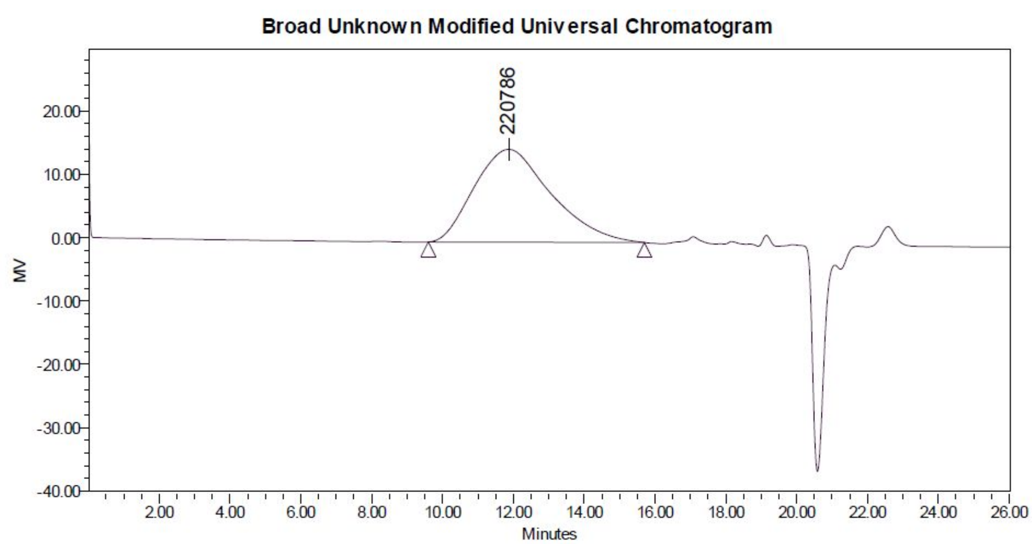

Broad Unknown Modified Universal Peak Table

	Distribution Name	Mv (Daltons)	K (dl/g)	alpha	Intrinsic Viscosity (dl/g)	Mn (Daltons)	Mw (Daltons)	MP (Daltons)	Mz (Daltons)	Mz+1 (Daltons)	Polydispersity	Mz/Mw
1						89222	289140	220786	612644	965680	3.240689	2.11885C

Figure S52. GPC curve of Et_3Si-end-functionalized poly(EPI) in Table 1, entry 8.

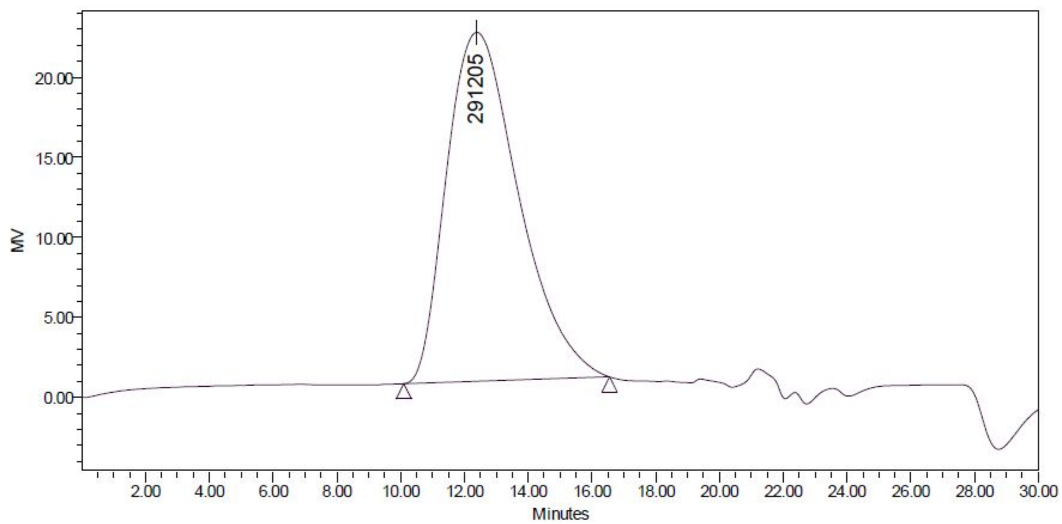

Broad Unknown Modified Universal Peak Table

	Distribution Name	Mv (Daltons)	K (dl/g)	alpha	Intrinsic Viscosity (dl/g)	Mn (Daltons)	Mw (Daltons)	MP (Daltons)	Mz (Daltons)	Mz+1 (Daltons)	Polydispersity	Mz/Mw
1						95716	355640	291205	783629	1253092	3.715588	2.203431

Figure S53. GPC curve of Et_3Si-End-Functionalized Poly(EPI) in Table 1, entry 9.

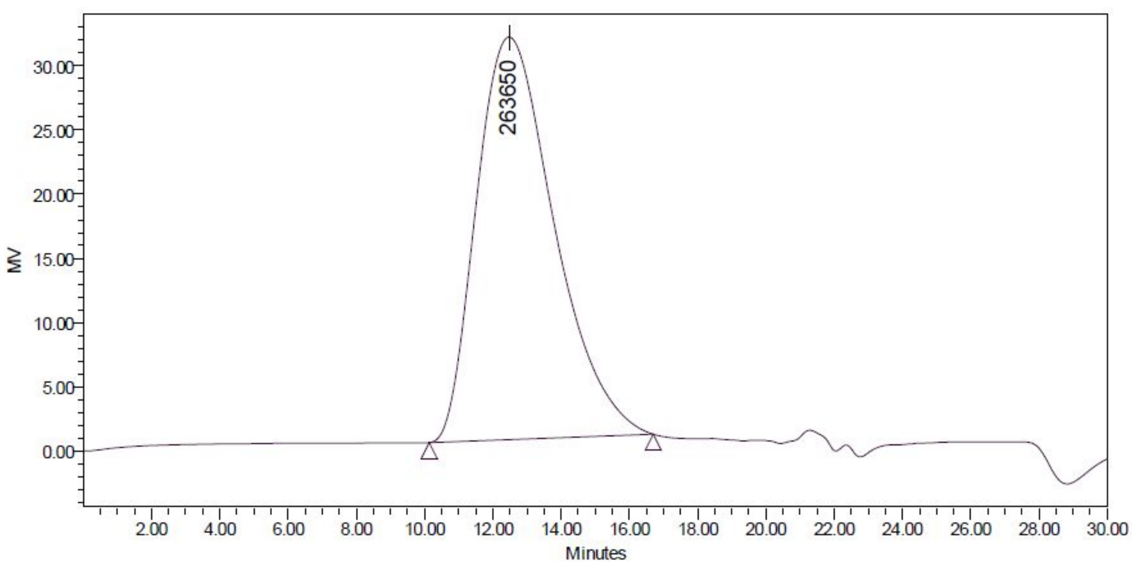

Broad Unknown Modified Universal Peak Table

	Distribution Name	Mv (Daltons)	K (dl/g)	alpha	Intrinsic Viscosity (dl/g)	Mn (Daltons)	Mw (Daltons)	MP (Daltons)	Mz (Daltons)	Mz+1 (Daltons)	Polydispersity	Mz/Mw
1						86536	326841	263650	733599	118999C	3.776956	2.244511

Figure S54. GPC curve of Et_3Si-end-functionalized poly(EPI) in Table 1, entry 10.

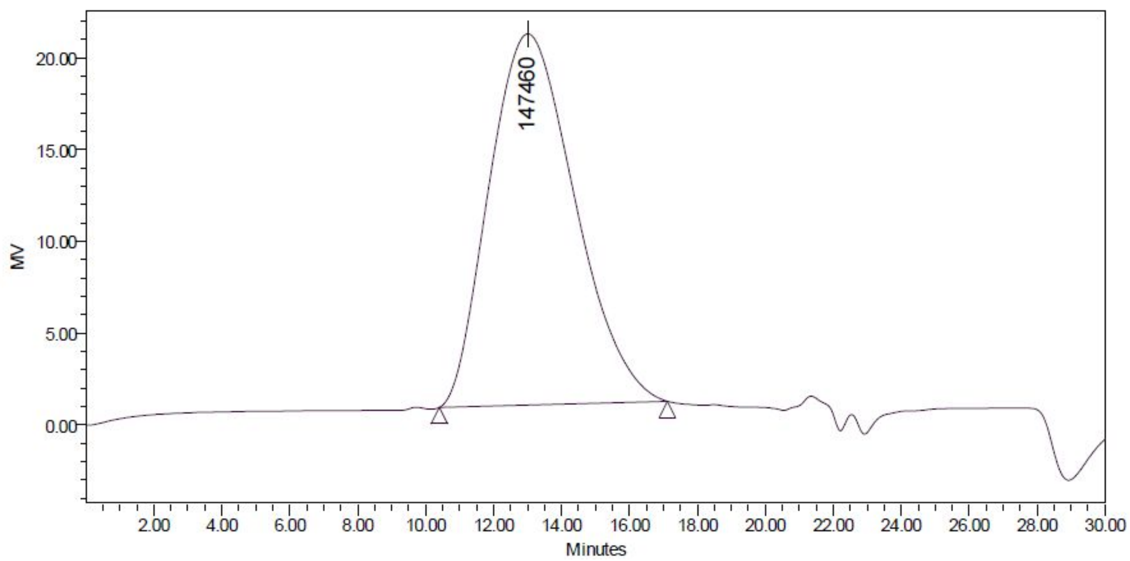

Broad Unknown Modified Universal Peak Table

	Distribution Name	Mv (Daltons)	K (dl/g)	alpha	Intrinsic Viscosity (dl/g)	Mn (Daltons)	Mw (Daltons)	MP (Daltons)	Mz (Daltons)	Mz+1 (Daltons)	Polydispersity	Mz/Mw
1						53165	224438	147460	579055	988682	4.221503	2.580021

Figure S55. GPC curve of Et_3Si-end-functionalized poly(EPI) in Table 1, entry 11.

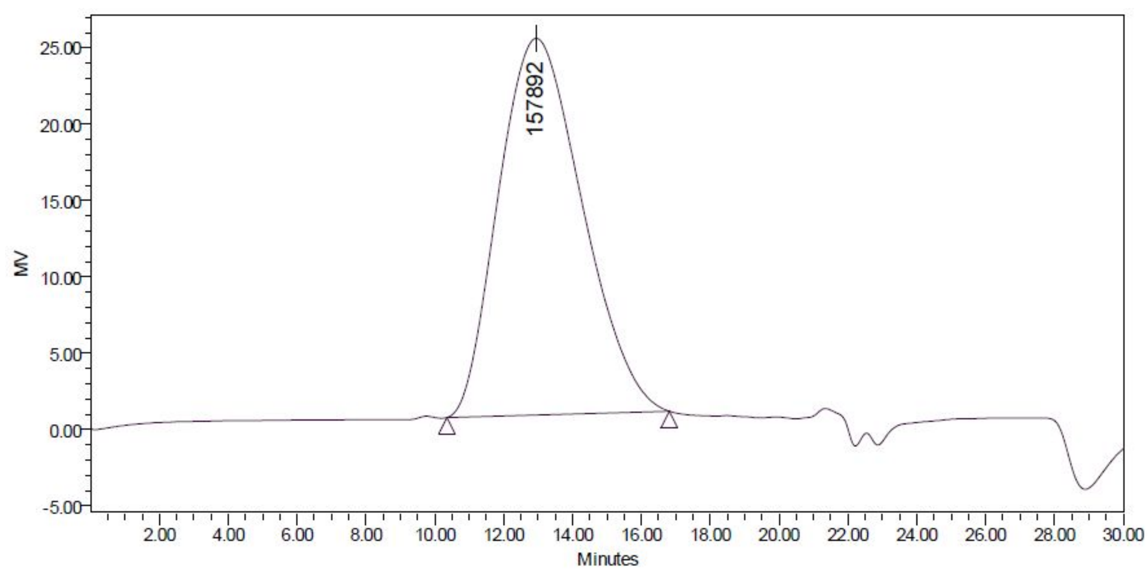

Broad Unknown Modified Universal Peak Table

	Distribution Name	Mv (Daltons)	K (dl/g)	alpha	Intrinsic Viscosity (dl/g)	Mn (Daltons)	Mw (Daltons)	MP (Daltons)	Mz (Daltons)	Mz+1 (Daltons)	Polydispersity	Mz/Mw
1						61134	231339	157892	576059	984709	3.784110	2.490105

Figure S56. GPC curve of Et_3Si-end-functionalized poly(EPI) in Table 1, entry 12.

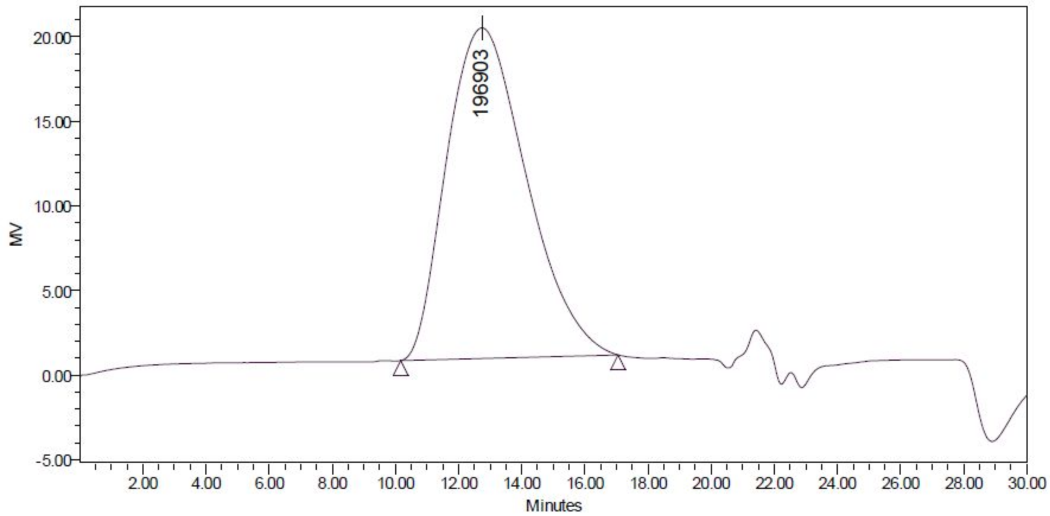

Broad Unknown Modified Universal Peak Table

	Distribution Name	Mv (Daltons)	K (dl/g)	alpha	Intrinsic Viscosity (dl/g)	Mn (Daltons)	Mw (Daltons)	MP (Daltons)	Mz (Daltons)	Mz+1 (Daltons)	Polydispersity	Mz/Mw
1						63580	286366	196903	726279	1225562	4.504001	2.536188

Figure S57. GPC curve of Et_3Si-end-functionalized poly(EPI) in Table 1, entry 13.

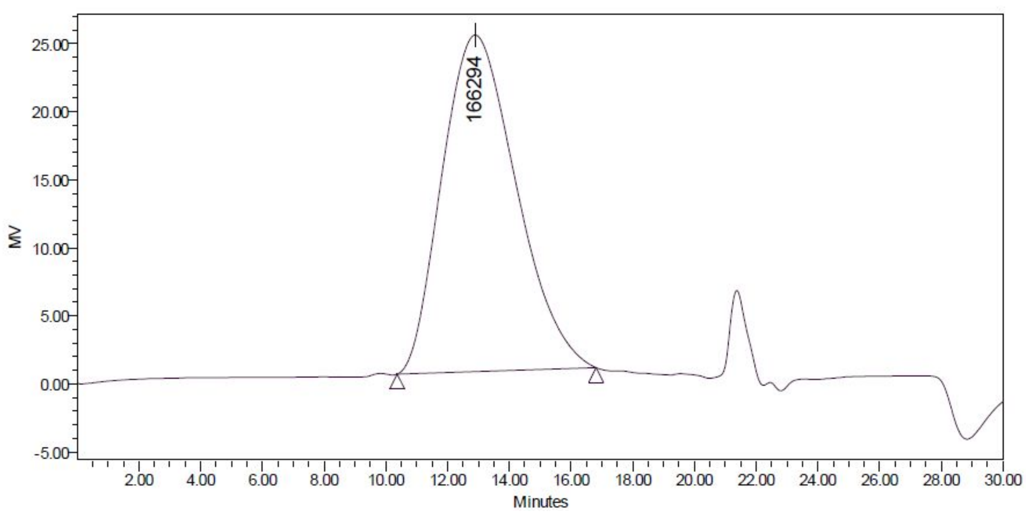

Broad Unknown Modified Universal Peak Table

	Distribution Name	Mv (Daltons)	K (dl/g)	alpha	Intrinsic Viscosity (dl/g)	Mn (Daltons)	Mw (Daltons)	MP (Daltons)	Mz (Daltons)	Mz+1 (Daltons)	Polydispersity	Mz/Mw
1						62297	239798	166294	590950	1002743	3.849237	2.464370

Figure S58. GPC curve of Et_3Si-end-functionalized poly(EPI) in Table 1, entry 14.

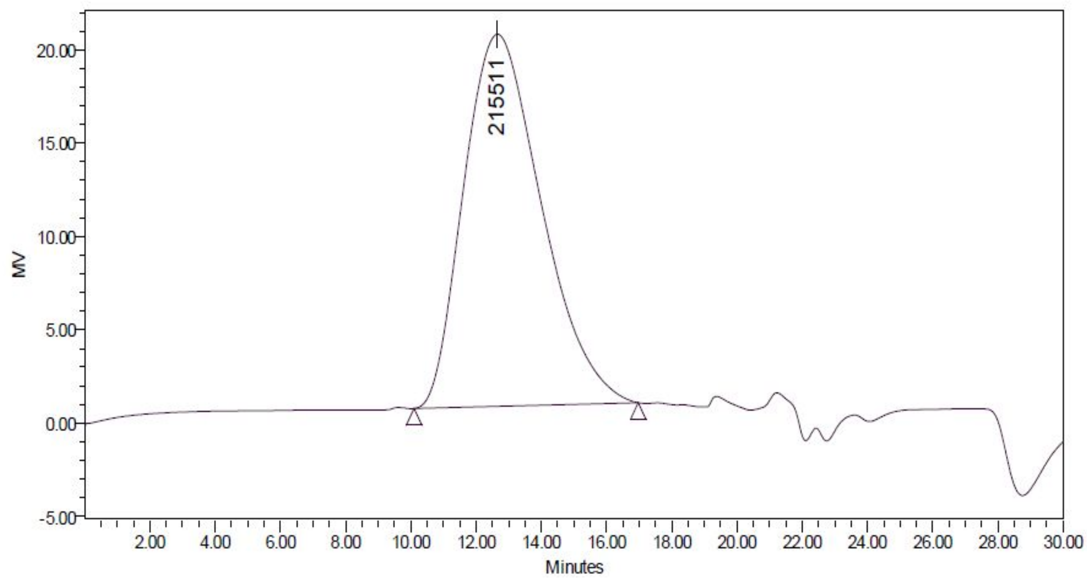

Broad Unknown Modified Universal Peak Table

	Distribution Name	Mv (Daltons)	K (dl/g)	alpha	Intrinsic Viscosity (dl/g)	Mn (Daltons)	Mw (Daltons)	MP (Daltons)	Mz (Daltons)	Mz+1 (Daltons)	Polydispersity	Mz/Mw
1						72213	295664	215511	721397	1226832	4.094348	2.439918

Figure S59. GPC curve of Et_3Si-end-functionalized poly(EPI) in Table 1, entry 15.

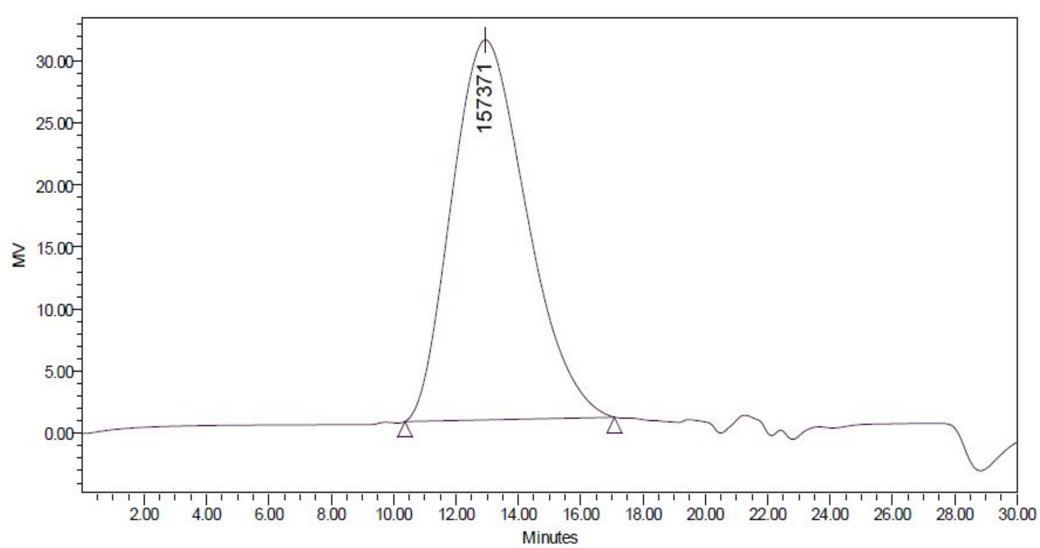

Broad Unknown Modified Universal Peak Table

	Distribution Name	Mv (Daltons)	K (dl/g)	alpha	Intrinsic Viscosity (dl/g)	Mn (Daltons)	Mw (Daltons)	MP (Daltons)	Mz (Daltons)	Mz+1 (Daltons)	Polydispersity	Mz/Mw
1						58365	232014	157371	585538	1012901	3.975224	2.523718

Figure S60. GPC curve of Et_3Si-end-functionalized poly(EPI) in Table 1, entry 16.

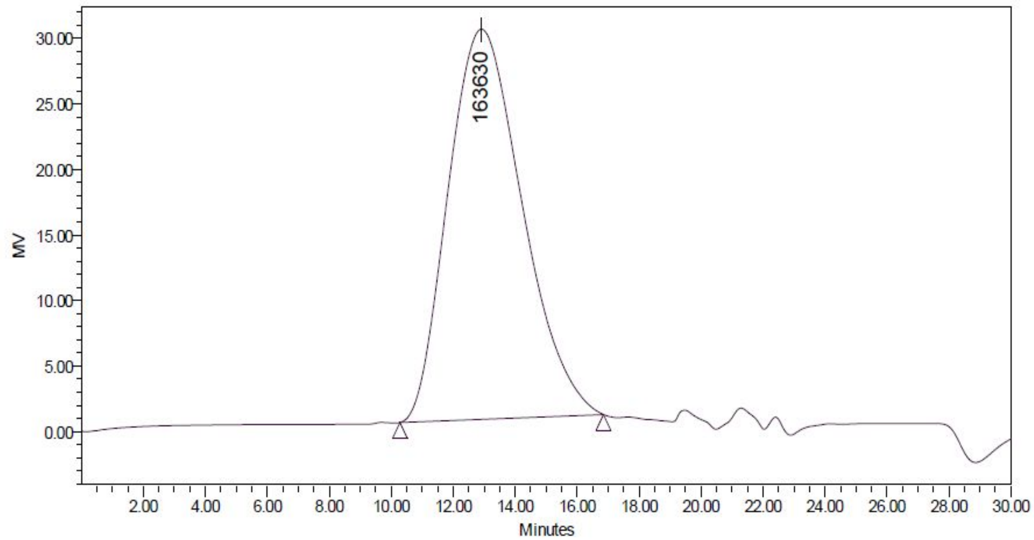

Broad Unknown Modified Universal Peak Table

	Distribution Name	Mv (Daltons)	K (dl/g)	alpha	Intrinsic Viscosity (dl/g)	Mn (Daltons)	Mw (Daltons)	MP (Daltons)	Mz (Daltons)	Mz+1 (Daltons)	Polydispersity	Mz/Mw
1						61905	238908	163630	596029	1033177	3.859246	2.494803

Figure S61. GPC curve of Et_3Si-end-functionalized poly(EPI) in Table 1, entry 17.

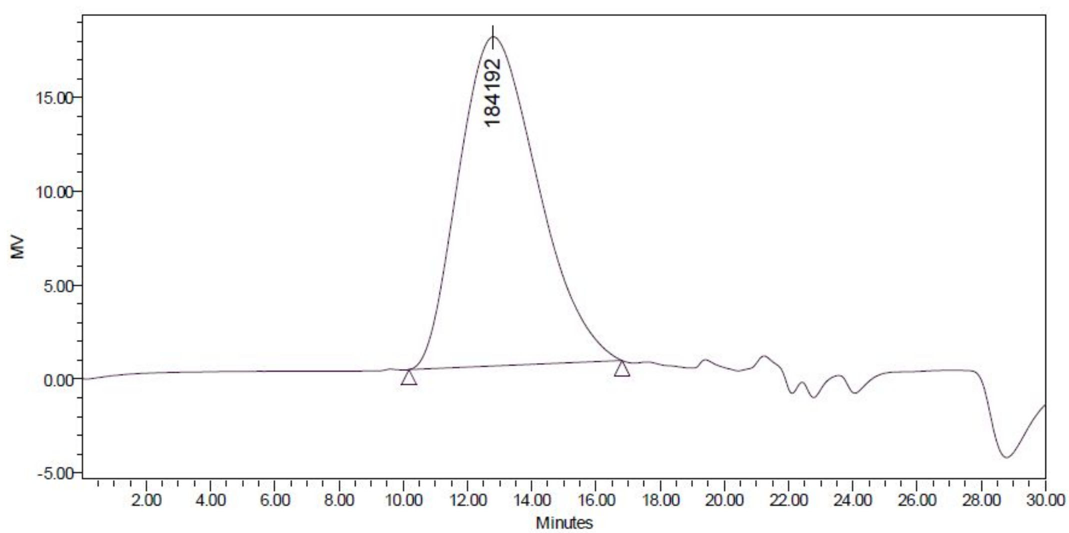

Broad Unknown Modified Universal Peak Table

	Distribution Name	Mv (Daltons)	K (dl/g)	alpha	Intrinsic Viscosity (dl/g)	Mn (Daltons)	Mw (Daltons)	MP (Daltons)	Mz (Daltons)	Mz+1 (Daltons)	Polydispersity	Mz/Mw
1						63232	262249	184192	672196	116829C	4.147401	2.563199

Figure S62. GPC curve of Et_3Si-end-functionalized poly(EPI) in Table 1, entry 18.

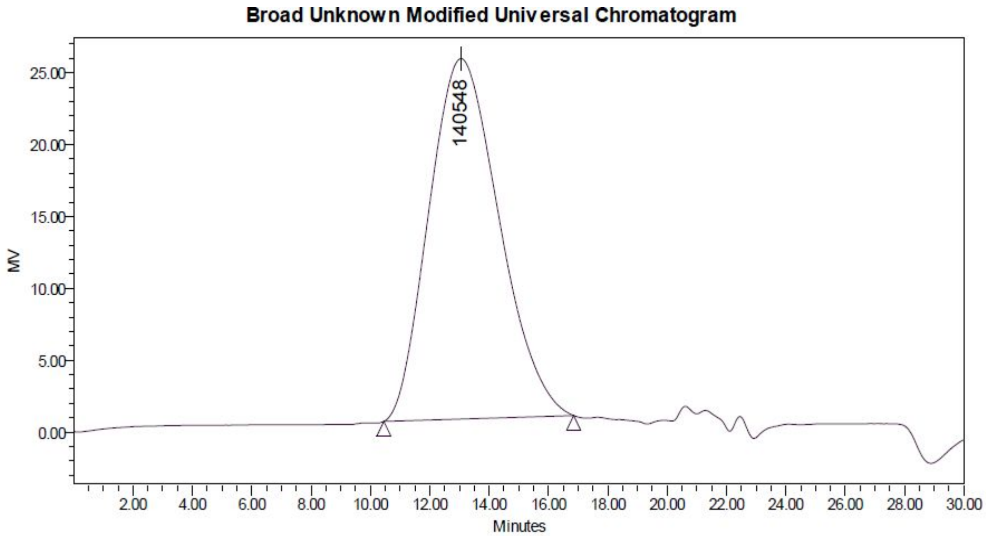

Broad Unknown Modified Universal Peak Table

	Distribution Name	Mv (Daltons)	K (dl/g)	alpha	Intrinsic Viscosity (dl/g)	Mn (Daltons)	Mw (Daltons)	MP (Daltons)	Mz (Daltons)	Mz+1 (Daltons)	Polydispersity	Mz/Mw
1						57855	209883	140548	521933	902777	3.627734	2.486782

Figure S63. GPC curve of $PhMe_2Si$-end-functionalized poly(EPI) in Table 2, entry 1.

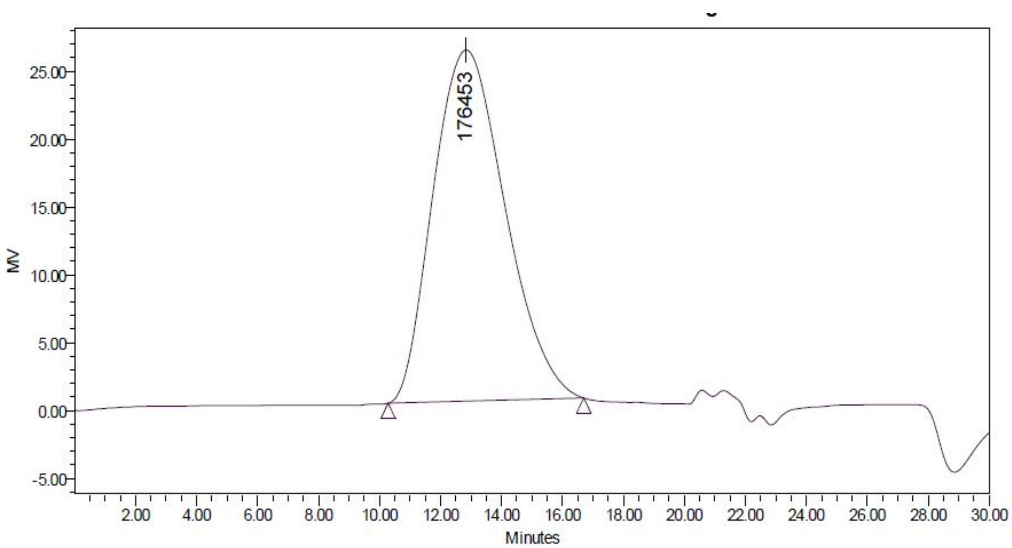

Broad Unknown Modified Universal Peak Table

	Distribution Name	Mv (Daltons)	K (dl/g)	alpha	Intrinsic Viscosity (dl/g)	Mn (Daltons)	Mw (Daltons)	MP (Daltons)	Mz (Daltons)	Mz+1 (Daltons)	Polydispersity	Mz/Mw
1						71822	260754	176453	629250	1064576	3.630539	2.413193

Figure S64. GPC curve of (4-^{i}PrC$_6$H$_4$)Me$_2$Si-end-functionalized poly(EPI) in Table 2, entry 2.

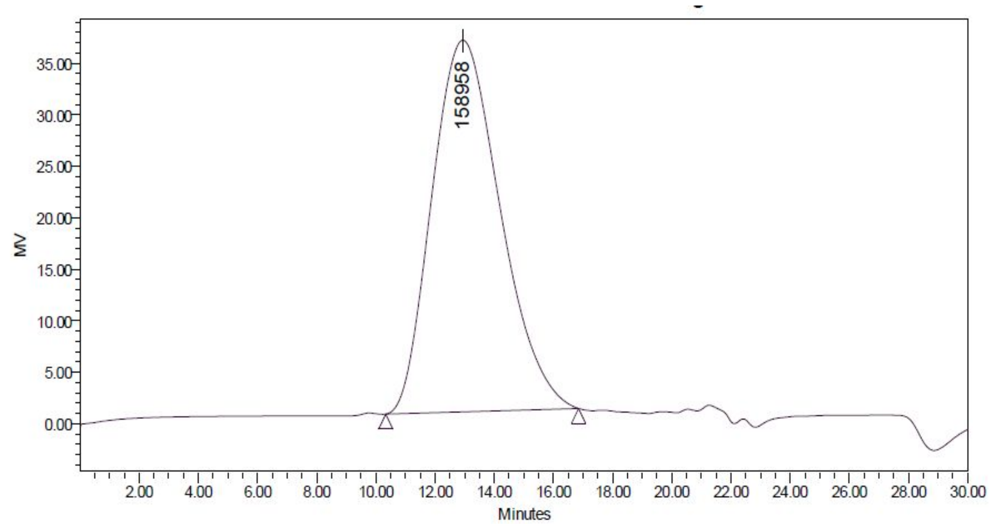

Broad Unknown Modified Universal Peak Table

	Distribution Name	Mv (Daltons)	K (dl/g)	alpha	Intrinsic Viscosity (dl/g)	Mn (Daltons)	Mw (Daltons)	MP (Daltons)	Mz (Daltons)	Mz+1 (Daltons)	Polydispersity	Mz/Mw
1						64122	226677	158958	540900	928216	3.535077	2.386221

Figure S65. GPC curve of Ph$_3$Si-end-functionalized poly(EPI) in Table 2, entry 3.

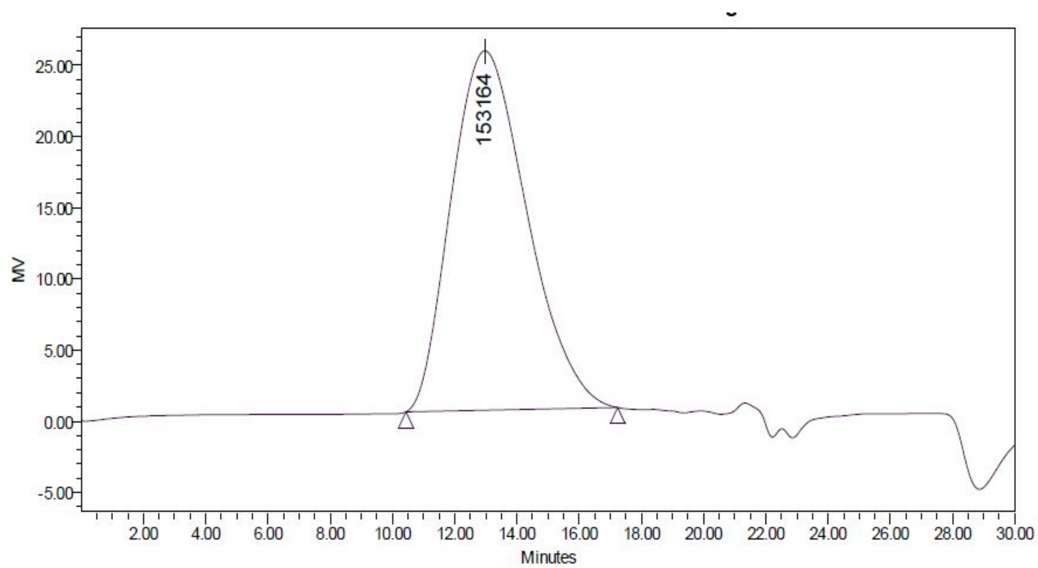

Broad Unknown Modified Universal Peak Table

	Distribution Name	Mv (Daltons)	K (dl/g)	alpha	Intrinsic Viscosity (dl/g)	Mn (Daltons)	Mw (Daltons)	MP (Daltons)	Mz (Daltons)	Mz+1 (Daltons)	Polydispersity	Mz/Mw
1						54327	220242	153164	546000	925151	4.054013	2.479095

Figure S66. GPC curve of $^{i}Pr_3Si$ -end-functionalized poly(EPI) in Table 2, entry 5.

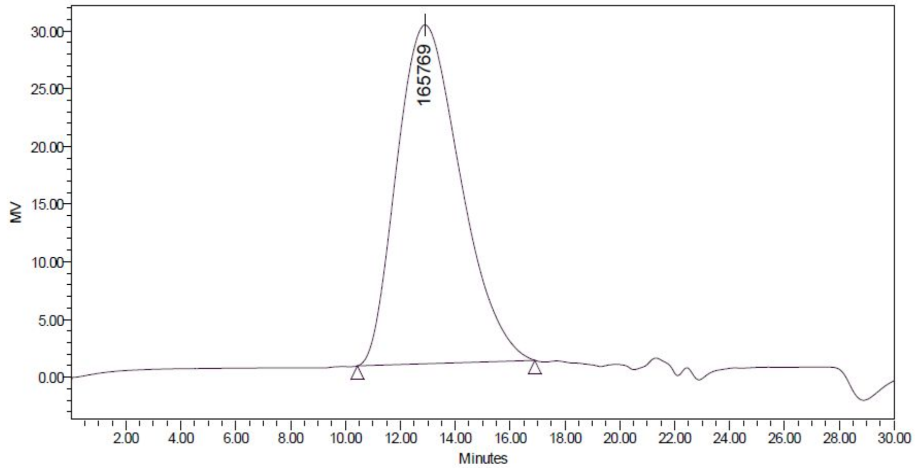

Broad Unknown Modified Universal Peak Table

	Distribution Name	Mv (Daltons)	K (dl/g)	alpha	Intrinsic Viscosity (dl/g)	Mn (Daltons)	Mw (Daltons)	MP (Daltons)	Mz (Daltons)	Mz+1 (Daltons)	Polydispersity	Mz/Mw
1						62394	225135	165769	522785	869546	3.608279	2.322095

Figure S67. GPC curve of $(OEt)_3Si$-end-functionalized poly(EPI) in Table 2, entry 6.

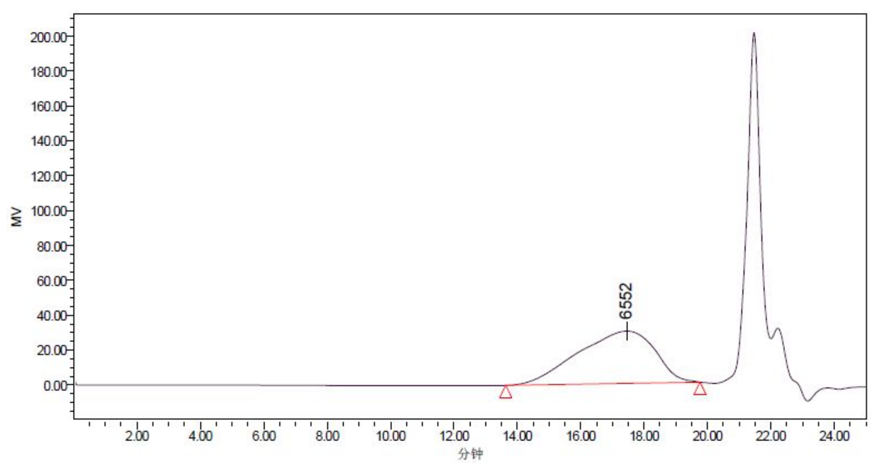

GPC Results

	Dist Name	Elution Volume (ml)	Retention Time (min)	Adjusted RT (min)	Mn	Mw	MP	Mz	Mz+1	Mz/Mw	Mz+1/Mw
1		17.457	17.457	17.457	6920	11488	6552	20113	32894	1.750815	2.863346

Figure S68. GPC curve of $(OEt)_3Si$-end-functionalized poly(EPI) in Table 2, entry 7.

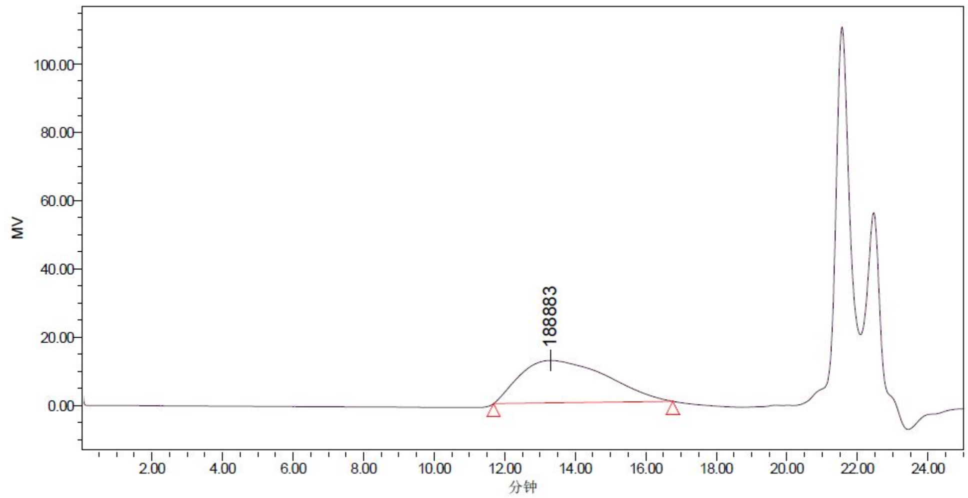

GPC Results

	Dist Name	Elution Volume (ml)	Retention Time (min)	Adjusted RT (min)	Mn	Mw	MP	Mz	Mz+1	Mz/Mw
1		13.307	13.307	13.307	68717	232328	188883	626163	1032547	2.695171

Figure S69. GPC curve of Et_3Si-end-functionalized poly(ITPP) in Table 2, entry 8.

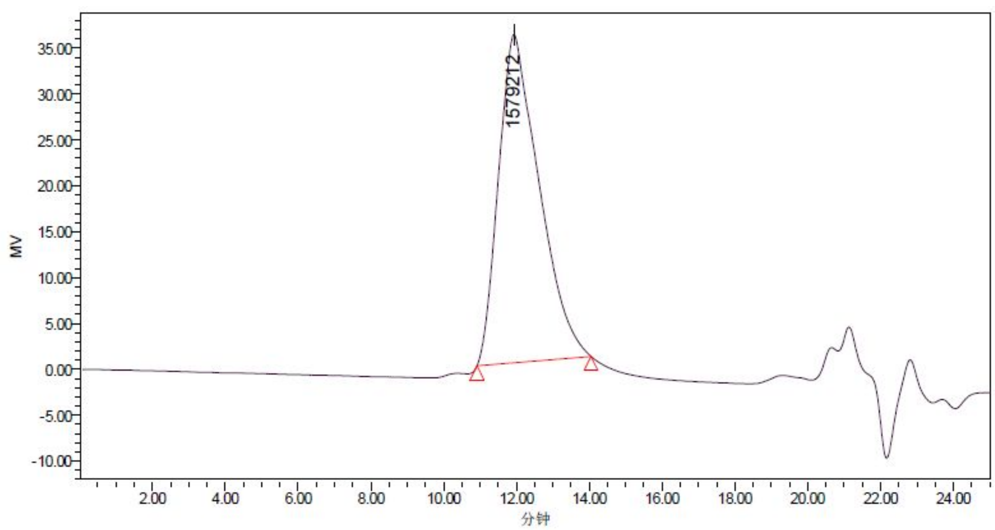

GPC Results

	Dist Name	Elution Volume (ml)	Retention Time (min)	Adjusted RT (min)	Mn	Mw	MP	Mz	Mz+1	Mz/Mw
1		11.930	11.930	11.930	711137	1643957	1579212	3131660	4798522	1.904953

Figure S70. GPC curve of Et_3Si-end-functionalized poly(ITPPA) in Table 2, entry 9.

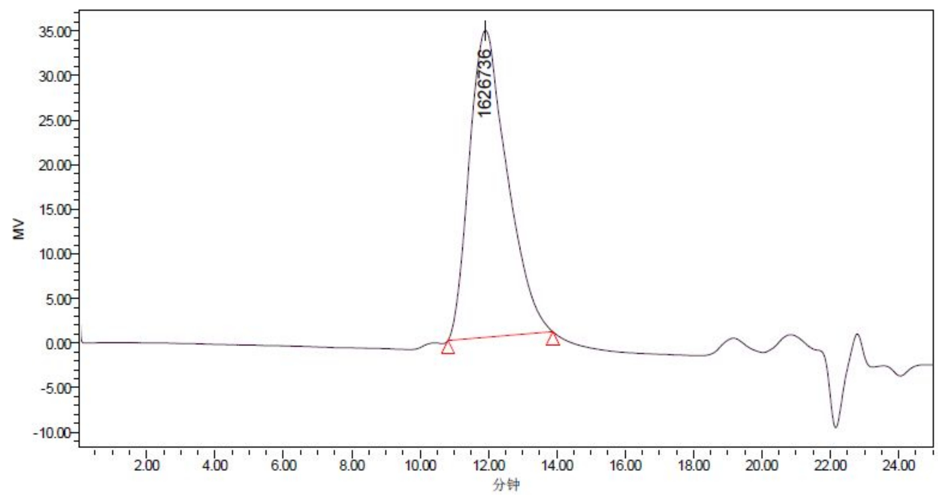

GPC Results

	Dist Name	Elution Volume (ml)	Retention Time (min)	Adjusted RT (min)	Mn	Mw	MP	Mz	Mz+1	Mz/Mw
1		11.914	11.914	11.914	837738	1919038	1626736	3708980	5803431	1.932729

Figure S71. GPC curve of Et_3Si-end-functionalized poly(D-IMCI) in Table 2, entry 10

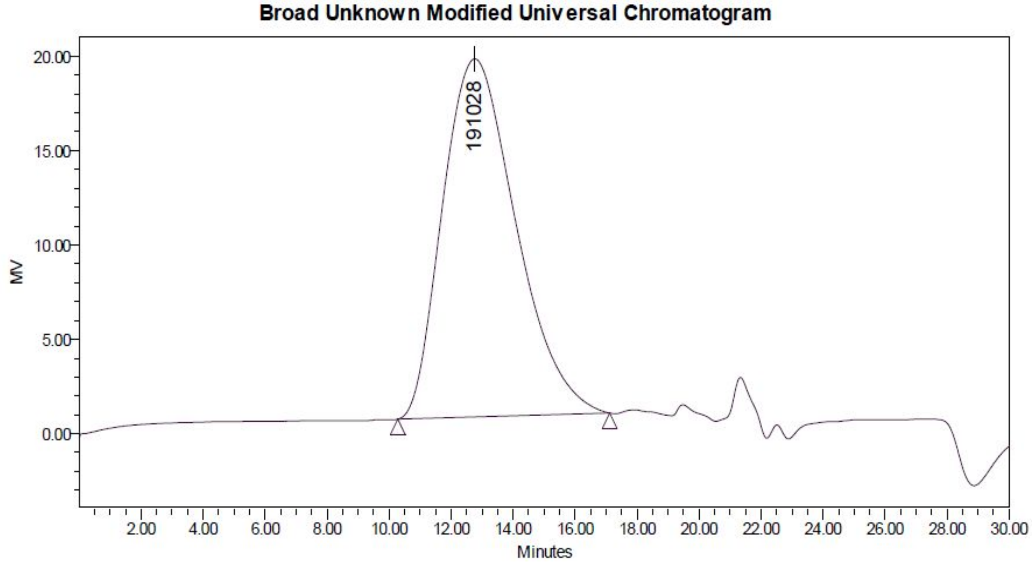

Broad Unknown Modified Universal Peak Table

	Distribution Name	Mv (Daltons)	K (dl/g)	alpha	Intrinsic Viscosity (dl/g)	Mn (Daltons)	Mw (Daltons)	MP (Daltons)	Mz (Daltons)	Mz+1 (Daltons)	Polydispersity	Mz/Mw
1						65341	262042	191028	623403	1043958	4.010387	2.379017

Figure S72. GPC curve of PhSi-end-functionalized star poly(EPI) in Table 3, entry 1.

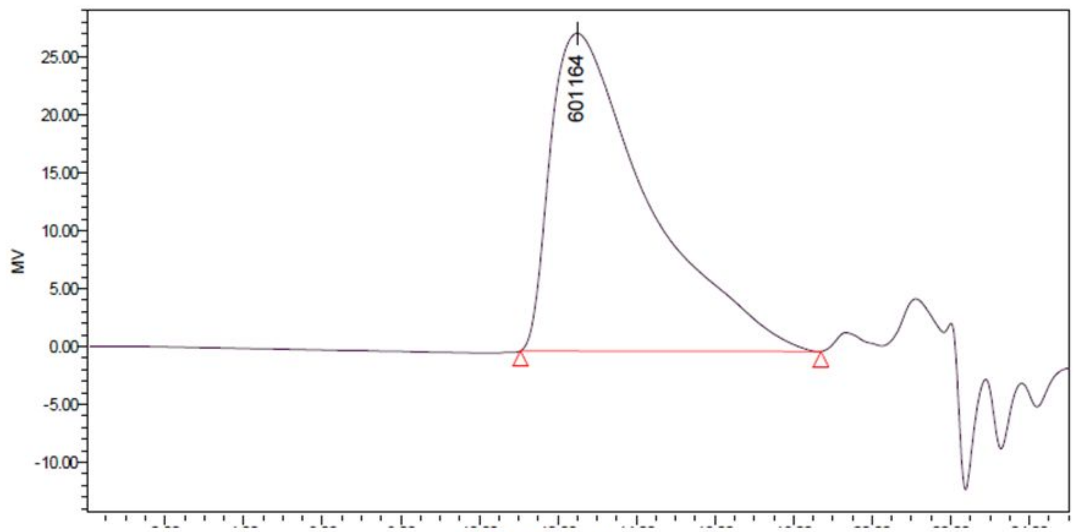

GPC Results

	Dist Name	Elution Volume (ml)	Retention Time (min)	Adjusted RT (min)	Mn	Mw	MP	Mz	Mz+1	Mz/Mw
1		12.492	12.492	12.492	59759	522016	601164	1683976	2884722	3.225910

Figure S73. GPC curve of C_6H_3-1,3,5-$(Me_2Si)_3$-end-functionalized poly(D-IMCI) in Table 3, entry 2.

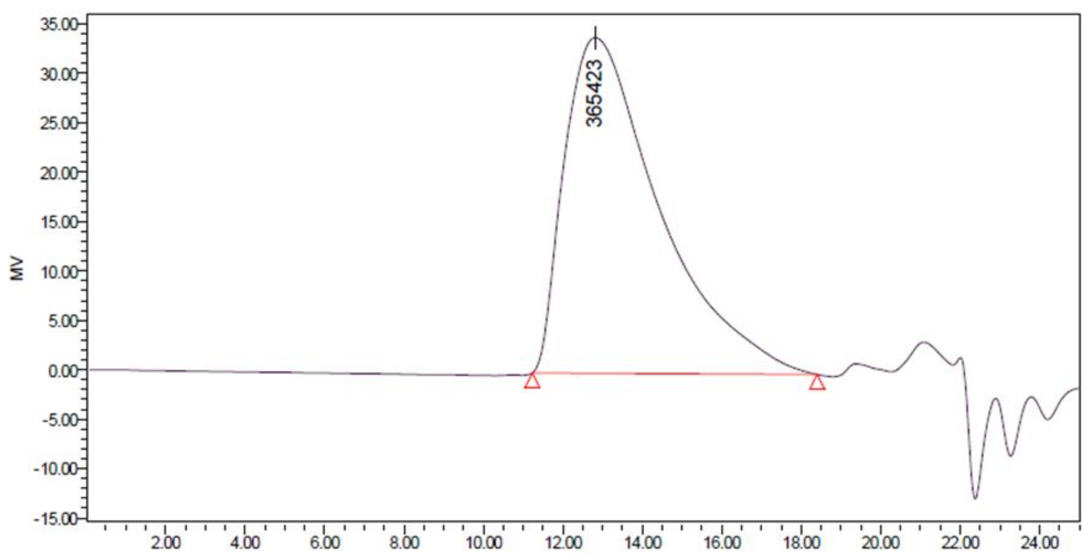

GPC Results

	Dist Name	Elution Volume (ml)	Retention Time (min)	Adjusted RT (min)	Mn	Mw	MP	Mz	Mz+1	Mz/Mw
1		12.820	12.820	12.820	66130	399174	365423	1205148	2055934	3.019107

Figure S74. GPC curve of C_6H_3-1,3,5-$(Me_2Si)_3$-end-functionalized poly(L-IMCI) in Table 3, entry 3.

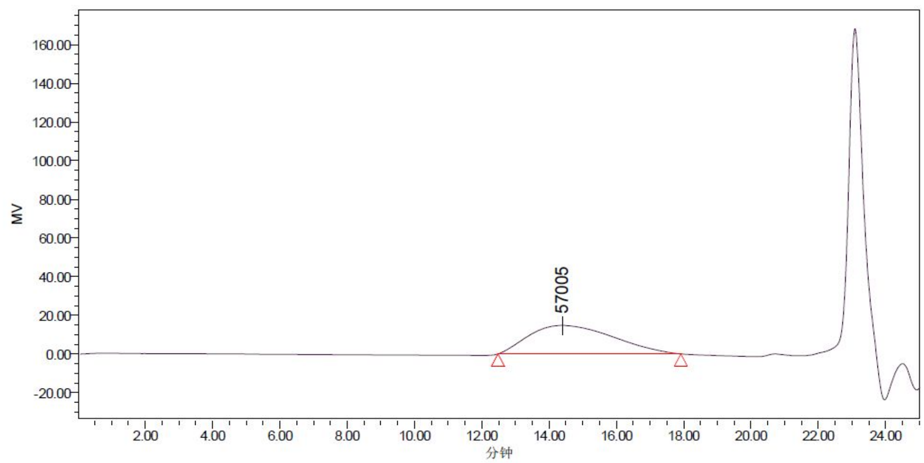

GPC Results

	Dist Name	Elution Volume (ml)	Retention Time (min)	Adjusted RT (min)	Mn	Mw	MP	Mz	Mz+1	Mz/Mw	Mz+1/Mw
1		14.408	14.408	14.408	30620	69992	57005	147851	236310	2.112394	3.376241

Figure S75. GPC curve of C_6H_3-1,3,5-$(Me_2Si)_3$-end-functionalized poly(D-IMCI-*co*-ITPPA) in Table 3, entry 4.

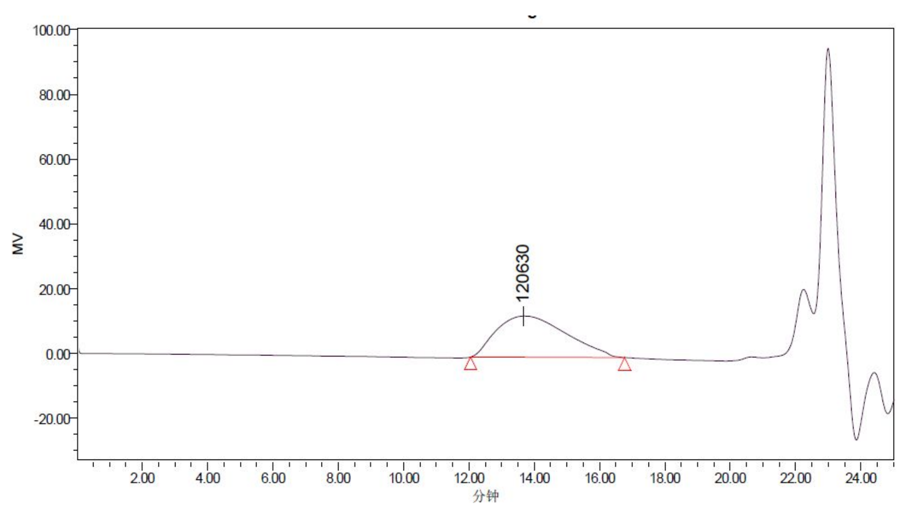

GPC Results

	Dist Name	Elution Volume (ml)	Retention Time (min)	Adjusted RT (min)	Mn	Mw	MP	Mz	Mz+1	Mz/Mw
1		13.681	13.681	13.681	61084	143429	120630	300062	469015	2.092061

Figure S76. GPC curve of C_6H_3-1,3,5-$(Me_2Si)_3$-end-functionalized poly(D-IMCI-*co*-ITPPA) in Table 3, entry 5.

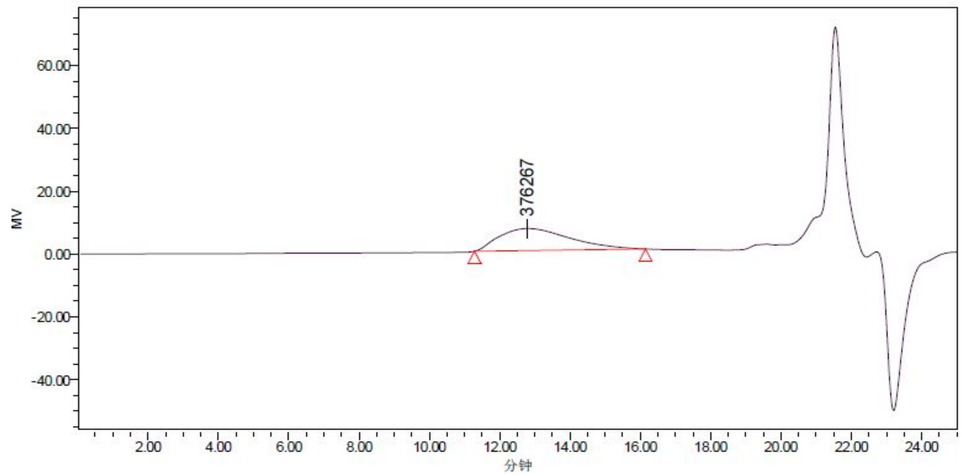

GPC Results

	Dist Name	Elution Volume (ml)	Retention Time (min)	Adjusted RT (min)	Mn	Mw	MP	Mz	Mz+1	Mz/Mw
1		12.800	12.800	12.800	142082	524779	376267	1376036	2241342	2.622126

Figure S77. GPC curve of C_6H_3-1,3,5-$(Me_2Si)_3$-end-functionalized poly(D-IMCI-*co*-ITPPA) in Table 3, entry 6.

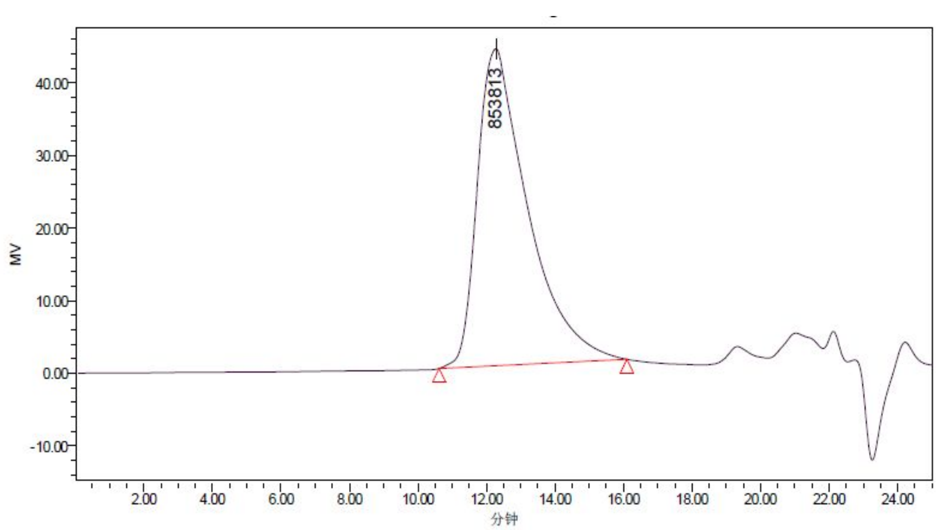

GPC Results

	Dist Name	Elution Volume (ml)	Retention Time (min)	Adjusted RT (min)	Mn	Mw	MP	Mz	Mz+1	Mz/Mw
1		12.278	12.278	12.278	251163	925273	853813	2518422	6204822	2.721816

Figure S78. GPC curve of C_6H_3-1,3,5-$(Me_2Si)_3$-end-functionalized poly(D-IMCI-*co*-ITPPA) in Table 3, entry 7.

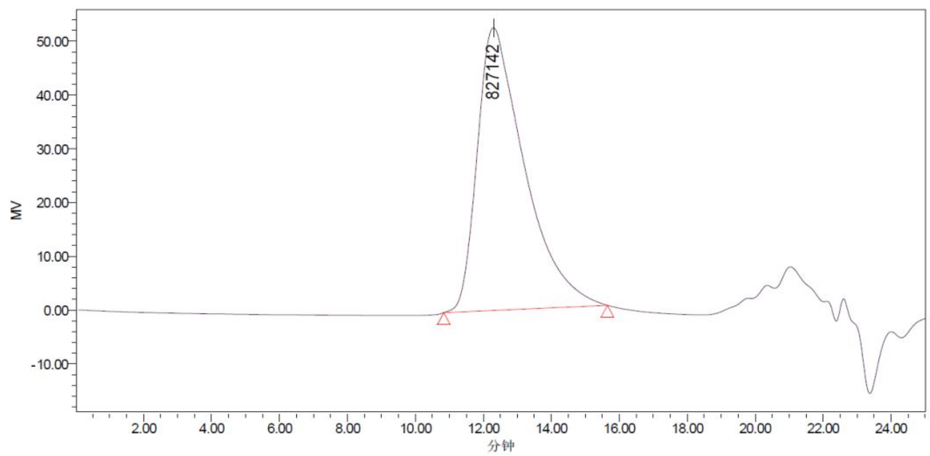

GPC Results

	Dist Name	Elution Volume (ml)	Retention Time (min)	Adjusted RT (min)	Mn	Mw	MP	Mz	Mz+1	Mz/Mw
1		12.297	12.297	12.297	270146	809970	827142	1831794	3505487	2.261558

Figure S79. GPC curve of C_6H_3-1,3,5-$(Me_2Si)_3$-end-functionalized poly(D-IMCI-*co*-ITPPA) in Table 3, entry 8.

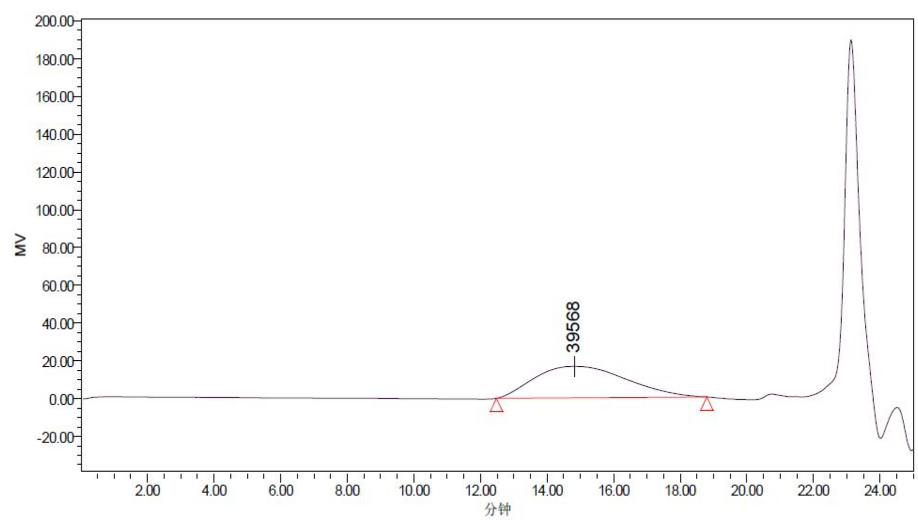

GPC Results

	Dist Name	Elution Volume (ml)	Retention Time (min)	Adjusted RT (min)	Mn	Mw	MP	Mz	Mz+1	Mz/Mw	Mz+1/Mw
1		14.821	14.821	14.821	22567	55195	39568	126988	216504	2.300719	3.922520

Figure S80. GPC curve of C_6H_3-1,3,5-$(Me_2Si)_3$-end-functionalized poly(L-IMCI-*co*-ITPPA) in Table 3, entry 9.

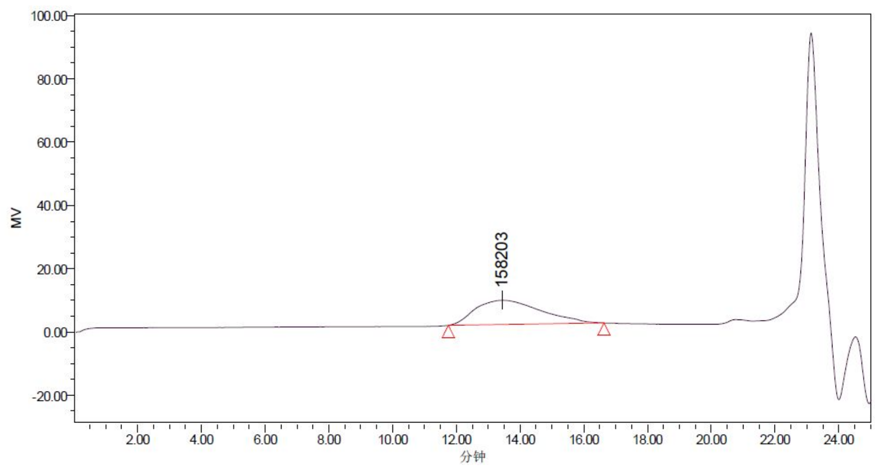

GPC Results

	Dist Name	Elution Volume (ml)	Retention Time (min)	Adjusted RT (min)	Mn	Mw	MP	Mz	Mz+1	Mz/Mw
1		13.450	13.450	13.450	78223	205982	158203	465004	763082	2.257500

Figure S81. GPC curve of C_6H_3-1,3,5-$(Me_2Si)_3$-end-functionalized poly(L-IMCI-*co*-ITPPA) in Table 3, entry 10.

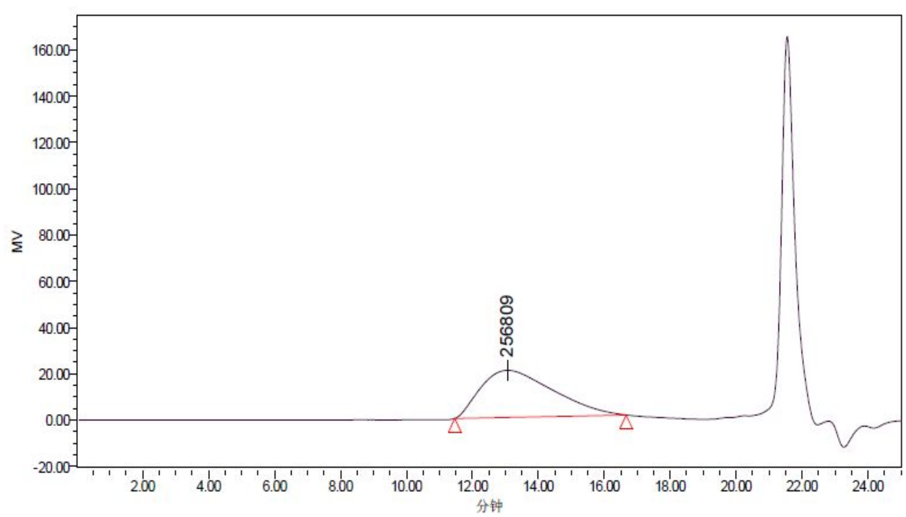

GPC Results

	Dist Name	Elution Volume (ml)	Retention Time (min)	Adjusted RT (min)	Mn	Mw	MP	Mz	Mz+1	Mz/Mw
1		13.072	13.072	13.072	91079	324849	256809	865924	1446682	2.665616

Figure S82. GPC curve of C_6H_3-1,3,5-$(Me_2Si)_3$-end-functionalized poly(L-IMCI-*co*-ITPPA) in Table 3, entry 11.

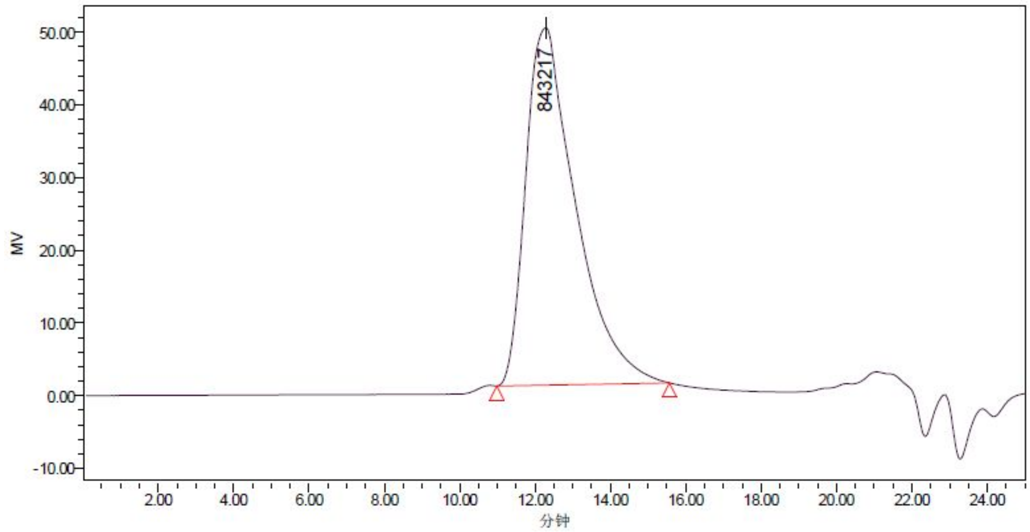

GPC Results

	Dist Name	Elution Volume (ml)	Retention Time (min)	Adjusted RT (min)	Mn	Mw	MP	Mz	Mz+1	Mz/Mw
1		12.285	12.285	12.285	323685	923617	843217	1871372	2980905	2.026134

Figure S83. GPC curve of C_6H_3-1,3,5-$(Me_2Si)_3$-end-functionalized poly(L-IMCI-*co*-ITPPA) in Table 3, entry 12.

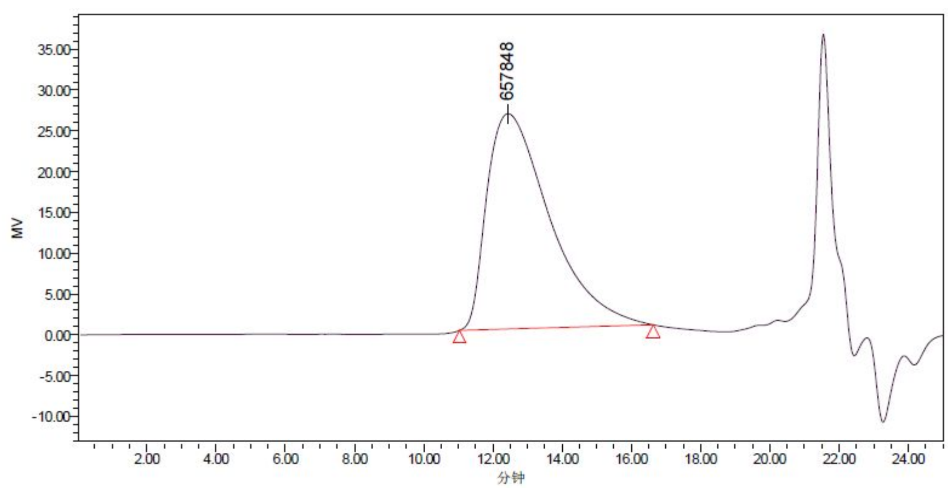

GPC Results

	Dist Name	Elution Volume (ml)	Retention Time (min)	Adjusted RT (min)	Mn	Mw	MP	Mz	Mz+1	Mz/Mw
1		12.436	12.436	12.436	162105	659013	657848	1618757	2721924	2.456336

Figure S84.GPC curve of C_6H_3-1,3,5-$(Me_2Si)_3$-end-functionalized poly(L-IMCI-*co*-ITPPA) in Table 3, entry 13.

COMPUTATIONALMETHODS

All calculations presented in this paper were performed using density functional theory (DFT) with the hybrid functional B3LYP[5–7] as implemented in Gaussian 09 package.[8] Geometry optimizations were carried out with the 6-31G(d, p) basis set. On the basis of the optimized geometries, more accurate energies were obtained by performing single-point calculations with a larger 6-311+G (2d, 2p) basis set. Using an empirical formula by Grimme et al,[9-12]dispersion effects were taken into account throughout geometry optimizations and single-point calculations. Solvation effects were also considered throughout geometry optimizations and single-point calculations, using a conductor-like polarizable continuum model (CPCM)[13-16]method with chlorobenzene as the solvent. Frequency calculations were performed at the same level of theory as in the optimizations to further confirm the nature of stationary points and to obtain zero-point energies (ZPE) and entropy effects. The energies reported in this paper are the free energies which have been corrected for dispersion, solvation, ZPE, and entropy effects.

Density functional calculations

Initiation

We first considered which species is the one essentially initiating the polymerization. The adduct of Ph_3C^+ and a substrate **a** (see $Ph_3C\text{-}(a)_1^+$ in Figure S85) was optimized, having an energy 1.6 kcal/mol higher than the reactant state of Ph_3C^+ + **a** (Figure S86). This indicates that Ph_3C^+ is an effective species to initiate the polymerization, especially considering that no transition state exists during the addition between Ph_3C^+ and **a** because the nature of this step is a simple one bond formation.

The species of A^+ (Figure S87) was also taken into account as an initiating species. Its formation should be activated by Ph_3C^+ via a hydride transfer transition state (see $\mathbf{TS_A}$ in Figure S85), which shows a barrier of 16.4 kcal/mol (Figure S87). Although such an activation is energetically accessible, the subsequent addition of the substrate **a** is unreachable with an accumulated barrier of 28.6 kcal/mol (see **TS1’** in Figure

S88 for structures and Figure S87 for energies). This means that A^+ is unable to work as a species to initiate the polymerization, at least in the first polymer chain.

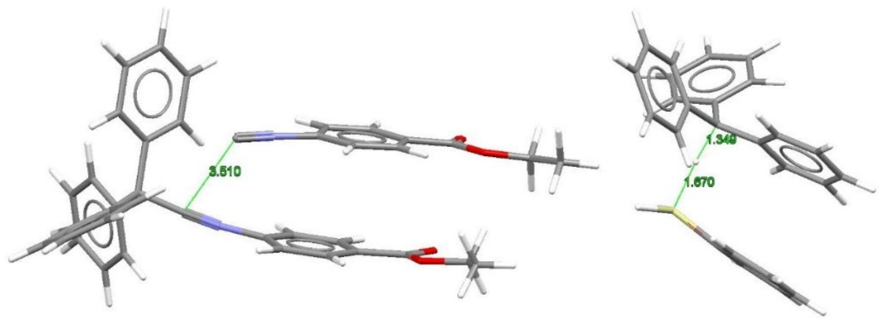

a TS$_A$

Figure S85. Optimized structures of the adduct between Ph_3C^+ and a substrate **a** ($Ph_3C\text{-}(a)_1^+$) and the transition state (**TS$_A$**) for the A^+ formation activated by Ph_3C^+.

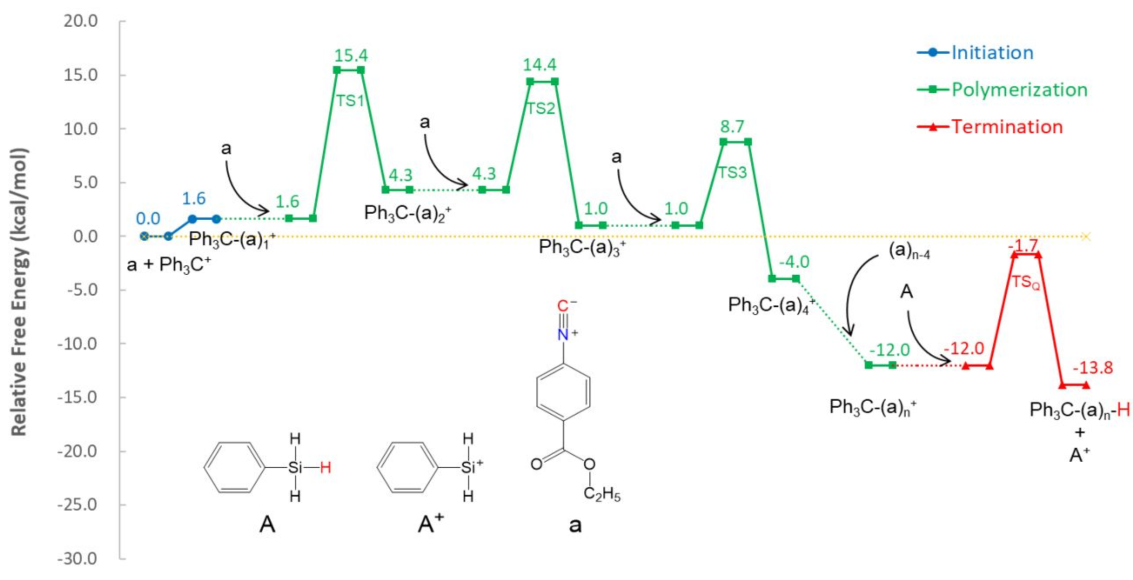

Figure S86. Free energy profile for the polymerization initiated by Ph_3C^+.

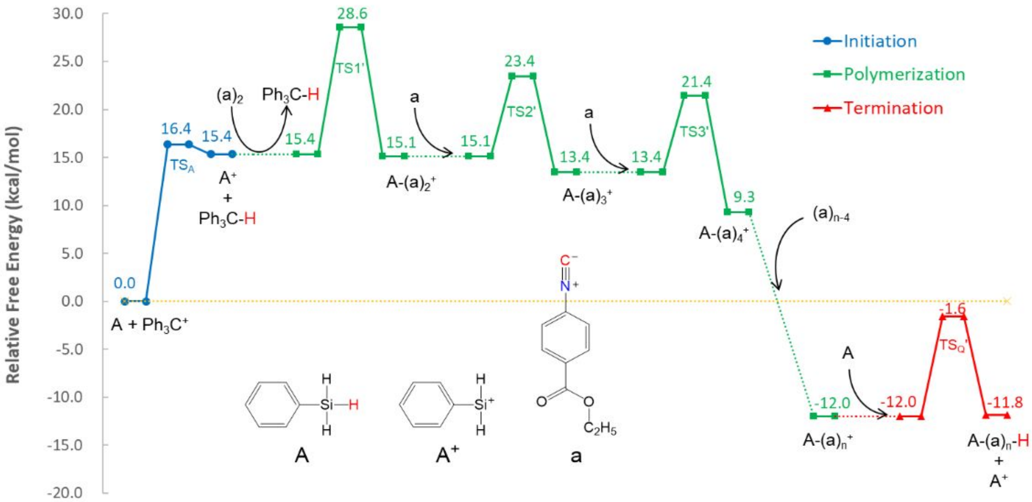

Figure S87. Free energy profile for the polymerization initiated by A^+.

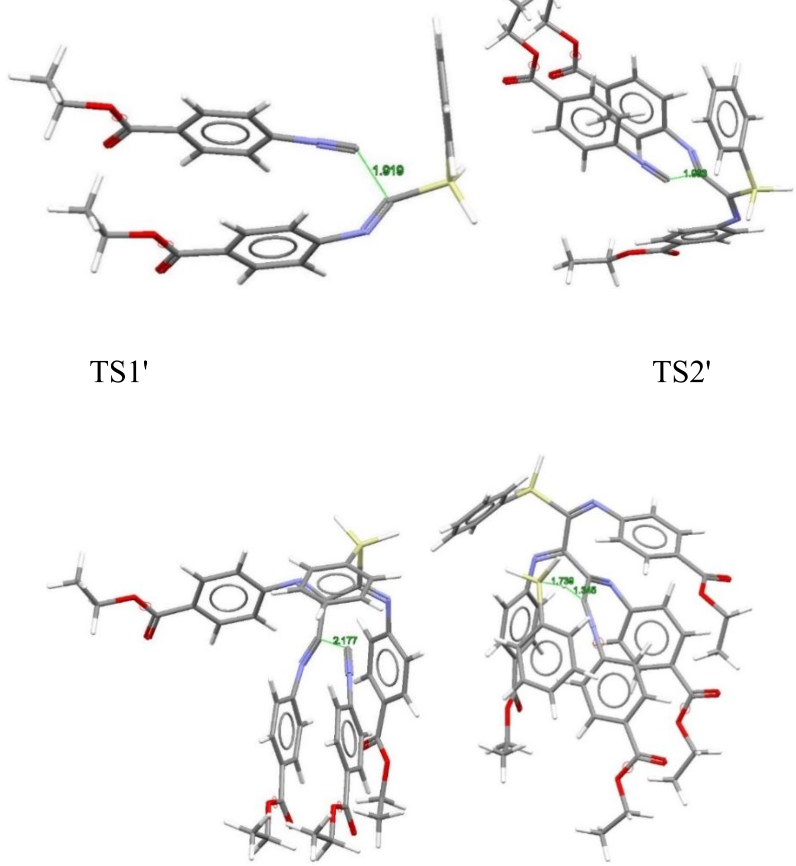

TS1' TS2'

TS3' TSQ'

Figure S88. Optimized structures of stationary points in the polymerization initiated by A^+.

Polymerization and termination

Once the adduct of $Ph_3C\text{-}(a)_1^+$ is formed, it is able to accept the addition of the second substrate **a** via a C-C bond formation transition state (see **TS1** in Figure S89 for structures and Figure S86 for energies). The barrier for this step is quite feasible, with a value of 15.4 kcal/mol accumulated from the initial state of Ph_3C^+ + **a** (Figure S86). The subsequent additions of the third and fourth substrates (via **TS2** and **TS3** in Figure S89, respectively) are both energetically reachable with a little exothermicity (see Figure S86 for energies). It is expected that the following polymerization steps should have the same nature with reasonable barrier and exothermicity, making the overall polymerization reaction energetically feasible. With an adequate number (estimated as n in Figure S86) of substrates polymerized, the accumulated exothermicity should be sufficient for the final chain termination through a hydride transfer transition state from an A to the cyano carbon of the late substrate in the chain (see $\mathbf{TS_Q}$ in Figure S89 for structures and Figure S86 for energies), which has a barrier of 10.3 kcal/mol. In summary, Ph_3C^+ is an effective species to initiate the polymerization, which is able to be terminated by A.

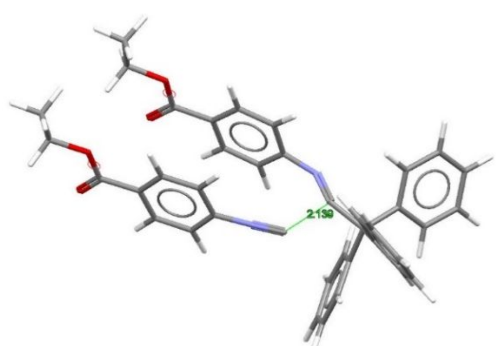

TS1

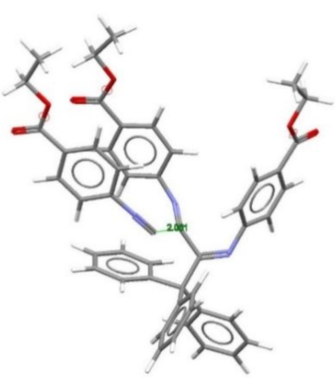

TS2

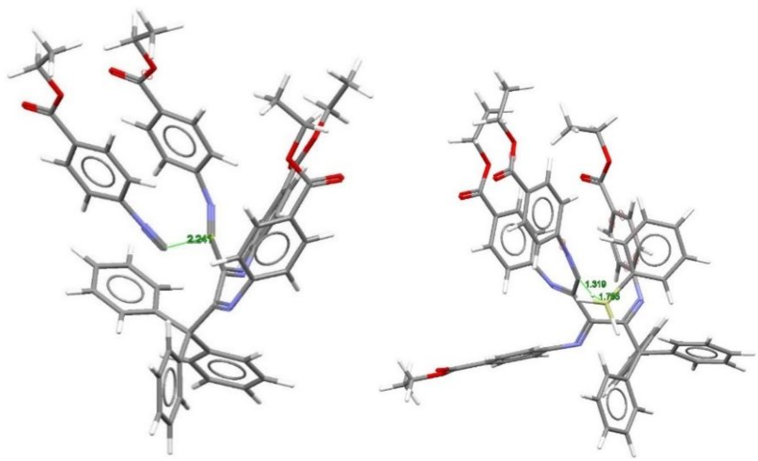

TS3 TSQ

Figure 89. Optimized structures of stationary points in the polymerization initiated by Ph_3C^+.

Interestingly, the termination step in the Ph_3C^+-initiated polymerization is slightly exothermic by 1.8 kcal/mol (see red curve in Figure S86), making the A^+ formation quite feasible, unlike the activation by Ph_3C^+described above (see the blue curve in Figure S87). The A^+ obtained from the termination of the Ph_3C^+-initiated polymerization is able to initiate the addition of substrate via **TS1’** with a reasonable barrier of 13.2 kcal/mol. The following addition of more substrates are also shown to have feasible barriers and slight exothermicities (see **TS2’** and **TS3’** in Figure xx4 for structures and the green curve in Figure S87 for energies), making the polymerization sustainable. Such an A^+-initiated polymerization chain can also be terminated by a hydride transfer from an A to the cyano carbon of the late substrate in the chain (see **TS$_Q$’** in Figure xx4 for structures and Figure S87 for energies), which has a barrier of 10.4 kcal/mol.

With these computational results, it can be concluded that the first polymerization chain should be initiated by Ph_3C^+, while the following chains can be initiated by Ph_3C^+ or A^+. The A^+ species is most likely formed in the termination steps of polymerization chains through a hydride transfer from A to the cyano carbon of the late substrate in the chain, instead in the activation by Ph_3C^+.

a

1 C1 3.9307 -0.0336 0.1056

2 C2 4.6797 0.1784 1.4417

3 C3 5.5291 1.2764 1.6016

4 C4 4.5618 -0.7639 2.4716

5 C5 6.2534 1.4292 2.7853

6 H6 5.6288 2.0078 0.8084

7 C7 5.2781 -0.6016 3.6564

8 H8 3.9230 -1.6345 2.3505

9 C9 6.1266 0.4964 3.8156

10 H10 6.9143 2.2824 2.8996

11 H11 5.1751 -1.3340 4.4505

12 H12 6.6858 0.6228 4.7371

13 C13 3.6910 1.2990 -0.6536

14 C14 4.3919 1.5935 -1.8243

15 C15 2.7899 2.2357 -0.1288

16 C16 4.1828 2.8143 -2.4705

17 H17 5.0965 0.8798 -2.2332

18 C18 2.5739 3.4460 -0.7836

19 H19 2.2603 2.0295 0.7972

20 C20 3.2695 3.7369 -1.9600

21 H21 4.7342 3.0373 -3.3783

22 H22 1.8675 4.1603 -0.3730

23 H23 3.1024 4.6790 -2.4722

24 C24 4.5640 -1.1361 -0.7826

25 C25 3.8552 -1.6008 -1.9008

26 C26 5.8345 -1.6436 -0.5031

27 C27 4.4156 -2.5741 -2.7254

28 H28 2.8827 -1.1810 -2.1450

29 C29 6.3946 -2.6116 -1.3405

30 H30 6.3902 -1.2875 0.3557

31 C31 5.6872 -3.0826 -2.4466

32 H32 3.8614 -2.9291 -3.5884

33 H33 7.3853 -2.9967 -1.1214

34 H34 6.1243 -3.8388 -3.0909

35 C35 0.1666 -1.1386 0.8732

36 C36 -0.4801 -2.0151 -0.0060

37 C37 -1.8533 -2.1767 0.1235

38 C38 -2.5550 -1.4765 1.1153

39 C39 -1.8755 -0.6438 2.0126

40 C40 -0.5034 -0.4649 1.9012

41 H41 0.0787 -2.5168 -0.7865

42 H42 -2.3889 -2.8202 -0.5624

43 H43 -2.4411 -0.1146 2.7700

44 H44 0.0372 0.2024 2.5617

45 N45 1.5066 -0.8582 0.6657

46 C46 2.5873 -0.5242 0.4396

47 C47 -4.0483 -1.5280 1.2121

48 O48 -4.6882 -0.9152 2.0482

49 O49 -4.5908 -2.2878 0.2542

50 C50 -6.0457 -2.3412 0.2196

51 H51 -6.3959 -2.8070 1.1452

52 H52 -6.4166 -1.3153 0.1859

53 C53 -6.4339 -3.1326 -1.0110

54 H54 -7.5239 -3.1979 -1.0740

55 H55 -6.0644 -2.6448 -1.9175

56 H56 -6.0290 -4.1475 -0.9690

57 C57 -1.5289 0.9736 -1.4904

58 C58 -2.6767 0.3569 -2.0058

59 C59 -3.9097 0.6228 -1.4212

60 C60 -3.9969 1.4940 -0.3263

61 C61 -2.8435 2.1217 0.1620

62 C62 -1.6063 1.8699 -0.4166

63 H63 -2.5884 -0.3323 -2.8373

64 H64 -4.8029 0.1423 -1.8001

65 H65 -2.9309 2.7921 1.0090

66 H66 -0.7022 2.3348 -0.0408

67 N67 -0.2883 0.6590 -2.0209

68 C68 0.7730 0.3564 -2.4328

69 C69 -5.2869 1.7644 0.3770

70 O70 -5.3857 2.4796 1.3570

71 O71 -6.3258 1.1298 -0.1942

72 C72 -7.6187 1.3074 0.4472

73 H73 -7.5745 0.8370 1.4344

74 H74 -7.7952 2.3770 0.5875

75 C75 -8.6591 0.6699 -0.4506

76 H76 -9.6501 0.7914 -0.0042

77 H77 -8.6629 1.1443 -1.4358

78 H78 -8.4718 -0.3996 -0.5810

TSA

1 Si1 0.6752 0.0534 -2.3839

2 H2 0.1528 -1.1786 -2.9890

3 H3 0.2982 1.3137 -3.0363

4 C39 2.3404 -0.0071 -1.6463

5 C40 2.8190 -1.2009 -1.0621

6 C41 3.1109 1.1717 -1.5302

7 C42 4.0302 -1.2120 -0.3771

8 H43 2.2447 -2.1198 -1.1408

9 C44 4.3298 1.1505 -0.8578

10 H45 2.7527 2.1027 -1.9610

11 C46 4.7826 -0.0370 -0.2734

12 H47 4.3880 -2.1300 0.0776

13 H48 4.9211 2.0570 -0.7777

14 H49 5.7260 -0.0473 0.2640

15 H4 -0.2797 0.0829 -1.0137

16 C5 -0.9437 0.0228 0.1592

17 C6 -1.6886 1.3299 0.1134

18 C7 -1.7460 2.1682 1.2375

19 C8 -2.4091 1.6859 -1.0404

20 C9 -2.5044 3.3401 1.2021

21 H10 -1.2185 1.8964 2.1442

22 C11 -3.1512 2.8613 -1.0786

23 H12 -2.3881 1.0339 -1.9096

24 C13 -3.2003 3.6935 0.0461

25 H14 -2.5477 3.9747 2.0814

26 H15 -3.6918 3.1291 -1.9808

27 H16 -3.7805 4.6105 0.0182

28 C17 0.1941 -0.0718 1.1253

29 C18 0.3604 -1.1789 1.9770

30 C19 1.1355 0.9764 1.1865

31 C20 1.4383 -1.2331 2.8593

32 H21 -0.3637 -1.9838 1.9691

33 C22 2.2157 0.9132 2.0577

34 H23 1.0205 1.8365 0.5360

35 C24 2.3728 -0.1964 2.8948

36 H25 1.5461 -2.0878 3.5193

37 H26 2.9403 1.7199 2.0757

38 H27 3.2180 -0.2488 3.5740

39 C28 -1.7809 -1.2088 -0.0506

40 C29 -1.1784 -2.4229 -0.4291

41 C30 -3.1686 -1.1788 0.1617

42 C31 -1.9404 -3.5738 -0.5972

43 H32 -0.1055 -2.4640 -0.5883

44 C33 -3.9297 -2.3386 0.0074

45 H34 -3.6498 -0.2571 0.4658

46 C35 -3.3222 -3.5340 -0.3778

47 H36 -1.4603 -4.4993 -0.8983

48 H37 -4.9996 -2.3028 0.1862

49 H38 -3.9188 -4.4315 -0.5079

TS1'

1 Si1 -2.3979 0.8078 1.5743

2 H2 -1.3459 0.1622 2.3728

3 H3 -2.3584 2.2775 1.5948

4 C4 -4.0895 0.1085 1.8129

5 C5 -4.2576 -1.2399 2.1849

6 C6 -5.2317 0.8968 1.5682

7 C7 -5.5356 -1.7845 2.3085

8 H8 -3.3911 -1.8661 2.3827

9 C9 -6.5087 0.3486 1.6927

10 H10 -5.1257 1.9405 1.2849

11 C11 -6.6599 -0.9909 2.0608

12 H12 -5.6556 -2.8235 2.5995

13 H13 -7.3827 0.9649 1.5061

14 H14 -7.6542 -1.4161 2.1592

15 C15 -0.9688 -0.5153 -2.2838

16 C16 -1.7085 -1.5772 -2.8223

17 C17 -1.6470 -1.8080 -4.1920

18 C18 -0.8464 -0.9974 -5.0075

19 C19 -0.0594 0.0136 -4.4376

20 C20 -0.1066 0.2594 -3.0714

21 H21 -2.3481 -2.1730 -2.1813

22 H22 -2.2452 -2.5943 -4.6347

23 H23 0.5625 0.6205 -5.0856

24 H24 0.4702 1.0591 -2.6215

25 N25 -1.1566 -0.1791 -0.9406

26 C26 -1.9471 0.4025 -0.2382

27 C27 -0.8329 -1.1391 -6.4957

28 O28 -0.1297 -0.4710 -7.2322

29 O29 -1.7041 -2.0646 -6.9228

30 C30 -1.7783 -2.2762 -8.3601

31 H31 -2.0242 -1.3232 -8.8362

32 H32 -0.7940 -2.5940 -8.7161

33 C33 -2.8447 -3.3288 -8.5878

34 H34 -2.9629 -3.5095 -9.6602

35 H35 -2.5713 -4.2719 -8.1067

36 H36 -3.8035 -2.9947 -8.1826

37 C37 -3.8849 0.7728 -3.7974

38 C38 -4.8131 -0.2043 -4.1853

39 C39 -4.9958 -0.4490 -5.5403

40 C40 -4.2589 0.2717 -6.4920

41 C41 -3.3485 1.2554 -6.0849

42 C42 -3.1544 1.5165 -4.7345

43 H43 -5.3563 -0.7645 -3.4333

44 H44 -5.6998 -1.2053 -5.8642

45 H45 -2.7853 1.7952 -6.8371

46 H46 -2.4392 2.2582 -4.4004

47 N47 -3.6273 0.9586 -2.4509

48 C48 -3.3782 1.0922 -1.3154

49 C49 -4.4002 0.0234 -7.9601

50 O50 -3.7299 0.5917 -8.8049

51 O51 -5.3331 -0.8973 -8.2389

52 C52 -5.5572 -1.1828 -9.6488

53 H53 -5.8940 -0.2624 -10.1346

54 H54 -4.6047 -1.4747 -10.0994

55 C55 -6.5903 -2.2874 -9.7216

56 H56 -6.7982 -2.5238 -10.7691

57 H57 -6.2269 -3.1938 -9.2289

58 H58 -7.5245 -1.9795 -9.2439

TS2'

1 Si1 -3.2060 1.0241 0.9868

2 H2 -2.8206 -0.2951 1.5187

3 H3 -2.7691 2.1247 1.8631

4 C4 -5.0185 1.0676 0.5659

5 C5 -5.7922 -0.1076 0.6086

6 C6 -5.6296 2.2571 0.1211

7 C7 -7.1330 -0.0969 0.2162

8 H8 -5.3468 -1.0397 0.9464

9 C9 -6.9675 2.2678 -0.2777

10 H10 -5.0610 3.1834 0.0807

11 C11 -7.7192 1.0889 -0.2342

12 H12 -7.7176 -1.0110 0.2622

13 H13 -7.4245 3.1929 -0.6163

14 H14 -8.7603 1.0976 -0.5429

15 C15 -0.1901 1.6054 -1.8029

16 C16 -0.2962 0.6582 -2.8401

17 C17 0.4932 0.7870 -3.9775

18 C18 1.3890 1.8594 -4.0933

19 C19 1.5145 2.7815 -3.0431

20 C20 0.7514 2.6448 -1.8917

21 H21 -0.9614 -0.1930 -2.7353

22 H22 0.4215 0.0567 -4.7746

23 H23 2.2239 3.5950 -3.1442

24 H24 0.8456 3.3457 -1.0695

25 N25 -0.9696 1.5294 -0.6385

26 C26 -2.2266 1.2864 -0.6427

27 C27 2.2422 2.0547 -5.3035

28 O28 3.0422 2.9657 -5.4288

29 O29 2.0240 1.1175 -6.2400

30 C30 2.8084 1.2293 -7.4573

31 H31 2.6095 2.2049 -7.9110

32 H32 3.8694 1.1916 -7.1924

33 C33 2.3998 0.0819 -8.3587

34 H34 2.9683 0.1276 -9.2920

35 H35 2.6003 -0.8801 -7.8784

36 H36 1.3344 0.1373 -8.5998

37 C37 -4.1721 1.9485 -3.9338

38 C38 -5.5602 2.0943 -3.8147

39 C39 -6.3473 1.8932 -4.9427

40 C40 -5.7514 1.5680 -6.1688

41 C41 -4.3545 1.4963 -6.2782

42 C42 -3.5498 1.6933 -5.1644

43 H43 -6.0031 2.3019 -2.8474

44 H44 -7.4255 1.9543 -4.8664

45 H45 -3.9162 1.2541 -7.2395

46 H46 -2.4705 1.6073 -5.2199

47 N47 -3.3934 1.9746 -2.7795

48 C48 -3.0046 1.2546 -1.9023

49 C49 -6.5634 1.2421 -7.3817

50 O50 -6.0783 0.9577 -8.4620

51 O51 -7.8799 1.2744 -7.1327

52 C52 -8.7615 0.9689 -8.2492

53 H53 -8.5677 1.6868 -9.0513

54 H54 -8.5163 -0.0312 -8.6164

55 C55 -10.1785 1.0598 -7.7194

56 H56 -10.8868 0.8044 -8.5128

57 H57 -10.3205 0.3649 -6.8876

58 H58 -10.4007 2.0720 -7.3703

59 C59 -5.5950 -1.2601 -3.7978

60 C60 -6.9461 -1.1884 -3.4283

61 C61 -7.9131 -1.4945 -4.3770

62 C62 -7.5335 -1.8614 -5.6771

63 C63 -6.1783 -1.9356 -6.0241

64 C64 -5.1963 -1.6371 -5.0875

65 H65 -7.2136 -0.8761 -2.4257

66 H66 -8.9630 -1.4398 -4.1176

67 H67 -5.9089 -2.2126 -7.0365

68 H68 -4.1442 -1.6718 -5.3426

69 N69 -4.6324 -0.8840 -2.8785

70 C70 -3.8435 -0.5443 -2.0819

71 C71 -8.5387 -2.1826 -6.7369

72 O72 -8.2395 -2.4527 -7.8874

73 O73 -9.7987 -2.1322 -6.2831

74 C74 -10.8440 -2.4735 -7.2372

75 H75 -10.7382 -1.8302 -8.1146

76 H76 -10.6907 -3.5088 -7.5556

77 C77 -12.1707 -2.2749 -6.5347

78 H78 -12.9864 -2.5360 -7.2150

79 H79 -12.2415 -2.9114 -5.6484

80 H80 -12.2975 -1.2325 -6.2284

TS3'

1 Si1 -6.2580 0.6503 -1.8228

2 H2 -7.2254 1.7631 -1.7523

3 H3 -6.3540 -0.0442 -3.1187

4 C4 -6.5257 -0.5169 -0.3852

5 C5 -6.9098 -0.0097 0.8707

6 C6 -6.3245 -1.9048 -0.5102

7 C7 -7.0929 -0.8608 1.9651

8 H8 -7.0765 1.0575 0.9989

9 C9 -6.5123 -2.7583 0.5792

10 H10 -6.0147 -2.3209 -1.4646

11 C11 -6.8979 -2.2369 1.8192

12 H12 -7.3967 -0.4519 2.9243

13 H13 -6.3626 -3.8276 0.4613

14 H14 -7.0488 -2.9008 2.6654

15 C15 -3.3868 3.3704 -0.7219

16 C16 -2.8505 3.0122 0.5288

17 C17 -1.7142 3.6525 1.0190

18 C18 -1.1076 4.6666 0.2712

19 C19 -1.7067 5.0870 -0.9308

20 C20 -2.8436 4.4617 -1.4214

21 H21 -3.3470 2.2500 1.1147

22 H22 -1.2822 3.3421 1.9636

23 H23 -1.2379 5.8886 -1.4914

24 H24 -3.2891 4.7706 -2.3605

25 N25 -4.5167 2.7062 -1.2128

26 C26 -4.5493 1.4760 -1.5746

27 C27 0.2161 5.2438 0.6328

28 O28 0.8667 5.9465 -0.1241

29 O29 0.6261 4.8696 1.8595

30 C30 1.9228 5.3525 2.3115

31 H31 2.1605 6.2752 1.7801

32 H32 1.7802 5.5710 3.3719

33 C33 2.9897 4.2913 2.1008

34 H34 3.9497 4.6573 2.4783

35 H35 2.7351 3.3811 2.6511

36 H36 3.1142 4.0487 1.0416

37 C37 -2.7044 -1.6709 -2.1013

38 C38 -2.6229 -2.6358 -1.0846

39 C39 -1.5360 -3.5030 -1.0469

40 C40 -0.5717 -3.4698 -2.0633

41 C41 -0.7517 -2.6144 -3.1587

42 C42 -1.8021 -1.7026 -3.1759

43 H43 -3.3897 -2.6664 -0.3201

44 H44 -1.4233 -4.1999 -0.2253

45 H45 -0.0248 -2.6323 -3.9639

46 H46 -1.9025 -0.9861 -3.9833

47 N47 -3.7025 -0.6735 -1.9993

48 C48 -3.3839 0.5348 -1.7004

49 C49 0.6838 -4.2680 -1.9895

50 O50 1.4237 -4.4802 -2.9324

51 O51 0.9389 -4.6726 -0.7284

52 C52 2.1768 -5.4032 -0.5199

53 H53 2.1186 -6.3514 -1.0627

54 H54 3.0000 -4.8216 -0.9457

55 C55 2.3291 -5.6067 0.9744

56 H56 3.2512 -6.1580 1.1793

57 H57 2.3795 -4.6466 1.4960

58 H58 1.4880 -6.1782 1.3775

59 C59 0.1769 1.6016 -2.2739

60 C60 1.0440 0.5259 -2.5202

61 C61 2.4104 0.6860 -2.3188

62 C62 2.9239 1.9128 -1.8772

63 C63 2.0610 3.0070 -1.7326

64 C64 0.6975 2.8627 -1.9539

65 H65 0.6406 -0.4382 -2.7997

66 H66 3.0736 -0.1609 -2.4465

67 H67 2.4566 3.9651 -1.4142

68 H68 0.0292 3.7007 -1.8347

69 N69 -1.2227 1.4244 -2.3757

70 C70 -1.9319 0.8866 -1.4711

71 C71 4.3403 2.0686 -1.4484

72 O72 4.7829 3.0708 -0.9100

73 O73 5.0678 0.9631 -1.6762

74 C74 6.4441 0.9807 -1.2136

75 H75 6.9795 1.7792 -1.7359

76 H76 6.4487 1.2041 -0.1435

77 C77 7.0194 -0.3900 -1.5113

78 H78 8.0473 -0.4479 -1.1415

79 H79 6.4283 -1.1689 -1.0215

80 H80 7.0277 -0.5866 -2.5870

81 C81 1.0319 -0.0998 0.6144

82 C82 1.5480 -1.3927 0.4228

83 C83 2.8822 -1.6283 0.7254

84 C84 3.6882 -0.6014 1.2350

85 C85 3.1431 0.6726 1.4517

86 C86 1.8184 0.9386 1.1420

87 H87 0.9156 -2.1794 0.0318

88 H88 3.3036 -2.6126 0.5637

89 H89 3.7843 1.4547 1.8406

90 H90 1.3937 1.9268 1.2698

91 N91 -0.2443 0.1654 0.2143

92 C92 -1.3566 0.3599 -0.1715

93 C93 5.1231 -0.8156 1.5750

94 O94 5.8469 0.0475 2.0437

95 O95 5.5332 -2.0645 1.3003

96 C96 6.9090 -2.3863 1.6408

97 H97 7.5677 -1.6577 1.1607

98 H98 7.0277 -2.2877 2.7242

99 C99 7.1644 -3.7988 1.1572

100 H100 8.1859 -4.0959 1.4115

101 H101 6.4714 -4.5022 1.6277

102 H102 7.0453 -3.8644 0.0718

103 Si103 -3.1758 -0.6000 2.0462

104 H104 -3.6572 0.6420 2.6635

105 H105 -4.1861 -1.5119 1.5110

106 C107 -1.6640 -1.3229 2.7683

107 C108 -0.7481 -0.4966 3.4570

108 C109 -1.3106 -2.6651 2.5040

109 C110 0.4867 -0.9979 3.8624

110 H111 -0.9955 0.5422 3.6602

111 C112 -0.0766 -3.1617 2.9117

112 H113 -2.0031 -3.3184 1.9818

113 C114 0.8254 -2.3247 3.5798

114 H115 1.1908 -0.3542 4.3790

115 H116 0.1911 -4.1913 2.6989

116 H117 1.7963 -2.7080 3.8780

117 H106 -2.3823 0.0430 0.6384

TSQ'

1 Si1 -6.2580 0.6503 -1.8228

2 H2 -7.2254 1.7631 -1.7523

3 H3 -6.3540 -0.0442 -3.1187

4 C4 -6.5257 -0.5169 -0.3852

5 C5 -6.9098 -0.0097 0.8707

6 C6 -6.3245 -1.9048 -0.5102

7 C7 -7.0929 -0.8608 1.9651

8 H8 -7.0765 1.0575 0.9989

9 C9 -6.5123 -2.7583 0.5792

10 H10 -6.0147 -2.3209 -1.4646

11 C11 -6.8979 -2.2369 1.8192

12 H12 -7.3967 -0.4519 2.9243

13 H13 -6.3626 -3.8276 0.4613

14 H14 -7.0488 -2.9008 2.6654

15 C15 -3.3868 3.3704 -0.7219

16 C16 -2.8505 3.0122 0.5288

17 C17 -1.7142 3.6525 1.0190

18 C18 -1.1076 4.6666 0.2712

19 C19 -1.7067 5.0870 -0.9308

20 C20 -2.8436 4.4617 -1.4214

21 H21 -3.3470 2.2500 1.1147

22 H22 -1.2822 3.3421 1.9636

23 H23 -1.2379 5.8886 -1.4914

24 H24 -3.2891 4.7706 -2.3605

25 N25 -4.5167 2.7062 -1.2128

26 C26 -4.5493 1.4760 -1.5746

27 C27 0.2161 5.2438 0.6328

28 O28 0.8667 5.9465 -0.1241

29 O29 0.6261 4.8696 1.8595

30 C30 1.9228 5.3525 2.3115

31 H31 2.1605 6.2752 1.7801

32 H32 1.7802 5.5710 3.3719

33 C33 2.9897 4.2913 2.1008

34 H34 3.9497 4.6573 2.4783

35 H35 2.7351 3.3811 2.6511

36 H36 3.1142 4.0487 1.0416

37 C37 -2.7044 -1.6709 -2.1013

38 C38 -2.6229 -2.6358 -1.0846

39 C39 -1.5360 -3.5030 -1.0469

40 C40 -0.5717 -3.4698 -2.0633

41 C41 -0.7517 -2.6144 -3.1587

42 C42 -1.8021 -1.7026 -3.1759

43 H43 -3.3897 -2.6664 -0.3201

44 H44 -1.4233 -4.1999 -0.2253

45 H45 -0.0248 -2.6323 -3.9639

46 H46 -1.9025 -0.9861 -3.9833

47 N47 -3.7025 -0.6735 -1.9993

48 C48 -3.3839 0.5348 -1.7004

49 C49 0.6838 -4.2680 -1.9895

50 O50 1.4237 -4.4802 -2.9324

51 O51 0.9389 -4.6726 -0.7284

52 C52 2.1768 -5.4032 -0.5199

53 H53 2.1186 -6.3514 -1.0627

54 H54 3.0000 -4.8216 -0.9457

55 C55 2.3291 -5.6067 0.9744

56 H56 3.2512 -6.1580 1.1793

57 H57 2.3795 -4.6466 1.4960

58 H58 1.4880 -6.1782 1.3775

59 C59 0.1769 1.6016 -2.2739

60 C60 1.0440 0.5259 -2.5202

61 C61 2.4104 0.6860 -2.3188

62 C62 2.9239 1.9128 -1.8772

63 C63 2.0610 3.0070 -1.7326

64 C64 0.6975 2.8627 -1.9539

65 H65 0.6406 -0.4382 -2.7997

66 H66 3.0736 -0.1609 -2.4465

67 H67 2.4566 3.9651 -1.4142

68 H68 0.0292 3.7007 -1.8347

69 N69 -1.2227 1.4244 -2.3757

70 C70 -1.9319 0.8866 -1.4711

71 C71 4.3403 2.0686 -1.4484

72 O72 4.7829 3.0708 -0.9100

73 O73 5.0678 0.9631 -1.6762

74 C74 6.4441 0.9807 -1.2136

75 H75 6.9795 1.7792 -1.7359

76 H76 6.4487 1.2041 -0.1435

77 C77 7.0194 -0.3900 -1.5113

78 H78 8.0473 -0.4479 -1.1415

79 H79 6.4283 -1.1689 -1.0215

80 H80 7.0277 -0.5866 -2.5870

81 C81 1.0319 -0.0998 0.6144

82 C82 1.5480 -1.3927 0.4228

83 C83 2.8822 -1.6283 0.7254

84 C84 3.6882 -0.6014 1.2350

85 C85 3.1431 0.6726 1.4517

86 C86 1.8184 0.9386 1.1420

87 H87 0.9156 -2.1794 0.0318

88 H88 3.3036 -2.6126 0.5637

89 H89 3.7843 1.4547 1.8406

90 H90 1.3937 1.9268 1.2698

91 N91 -0.2443 0.1654 0.2143

92 C92 -1.3566 0.3599 -0.1715

93 C93 5.1231 -0.8156 1.5750

94 O94 5.8469 0.0475 2.0437

95 O95 5.5332 -2.0645 1.3003

96 C96 6.9090 -2.3863 1.6408

97 H97 7.5677 -1.6577 1.1607

98 H98 7.0277 -2.2877 2.7242

99 C99 7.1644 -3.7988 1.1572

100 H100 8.1859 -4.0959 1.4115

101 H101 6.4714 -4.5022 1.6277

102 H102 7.0453 -3.8644 0.0718

103 Si103 -3.1758 -0.6000 2.0462

104 H104 -3.6572 0.6420 2.6635

105 H105 -4.1861 -1.5119 1.5110

106 C107 -1.6640 -1.3229 2.7683

107 C108 -0.7481 -0.4966 3.4570

108 C109 -1.3106 -2.6651 2.5040

109 C110 0.4867 -0.9979 3.8624

110 H111 -0.9955 0.5422 3.6602

111 C112 -0.0766 -3.1617 2.9117

112 H113 -2.0031 -3.3184 1.9818

113 C114 0.8254 -2.3247 3.5798

114 H115 1.1908 -0.3542 4.3790

115 H116 0.1911 -4.1913 2.6989

116 H117 1.7963 -2.7080 3.8780

117 H106 -2.3823 0.0430 0.6384

TS1

1 C1 3.7941 -0.0178 0.0729

2 C2 4.6931 1.1121 -0.5044

3 C3 5.8245 0.7910 -1.2626

4 C4 4.4597 2.4478 -0.1548

5 C5 6.6980 1.7972 -1.6801

6 H6 6.0299 -0.2384 -1.5304

7 C7 5.3287 3.4506 -0.5810

8 H8 3.6075 2.7149 0.4614

9 C9 6.4512 3.1290 -1.3475

10 H10 7.5707 1.5328 -2.2688

11 H11 5.1300 4.4821 -0.3078

12 H12 7.1286 3.9098 -1.6781

13 C13 3.7717 -1.3055 -0.7927

14 C14 3.8021 -2.5813 -0.2181

15 C15 3.5854 -1.1840 -2.1793

16 C16 3.6921 -3.7167 -1.0234

17 H17 3.9109 -2.6936 0.8530

18 C18 3.4707 -2.3188 -2.9792

19 H19 3.5376 -0.2001 -2.6346

20 C20 3.5287 -3.5903 -2.4029

21 H21 3.7284 -4.7000 -0.5654

22 H22 3.3350 -2.2084 -4.0503

23 H23 3.4416 -4.4751 -3.0254

24 C24 4.2132 -0.2131 1.5386

25 C25 3.4603 0.2957 2.6014

26 C26 5.4489 -0.8178 1.8053

27 C27 3.9224 0.1794 3.9142

28 H28 2.5100 0.7888 2.4211

29 C29 5.9065 -0.9374 3.1155

30 H30 6.0540 -1.1915 0.9861

31 C31 5.1432 -0.4413 4.1759

32 H32 3.3242 0.5765 4.7281

33 H33 6.8628 -1.4139 3.3067

34 H34 5.5015 -0.5335 5.1963

35 C35 0.2339 1.4107 -0.7715

36 C36 -0.4815 2.2598 0.0809

37 C37 -1.8599 2.3421 -0.0724

38 C38 -2.5056 1.5955 -1.0690

39 C39 -1.7597 0.8091 -1.9559

40 C40 -0.3813 0.7134 -1.8195

41 H41 0.0318 2.7972 0.8696

42 H42 -2.4431 2.9569 0.6014

43 H43 -2.2781 0.2453 -2.7220

44 H44 0.2085 0.0750 -2.4668

45 N45 1.5794 1.1670 -0.5157

46 C46 2.3715 0.4244 -0.0385

47 C47 -3.9955 1.5505 -1.1839

48 O48 -4.5882 0.8543 -1.9897

49 O49 -4.5984 2.3311 -0.2780

50 C50 -6.0531 2.3271 -0.2873

51 H51 -6.3927 2.7465 -1.2388

52 H52 -6.3899 1.2909 -0.2275

53 C53 -6.5081 3.1476 0.9010

54 H54 -7.6010 3.1862 0.9228

55 H55 -6.1587 2.7001 1.8359

56 H56 -6.1286 4.1712 0.8388

57 C57 -1.3331 -1.4553 0.6325

58 C58 -2.1944 -0.7407 1.4738

59 C59 -3.5665 -0.8298 1.2626

60 C60 -4.0677 -1.6193 0.2195

61 C61 -3.1903 -2.3418 -0.6009

62 C62 -1.8193 -2.2689 -0.4001

63 H63 -1.7868 -0.1142 2.2578

64 H64 -4.2479 -0.2728 1.8932

65 H65 -3.5996 -2.9475 -1.4008

66 H66 -1.1258 -2.8046 -1.0376

67 N67 0.0364 -1.2962 0.7744

68 C68 1.1935 -1.1256 0.8478

69 C69 -5.5313 -1.7221 -0.0692

70 O70 -5.9967 -2.4026 -0.9639

71 O71 -6.2734 -0.9877 0.7773

72 C72 -7.7159 -1.0689 0.6035

73 H73 -7.9686 -0.6602 -0.3797

74 H74 -8.0072 -2.1226 0.6157

75 C75 -8.3473 -0.2845 1.7346

76 H76 -9.4363 -0.3197 1.6404

77 H77 -8.0693 -0.7094 2.7029

78 H78 -8.0339 0.7626 1.7114

TS2

1 C1 3.8815 -1.3763 0.0199

2 C2 5.3567 -1.2667 -0.4491

3 C3 5.8964 -2.1072 -1.4297

4 C4 6.2202 -0.3773 0.2136

5 C5 7.2505 -2.0322 -1.7703

6 H6 5.2745 -2.8369 -1.9323

7 C7 7.5663 -0.2958 -0.1329

8 H8 5.8400 0.2449 1.0138

9 C9 8.0887 -1.1202 -1.1331

10 H10 7.6433 -2.6960 -2.5345

11 H11 8.2106 0.4053 0.3889

12 H12 9.1394 -1.0602 -1.4001

13 C13 3.0249 -2.3179 -0.8657

14 C14 2.2447 -3.3590 -0.3454

15 C15 2.9293 -2.0388 -2.2421

16 C16 1.4038 -4.1051 -1.1758

17 H17 2.2803 -3.5877 0.7121

18 C18 2.0936 -2.7825 -3.0716

19 H19 3.5105 -1.2241 -2.6635

20 C20 1.3249 -3.8226 -2.5394

21 H21 0.8133 -4.9108 -0.7503

22 H22 2.0402 -2.5480 -4.1299

23 H23 0.6722 -4.4044 -3.1825

24 C24 3.9434 -1.8255 1.5008

25 C25 3.5142 -1.0269 2.5643

26 C26 4.5280 -3.0690 1.7891

27 C27 3.6413 -1.4676 3.8854

28 H28 3.0896 -0.0468 2.3832

29 C29 4.6484 -3.5128 3.1032

30 H30 4.8940 -3.6873 0.9756

31 C31 4.2025 -2.7125 4.1599

32 H32 3.3011 -0.8294 4.6950

33 H33 5.0985 -4.4804 3.3027

34 H34 4.3008 -3.0555 5.1850

35 C35 3.0498 2.3559 -0.0133

36 C36 1.9679 2.6131 0.8502

37 C37 1.3503 3.8582 0.8337

38 C38 1.7952 4.8521 -0.0490

39 C39 2.8889 4.5982 -0.8898

40 C40 3.5320 3.3686 -0.8583

41 H41 1.6332 1.8497 1.5451

42 H42 0.5230 4.0626 1.5026

43 H43 3.2286 5.3826 -1.5565

44 H44 4.3856 3.1646 -1.4949

45 N45 3.7188 1.1264 -0.0166

46 C46 3.1613 -0.0122 -0.0944

47 C47 1.1498 6.1961 -0.1223

48 O48 1.5223 7.0884 -0.8639

49 O49 0.1077 6.3094 0.7179

50 C50 -0.5849 7.5864 0.7158

51 H51 0.1327 8.3719 0.9707

52 H52 -0.9518 7.7817 -0.2963

53 C53 -1.7094 7.4859 1.7256

54 H54 -2.2598 8.4304 1.7578

55 H55 -2.4067 6.6886 1.4531

56 H56 -1.3166 7.2804 2.7254

57 C57 -0.4624 0.3335 -1.4576

58 C58 -1.2315 1.4146 -1.0056

59 C59 -2.6137 1.3319 -1.1155

60 C60 -3.2108 0.1968 -1.6849

61 C61 -2.4153 -0.8325 -2.2049

62 C62 -1.0325 -0.7723 -2.1025

63 H63 -0.7491 2.2650 -0.5379

64 H64 -3.2354 2.1303 -0.7302

65 H65 -2.8972 -1.6951 -2.6491

66 H66 -0.4005 -1.5805 -2.4515

67 N67 0.8982 0.3125 -1.1769

68 C68 1.7023 -0.0765 -0.3847

69 C69 -4.6927 0.0030 -1.6997

70 O70 -5.2372 -0.9923 -2.1455

71 O71 -5.3452 1.0252 -1.1308

72 C72 -6.7940 0.9100 -1.0636

73 H73 -7.1891 0.9471 -2.0831

74 H74 -7.0381 -0.0633 -0.6346

75 C75 -7.2931 2.0553 -0.2086

76 H76 -8.3847 2.0196 -0.1490

77 H77 -6.8885 1.9850 0.8052

78 H78 -7.0037 3.0194 -0.6358

79 C79 -1.7683 -1.7120 1.0935

80 C80 -2.7404 -0.8317 1.5838

81 C81 -4.0822 -1.1688 1.4406

82 C82 -4.4427 -2.3664 0.8095

83 C83 -3.4535 -3.2437 0.3426

84 C84 -2.1103 -2.9268 0.4826

85 H85 -2.4414 0.1022 2.0440

86 H86 -4.8500 -0.4946 1.7987

87 H87 -3.7563 -4.1637 -0.1431

88 H88 -1.3306 -3.5759 0.1014

89 N89 -0.4350 -1.3445 1.1432

90 C90 0.6993 -1.0507 1.1298

91 C91 -5.8715 -2.7525 0.5936

92 O92 -6.2165 -3.7767 0.0349

93 O93 -6.7267 -1.8455 1.0941

94 C94 -8.1430 -2.1504 0.9581

95 H95 -8.3893 -2.1710 -0.1080

96 H96 -8.3235 -3.1484 1.3664

97 C97 -8.9043 -1.0762 1.7064

98 H98 -9.9782 -1.2678 1.6288

99 H99 -8.6286 -1.0719 2.7644

100 H100 -8.7005 -0.0859 1.2902

TS3

1 C1 3.7991 -2.4783 -0.0211

2 C2 5.1854 -1.8911 -0.3821

3 C3 5.7748 -2.1038 -1.6335

4 C4 5.9215 -1.2092 0.5975

5 C5 7.0552 -1.6183 -1.9097

6 H6 5.2400 -2.6551 -2.3981

7 C7 7.1975 -0.7210 0.3231

8 H8 5.4990 -1.0652 1.5863

9 C9 7.7682 -0.9178 -0.9365
10 H10 7.4933 -1.7934 -2.8876
11 H11 7.7454 -0.1884 1.0944
12 H12 8.7608 -0.5355 -1.1538
13 C13 2.9021 -2.6872 -1.2849
14 C14 2.1423 -3.8485 -1.4804
15 C15 2.7706 -1.6623 -2.2437
16 C16 1.2462 -3.9586 -2.5477
17 H17 2.2338 -4.6814 -0.7972
18 C18 1.8660 -1.7624 -3.3004
19 H19 3.4006 -0.7853 -2.1890
20 C20 1.0841 -2.9092 -3.4509
21 H21 0.6711 -4.8721 -2.6635
22 H22 1.7896 -0.9477 -4.0141
23 H23 0.3824 -2.9934 -4.2752
24 C24 3.9743 -3.7928 0.7751
25 C25 2.8943 -4.3639 1.4731
26 C26 5.1940 -4.4794 0.7784
27 C27 3.0349 -5.5705 2.1545
28 H28 1.9318 -3.8671 1.4742
29 C29 5.3370 -5.6911 1.4607
30 H30 6.0464 -4.0735 0.2483
31 C31 4.2613 -6.2403 2.1552
32 H32 2.1841 -5.9871 2.6854
33 H33 6.2957 -6.2006 1.4456
34 H34 4.3729 -7.1793 2.6889
35 C35 2.0833 -0.5732 2.7627
36 C36 0.7557 -0.8670 3.1185
37 C37 -0.0613 0.1344 3.6300
38 C38 0.4521 1.4207 3.8528
39 C39 1.8091 1.6751 3.6087
40 C40 2.6221 0.6911 3.0573
41 H41 0.3662 -1.8619 2.9376
42 H42 -1.1017 -0.0747 3.8498
43 H43 2.2041 2.6633 3.8175
44 H44 3.6580 0.9017 2.8152
45 N45 2.8298 -1.5705 2.0897
46 C46 3.0693 -1.4197 0.8469
47 C47 -0.4033 2.5454 4.3197
48 O48 0.0239 3.5943 4.7674
49 O49 -1.7163 2.2849 4.1498
50 C50 -2.6380 3.3168 4.5948
51 H51 -2.5388 3.4212 5.6796
52 H52 -2.3483 4.2664 4.1367
53 C53 -4.0313 2.8847 4.1878
54 H54 -4.7624 3.6112 4.5535
55 H55 -4.1200 2.8318 3.0993
56 H56 -4.2758 1.9056 4.6091
57 C57 3.2144 2.0317 -0.6864
58 C58 2.3949 2.9622 -0.0218
59 C59 2.2384 4.2374 -0.5513
60 C60 2.8744 4.5881 -1.7503
61 C61 3.7060 3.6614 -2.3964
62 C62 3.9044 2.3995 -1.8552

63 H63 1.9220 2.6974 0.9167

64 H64 1.6192 4.9629 -0.0381

65 H65 4.2050 3.9554 -3.3126

66 H66 4.5704 1.6841 -2.3252

67 N67 3.4652 0.7535 -0.1829

68 C68 2.6252 -0.1295 0.1840

69 C69 2.7147 5.9371 -2.3702

70 O70 3.2519 6.2728 -3.4115

71 O71 1.9099 6.7376 -1.6530

72 C72 1.6932 8.0738 -2.1807

73 H73 2.6626 8.5723 -2.2741

74 H74 1.2618 7.9864 -3.1824

75 C75 0.7691 8.7895 -1.2173

76 H76 0.5791 9.8050 -1.5765

77 H77 -0.1881 8.2668 -1.1357

78 H78 1.2187 8.8530 -0.2225

79 C79 -1.0651 1.0366 -0.4524

80 C80 -1.9025 1.3635 0.6235

81 C81 -3.2730 1.3643 0.4024

82 C82 -3.7885 1.0605 -0.8662

83 C83 -2.9260 0.8097 -1.9405

84 C84 -1.5519 0.7989 -1.7450

85 H85 -1.4935 1.5586 1.6079

86 H86 -3.9507 1.5613 1.2228

87 H87 -3.3478 0.5814 -2.9118

88 H88 -0.8652 0.5536 -2.5465

89 N89 0.2806 0.8135 -0.2125

90 C90 1.1726 0.0862 0.0410

91 C91 -5.2590 0.9258 -1.1072

92 O92 -5.7400 0.6353 -2.1882

93 O93 -5.9715 1.1214 0.0088

94 C94 -7.4148 0.9793 -0.1089

95 H95 -7.7877 1.7837 -0.7497

96 H96 -7.6226 0.0253 -0.5959

97 C97 -7.9829 1.0462 1.2927

98 H98 -9.0733 0.9700 1.2509

99 H99 -7.6016 0.2231 1.9040

100 H100 -7.7225 1.9919 1.7760

101 C101 -2.2497 -2.3175 -0.5059

102 C102 -3.2651 -2.1047 0.4343

103 C103 -4.5910 -2.2171 0.0290

104 C104 -4.8949 -2.5288 -1.3029

105 C105 -3.8638 -2.7527 -2.2263

106 C106 -2.5357 -2.6542 -1.8360

107 H107 -3.0101 -1.8372 1.4528

108 H108 -5.3901 -2.0430 0.7386

109 H109 -4.1216 -2.9930 -3.2510

110 H110 -1.7227 -2.8074 -2.5363

111 N111 -0.9303 -2.1273 -0.1317

112 C112 0.1897 -1.9247 0.1499

113 C113 -6.3027 -2.6285 -1.7965

114 O114 -6.5975 -2.8693 -2.9522

115 O115 -7.2039 -2.4351 -0.8180

116 C116 -8.6030 -2.5574 -1.1982

117 H117 -8.8398 -1.7539 -1.9025

118 H118 -8.7401 -3.5108 -1.7154

119 C119 -9.4206 -2.4712 0.0738

120 H120 -10.4835 -2.5598 -0.1676

121 H121 -9.1528 -3.2786 0.7608

122 H122 -9.2620 -1.5161 0.5817

TSQ

1 C1 4.5515 -1.3926 0.1447

2 C2 5.1279 -0.7964 1.4639

3 C3 5.8389 0.4096 1.5106

4 C4 4.8295 -1.4373 2.6784

5 C5 6.2641 0.9415 2.7291

6 H6 6.0467 0.9513 0.5975

7 C7 5.2526 -0.9070 3.8981

8 H8 4.2623 -2.3622 2.6686

9 C9 5.9740 0.2876 3.9284

10 H10 6.8176 1.8759 2.7372

11 H11 5.0128 -1.4274 4.8204

12 H12 6.3019 0.7067 4.8749

13 C13 5.0884 -0.7305 -1.1403

14 C14 6.4764 -0.6528 -1.3341

15 C15 4.2608 -0.3390 -2.1983

16 C16 7.0120 -0.1609 -2.5237

17 H17 7.1434 -0.9912 -0.5480

18 C18 4.7891 0.1466 -3.3963

19 H19 3.1853 -0.4024 -2.0988

20 C20 6.1704 0.2458 -3.5624

21 H21 8.0901 -0.1043 -2.6412

22 H22 4.1162 0.4506 -4.1930

23 H23 6.5865 0.6280 -4.4894

24 C24 4.9088 -2.8895 -0.0387

25 C25 4.2669 -3.6156 -1.0541

26 C26 5.9382 -3.5164 0.6689

27 C27 4.6108 -4.9350 -1.3290

28 H28 3.4989 -3.1287 -1.6433

29 C29 6.2923 -4.8424 0.3927

30 H30 6.4758 -2.9783 1.4403

31 C31 5.6276 -5.5604 -0.5989

32 H32 4.0973 -5.4758 -2.1194

33 H33 7.0948 -5.3070 0.9581

34 H34 5.9018 -6.5893 -0.8111

35 C35 1.1735 -2.2061 1.5096

36 C36 0.1125 -3.0499 1.1278

37 C37 -1.1079 -2.9673 1.7853

38 C38 -1.2734 -2.0786 2.8608

39 C39 -0.1749 -1.3359 3.3188

40 C40 1.0416 -1.3980 2.6584

41 H41 0.2476 -3.7266 0.2938

42 H42 -1.9407 -3.5768 1.4549

43 H43 -0.2986 -0.6932 4.1835

44 H44 1.8923 -0.8189 3.0024

45 N45 2.3828 -2.2554 0.8205

46 C46 3.0256 -1.2238 0.4105

47 C47 -2.5893 -1.8410 3.5124

48 O48 -2.8053 -0.9057 4.2672

49 O49 -3.5133 -2.7505 3.1498

50 C50 -4.8438 -2.6150 3.7213

51 H51 -5.1906 -3.6413 3.8563

52 H52 -4.7619 -2.1278 4.6943

53 C53 -5.7479 -1.8390 2.7797

54 H54 -6.7478 -1.7568 3.2163

55 H55 -5.3647 -0.8295 2.6067

56 H56 -5.8362 -2.3573 1.8209

57 C57 2.9267 2.4698 -0.0802

58 C58 3.3242 3.4663 0.8257

59 C59 3.0562 4.7999 0.5437

60 C60 2.4339 5.1615 -0.6617

61 C61 2.0869 4.1651 -1.5847

62 C62 2.3241 2.8265 -1.3010

63 H63 3.8183 3.1762 1.7466

64 H64 3.3372 5.5694 1.2530

65 H65 1.6244 4.4572 -2.5213

66 H66 2.0698 2.0545 -2.0201

67 N67 3.2525 1.1420 0.1984

68 C68 2.4360 0.1671 0.3087

69 C69 2.1295 6.5760 -1.0114

70 O70 1.5897 6.9221 -2.0499

71 O71 2.5121 7.4378 -0.0521

72 C72 2.2492 8.8412 -0.3068

73 H73 2.7534 9.1295 -1.2344

74 H74 1.1731 8.9744 -0.4553

75 C75 2.7630 9.6165 0.8898

76 H76 2.5848 10.6855 0.7405

77 H77 2.2502 9.3048 1.8043

78 H78 3.8374 9.4600 1.0219

79 C79 -0.8629 1.8084 0.9146

80 C80 -1.7638 1.4274 1.9222

81 C81 -3.1193 1.6875 1.7567

82 C82 -3.5790 2.3664 0.6188

83 C83 -2.6513 2.8648 -0.3076

84 C84 -1.2960 2.5981 -0.1656

85 H85 -1.4219 0.8641 2.7793

86 H86 -3.8213 1.3266 2.4990

87 H87 -3.0148 3.4165 -1.1672

88 H88 -0.5760 2.9367 -0.9025

89 N89 0.4721 1.3780 0.9642

90 C90 0.9403 0.4061 0.2881

91 C91 -5.0251 2.5087 0.2984

92 O92 -5.4497 3.0874 -0.6885

93 O93 -5.8192 1.8884 1.1904

94 C94 -7.2454 1.9691 0.9282

95 H95 -7.5405 3.0226 0.9354

96 H96 -7.4368 1.5677 -0.0700

97 C97 -7.9502 1.1687 2.0034

98 H98 -9.0332 1.2624 1.8791

99 H99 -7.6850 0.1109 1.9357

100 H100 -7.6854 1.5332 2.9999

101 C101 -2.4641 -0.4817 -1.0632
102 C102 -3.4978 -1.0057 -0.2674
103 C103 -4.8050 -0.9285 -0.7266
104 C104 -5.0917 -0.3190 -1.9567
105 C105 -4.0509 0.1782 -2.7525
106 C106 -2.7360 0.1000 -2.3176
107 H107 -3.2683 -1.4433 0.6954
108 H108 -5.6146 -1.3080 -0.1179
109 H109 -4.2911 0.6462 -3.7002
110 H110 -1.9294 0.5309 -2.8988
111 N111 -1.1999 -0.3842 -0.5458
112 C112 0.0088 -0.4014 -0.5978
113 C113 -6.4910 -0.1490 -2.4509
114 O114 -6.7711 0.3012 -3.5468
115 O115 -7.4020 -0.5392 -1.5435
116 C116 -8.7968 -0.4261 -1.9395
117 H117 -9.0223 0.6315 -2.1070
118 H118 -8.9325 -0.9555 -2.8868
119 C119 -9.6280 -1.0223 -0.8223
120 H120 -10.6887 -0.9588 -1.0814
121 H121 -9.3718 -2.0741 -0.6668
122 H122 -9.4691 -0.4825 0.1148
123 Si123 0.6667 -1.9468 -3.0707
124 H124 -0.1770 -1.0597 -3.8792
125 H125 2.0890 -1.9897 -3.4246
126 C127 -0.0649 -3.5105 -2.4770
127 C128 -1.4467 -3.6112 -2.2056
128 C129 0.7767 -4.6009 -2.1641
129 C130 -1.9671 -4.7653 -1.6247
130 H131 -2.1155 -2.7886 -2.4388
131 C132 0.2489 -5.7576 -1.5942
132 H133 1.8421 -4.5455 -2.3593
133 C134 -1.1199 -5.8353 -1.3151
134 H135 -3.0292 -4.8303 -1.4113
135 H136 0.9035 -6.5900 -1.3574
136 H137 -1.5270 -6.7308 -0.8561
137 H126 -0.6344 -1.0179 -1.582

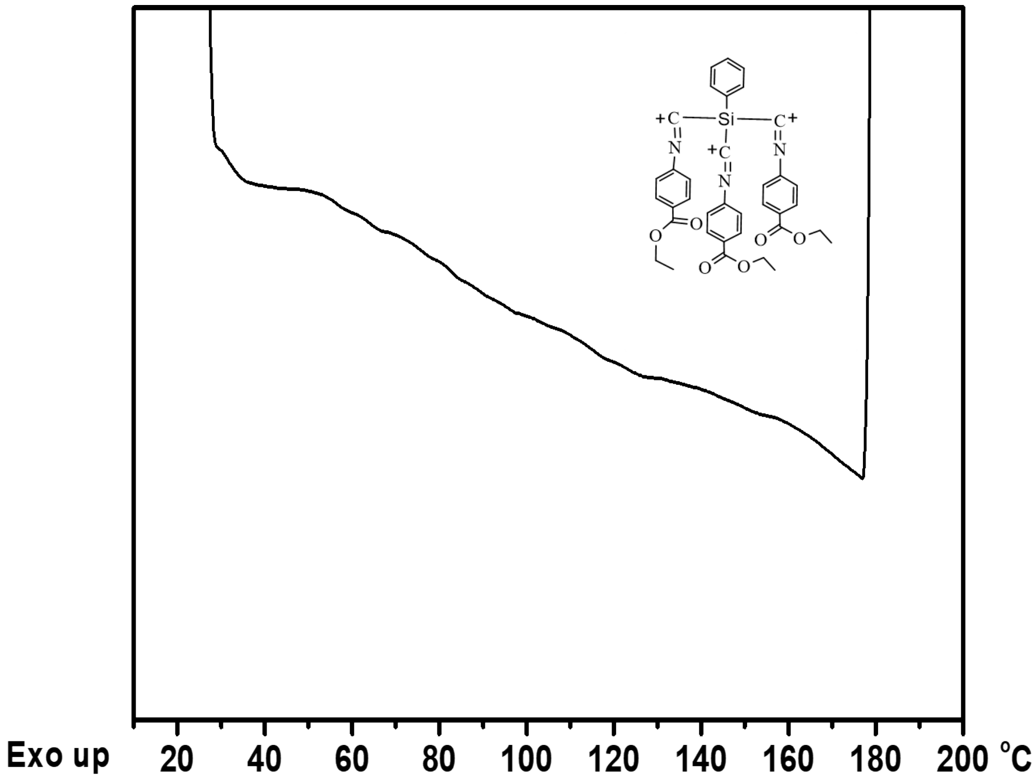

Figure S90. DSC curve of PhSi-end-functionalized star poly(EPI) in Table 3, entry 1.

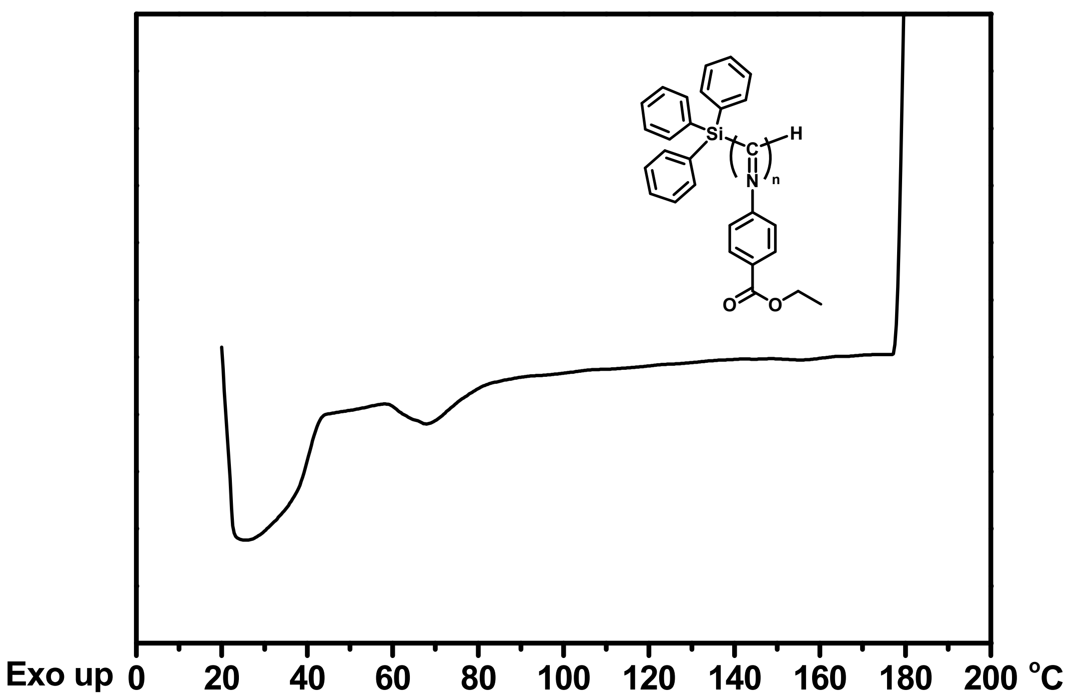

Figure S91. DSC curve of Ph_3Si-end-functionalized poly(EPI) in Table 2, entry 3.

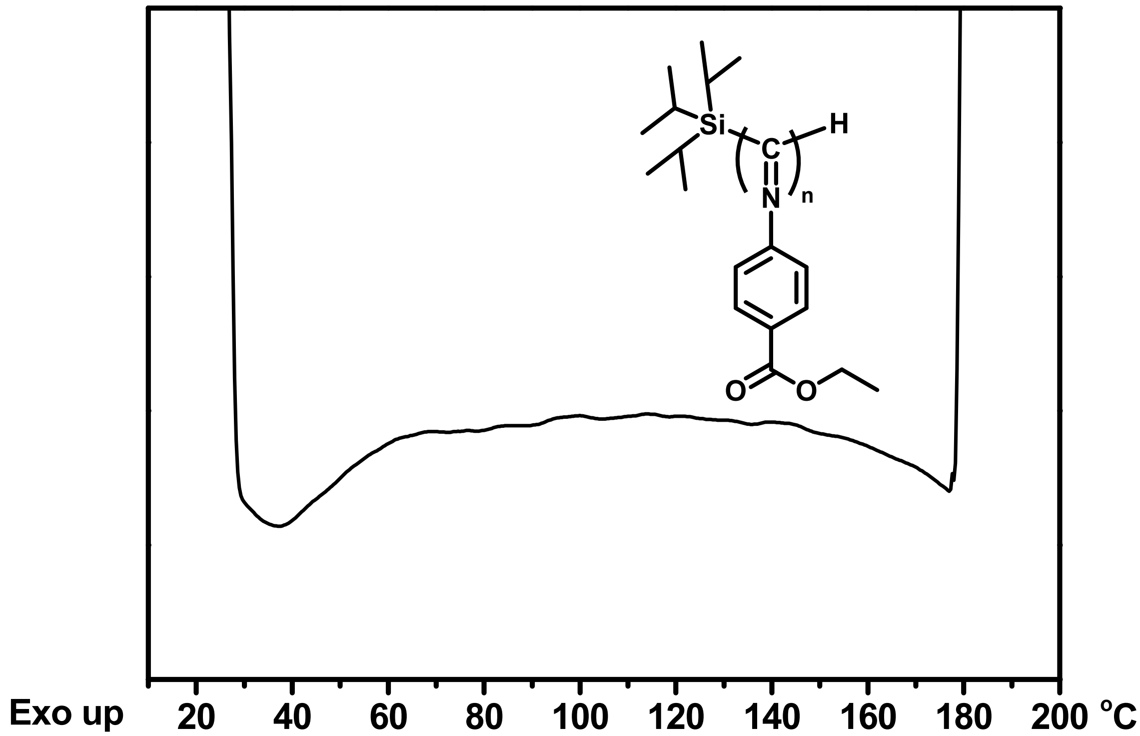

Figure S92. DSC curve of $^{i}Pr_3Si$-end-functionalized poly(EPI) in Table 2, entry 5.

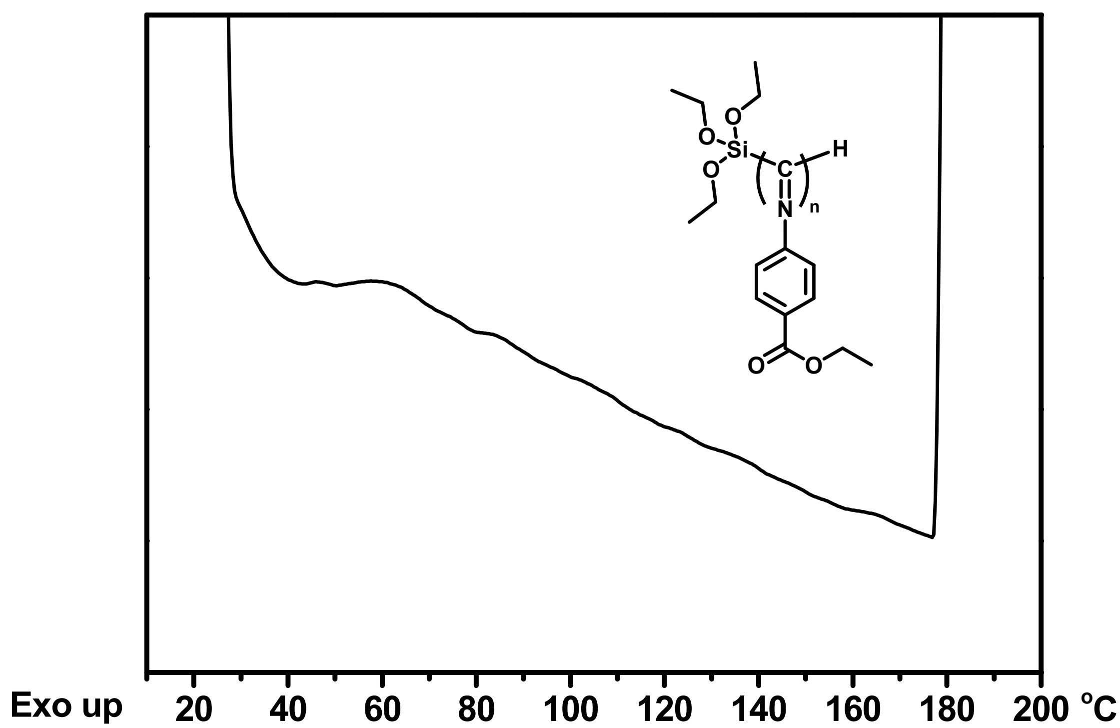

Figure S93. DSC curve of $(OEt)_3Si$-end-functionalized poly(EPI) in Table 2, entry 6.

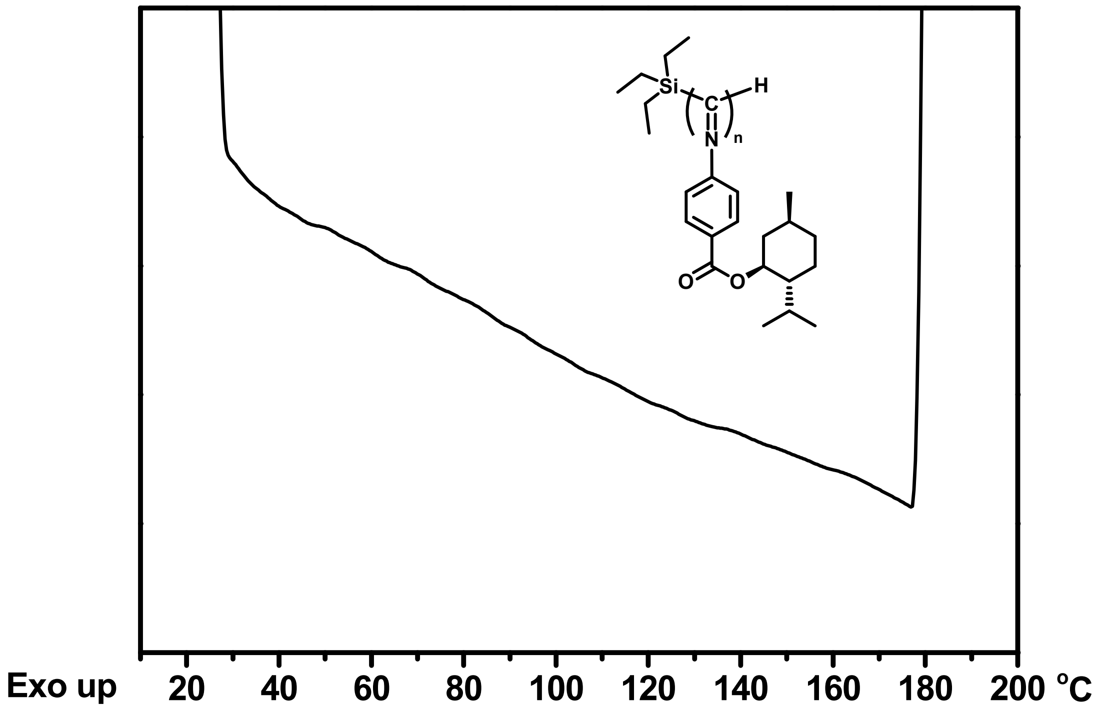

Figure S94. DSC curve of triethylsilane-end-capped Poly(D-IMCI) Table 2, entry 9.

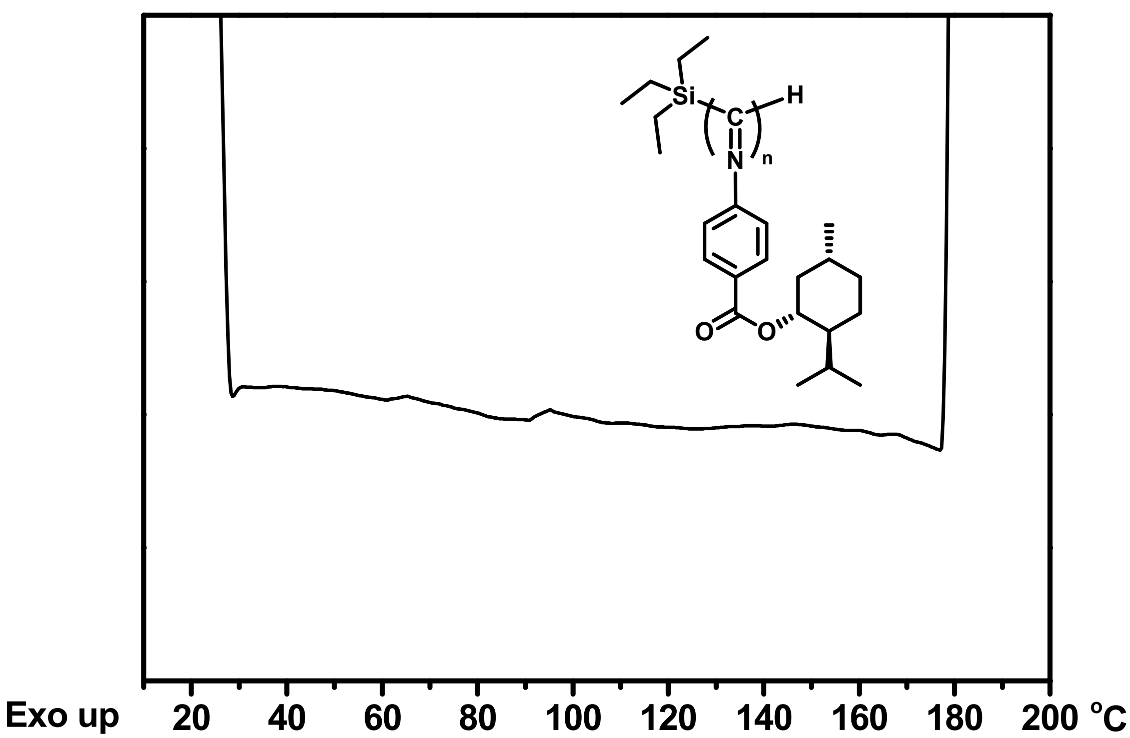

Figure S95. DSC curve of triethylsilane-end-capped Poly(L-IMCI) in Table 2, entry 10.

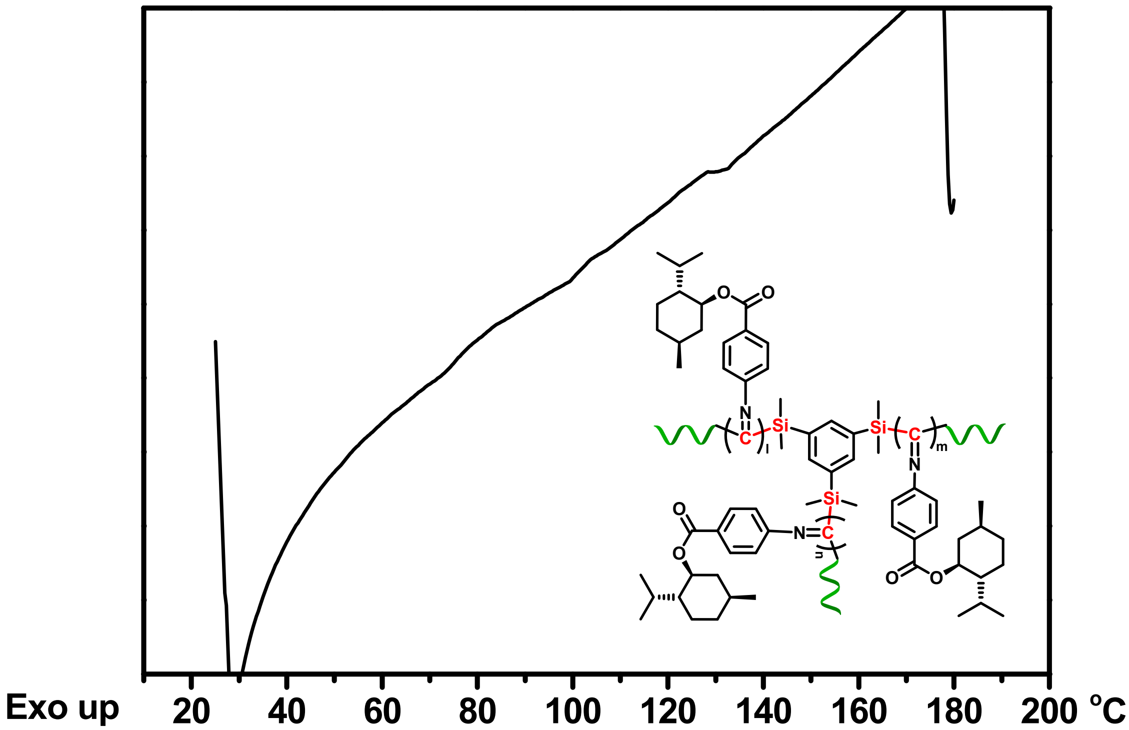

Figure S96. DSC curve of silane-end-capped star Poly(D-IMCI) in Table 3, entry 2.

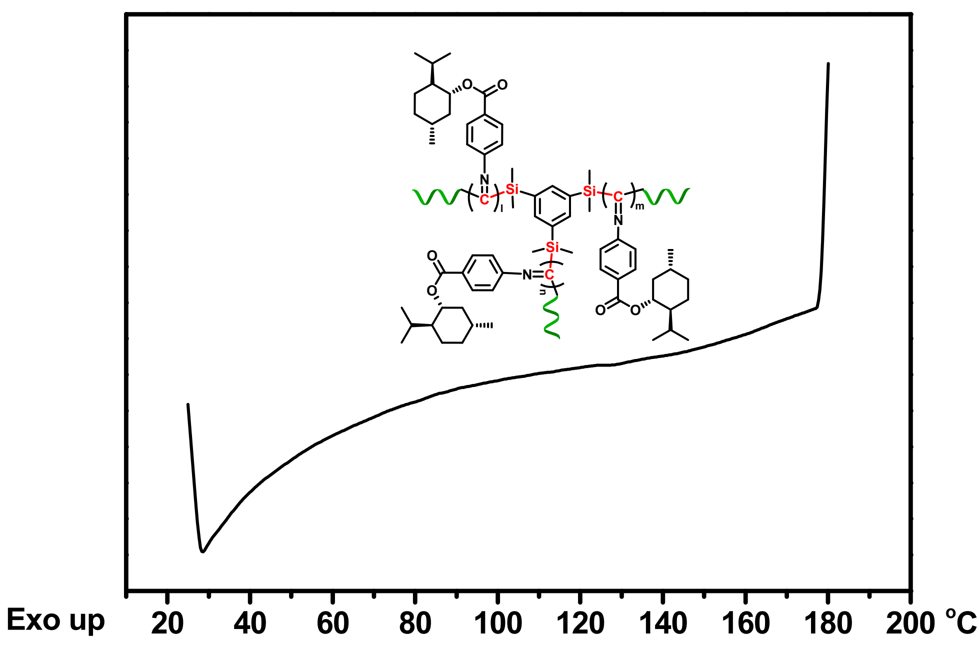

Figure S97. DSC curve of silane-end-capped star Poly(L-IMCI) in Table 3, entry 3.

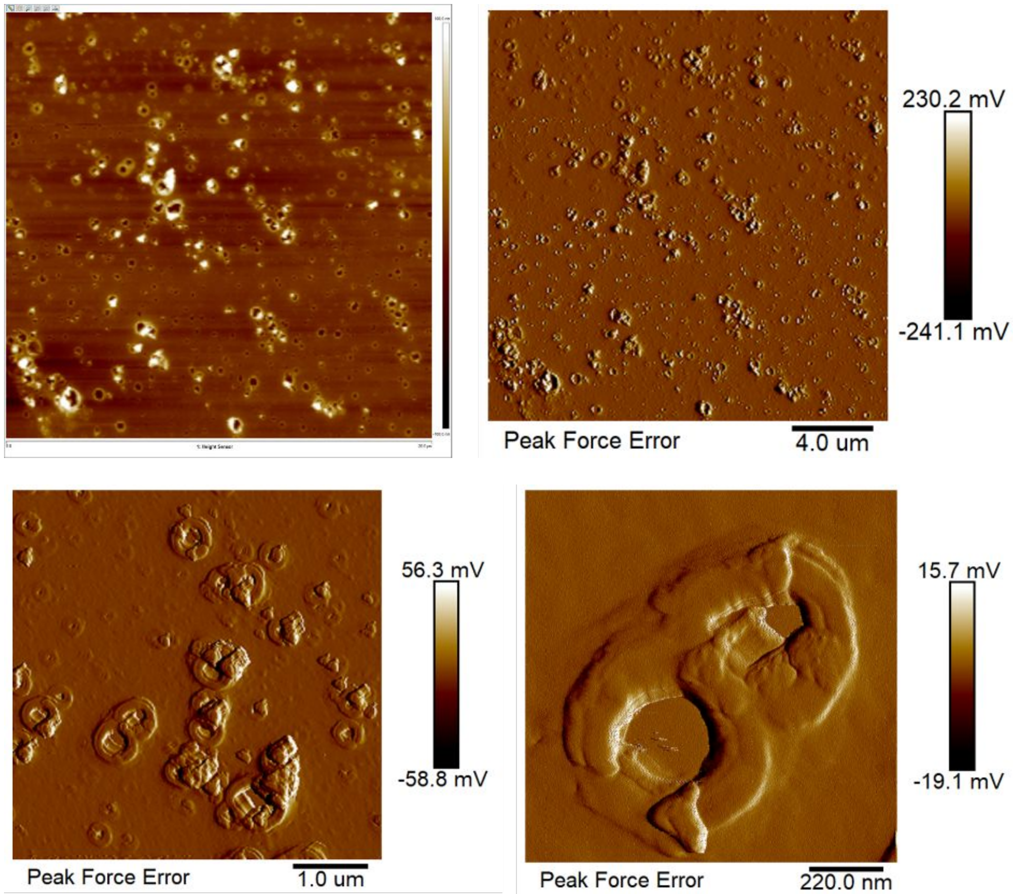

Figure S98. AFM image of silane-end-capped star Poly(L-IMCI) in Table 3, entry 3.

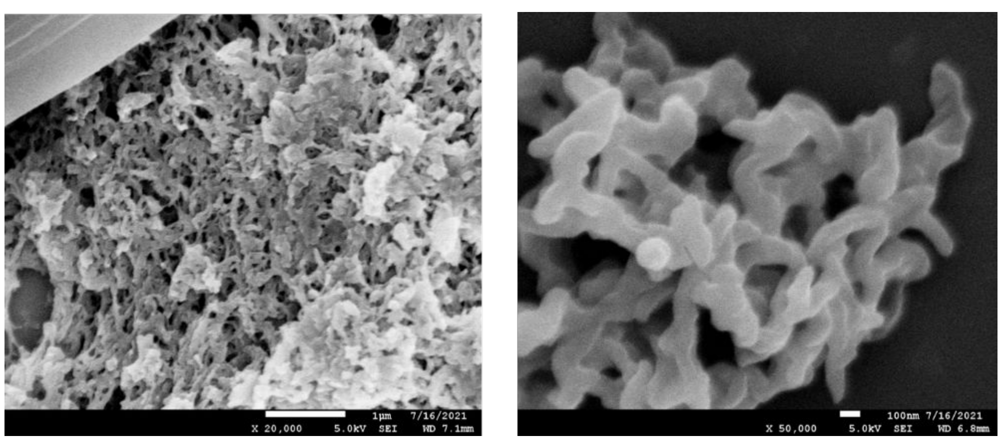

Figure S99. SEM image of silane-end-capped star Poly(L-IMCI) in Table 3, entry 3.

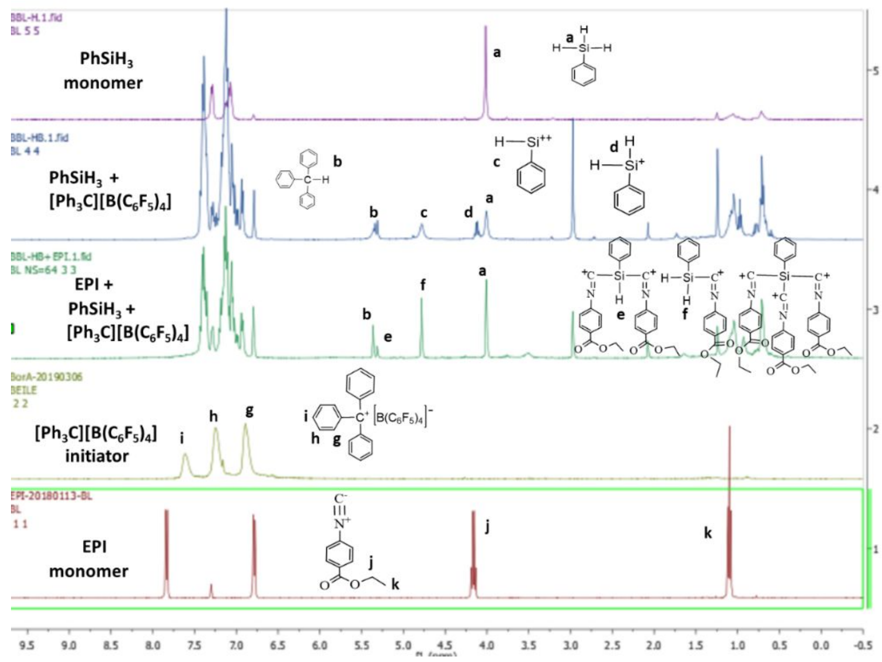

Figure S100. The *in situ* ^{1}H NMR spectra of the polymerization of EPI by the $[Ph_3C][B(C_6F_5)_4]/PhSiH_3$ binary system under the molar ratio of $[EPI]/\{[Ph_3C][B(C_6F_5)_4]\}/[PhSiH_3]$ as 10:1:10 at room temperature in d^8-THF.

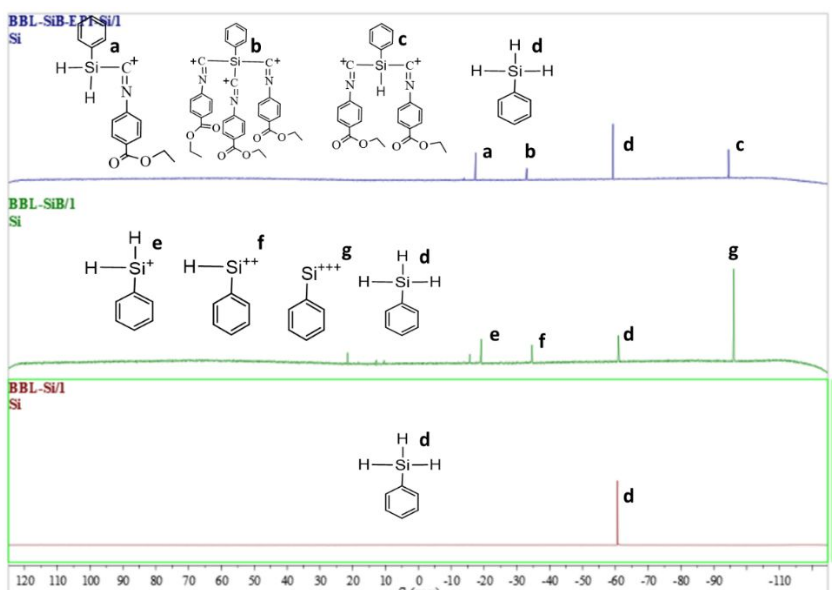

Figure S101. The *in situ* ^{29}Si NMR spectra of the polymerization of EPI by the $[Ph_3C][B(C_6F_5)_4]/PhSiH_3$ binary system under the molar ratio of $[EPI]/\{[Ph_3C][B(C_6F_5)_4]\}/[PhSiH_3]$ as 10:1:10 at room temperature in d^8-THF.

$$[Ph_3C]^+[B(C_6F_5)_4]^- + PhSiH_3 \longrightarrow Ph_3CH + [PhSiH_2]^+[B(C_6F_5)_4]^-$$

$$2[Ph_3C]^+[B(C_6F_5)_4]^- + PhSiH_3 \longrightarrow 2Ph_3CH + [PhSiH]^{2+}[B(C_6F_5)_4]^-_2$$

$$3[Ph_3C]^+[B(C_6F_5)_4]^- + PhSiH_3 \longrightarrow 3Ph_3CH + [PhSi]^{3+}[B(C_6F_5)_4]^-_3$$

Figure S102. The reaction of $[Ph_3C][B(C_6F_5)_4]$ and $PhSiH_3$ under the molar ratio of $[EPI]/\{[Ph_3C][B(C_6F_5)_4]\}/[PhSiH_3]$ as 10:1:10 at room temperature in 1h.

References

(1) X. W. Yan, S. W. Zhang, D. Q. Peng, J.G. Zhi, P. F. Zhang, X. L. Wu, L. Wang,Y. P. Dong, and X. F. Li*,*Polym. Chem.***2018**, *9*, 984–993.

(2) (a) M. A-Cortes, B. Heinrich, B. Donnio, K. E. Evans, C. W. Smith and D. W. Bruce*, *J. Mater. Chem.***2011**, *21*, 8427–8435. (b) A. Naka, Y. Matsumoto, T. Itano, K. Hasegawa, T. Shimamura, J. Osshita, A. Kunai, T. Takae, and M. Ishikawa*, *J. Organomet. Chem.***2009**, *694*, 345–352.

(3) (a), M. Amela-Cort, B. Heinrıch, B. Donnio, K. E. Evans, C. W. Smitha, D. W. Bruce, J. Mater. Chem., 2011, 21, 8427–8435. (b), H. Pleino, *J. Organomet. Chem.***1992**, *435*, 21.

(4) Z.J. Zhao, J.W.Y. Lam, B.Z. Tang, *J. Mater. Chem.***2012**, *22*, 23723–23740.

(5) A. D. Becke, *J. Chem. Phys.*, 1993, **98**, 1372−1377.

(6) A. D. Becke, *J. Chem. Phys.*, 1993, **98**, 5648−5652.

(7) C. Lee, W. Yang and R. G. Parr, *Phys. Rev. B.*, 1988, **37**, 785-789.

(8) M. J. Frisch, G. W.Trucks,H. B.Schlegel, G. E.Scuseria, M. A.Robb,J. R.Cheeseman, G. Scalmani,V. Barone,B. Mennucci,G. A. Petersson,H. Nakatsuji, M. Caricato,X. Li,H. P. Hratchian,A. F. Izmaylov, J. Bloino,G. Zheng,J. L. Sonnenberg, M. Hada, M. Ehara, K. Toyota, R. Fukuda, J. Hasegawa, M. Ishida, T. Nakajima, Y. Honda, O. Kitao, H. Nakai, T. Vreven, J. A. Montgomery, J. E. Peralta, F. Ogliaro, M. Bearpark, J. J. Heyd, E. Brothers, K. N.Kudin, V. N. Staroverov, T. Keith, R. Kobayashi, J. Normand, K.Raghavachari, A. Rendell, J. C. Burant, S. S. Iyengar, J. Tomasi, M. Cossi, N. Rega, J. M. Millam, M. Klene, J. E. Knox, J. B. Cross, V. Bakken, C. Adamo, J. Jaramillo, R. Gomperts, R. E. Stratmann, O. Yazyev, A. J. Austin, R. Cammi,C.Pomelli, J. W.Ochterski, R. L. Martin, K. Morokuma, V. G. Zakrzewski, G. A.

Voth, P. Salvador, J. J. Dannenberg, S. Dapprich, A. D. Daniels, O. Farkas, J. B. Foresman, J. V. Ortiz, J. Cioslowski, D. J. Fox, *Gaussian 09*, Revision D.01; Gaussian: Wallingford, CT, USA, 2013.

(9) S. Grimme, *J. Comput. Chem*., 2004, **25**, 1463.

(10) S. Grimme, *J. Comput. Chem*., 2006, **27**, 1787.

(11) S. Grimme, J. Antony,S. Ehrlich,H. Krieg,*J. Chem. Phys.,* 2010, **132**, 154104.

(12) L. Goerigk,S. Grimme,*Phys. Chem. Chem. Phys*., 2011, **13**, 6670−6688.

(13) A. Klamt, G. Schüürmann, *J. Chem. Soc. Perkin. Trans*., 1993, **2**, 799.

(14) R. Cammi, B. Mennucci, J. Tomasi, *J. Phys. Chem. A*, 1999, **103**, 9100.

(15) V. Barone, M. Cossi, *J. Phys. Chem. A*, 1998, **102**, 1995.

(16) J. Tomasi, B. Mennucci, R. Cammi, *Chem. Rev*., 2005, **105**, 2999.